

Supporting Information

Photo-Catalyzed Bis-Disulfidation of Vinyl Arenes with Tetrasulfides in Aqueous Phase

Ying-Ming Song,^a Binbin Huang,^b Yao Xiao,^b Zi-Shan Liu,^a Chen Zhang,^{*a} Hua Cao,^{*a} Yue Yu^{*a}

^a School of Chemistry and Chemical Engineering, Guangdong Provincial Key Laboratory of Advanced Drug Delivery, Guangdong Provincial Engineering Center of Topical Precise Drug Delivery System, Guangdong Pharmaceutical University, Guangzhou, Guangdong 510006, P. R. China.

^b EVE Energy Co., Ltd., Huizhou, Guangdong 516000, P. R. China.

E-mail: zhangch12020@gdpu.edu.cn; caohua@gdpu.edu.cn; yuyue@gdpu.edu.cn

Index

1	General Information	S2
2	Experimental Procedure	S4
3	Conditions Optimization	S8
4	Mechanistic Studies	S10
5	Electrochemical Analysis	S17
6	Characterization of Products	S20
7	References	S33
8	NMR Spectra	S35

1. General Information

1.1 NMR Spectrum

^1H and ^{13}C NMR spectra were acquired on 400 MHz NMR spectrometers (Bruker AVANCE). Chemical shifts for protons are reported in parts per million (ppm) downfield and are referenced to residual protium in the NMR solvent ($\text{CHCl}_3 = \delta$ 7.26 ppm). Chemical shifts for carbon are reported in parts per million downfield and are referenced to the carbon resonances of solvent ($\text{CHCl}_3 = \delta$ 77.16 ppm). Data is represented as follows: chemical shift, multiplicity (bs = broad singlet, s = singlet, d = doublet, t = triplet, q = quartet, m = multiplet), coupling constants in Hertz (Hz), integration.

1.2 Mass Spectroscopy

High-resolution mass spectra (HRMS) were performed on an Agilent 7250 GC/QTOF or a WATERS Xevo G2-XS QTOF mass spectrometer with an ESI or EI source. The column model is ACQUITY UPLC BEH C18 (with a packing particle size of 1.7 μm and available in dimensions of 2.1 \times 50 mm or 2.1 \times 100 mm).

1.3 TLC/Chromatography

Analytical thin-layer chromatography (TLC) was performed on silica gel. Column chromatography was performed with silica gel (300-400 mesh).

1.4 Solvents

Solvents were obtained from commercial sources.

1.5 Starting Materials

Styrene was commercially available, while the tetrasulfides were prepared according to literature-reported procedures.

1.6 Photochemical System

Photosyn-10 was manufactured by Shanghai Quanhuan Technology Co., Ltd.

1.7 UV-Vis Absorption

UV-vis absorption spectra were obtained with Shimadzu UV-2600i spectrophotometer.

1.8 Fluorescence Quenching Studies

Fluorescence quenching studies were performed using a Thermo Scientific Lumina Fluorescence spectrophotometer.

1.9 Raman Shift

Raman shift was performed with Thermo Scientific DXR3xi Raman Imaging Microscope.

1.10 Cyclic Voltammetry (CV)

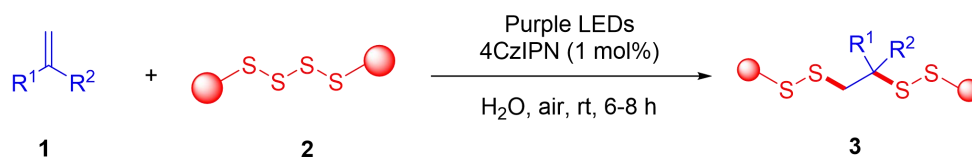
Cyclic voltammetry (CV) was performed on a Bio-Logic VSP potentiostat.

1.11 Voltage-Capacity Profile and Coulombic Efficiency (CE)

The battery was subjected to galvanostatic cycling at various C-rates on an Arbin BT 2000 multi-function battery testing system.

2. Experimental Procedure

2.1 General Procedure for Bis-disulfidation Reaction



Firstly, alkene **1** (0.40 mmol, 1.0 equiv.), tetrasulfides **2** (0.40 mmol, 1.0 equiv.), 4CzIPN (4.0 mg, 1.0 mol%), and H₂O (1 mL) were added to a 10 mL test tube at room temperature under an air atmosphere. The reaction mixture was irradiated with purple LEDs (6 W, 390-395 nm) for 6 hours. Upon complete consumption of compound **2** (as monitored by TLC), the reaction was quenched by adding water, and the organic phase was extracted with ethyl acetate. The organic layer was subsequently washed with brine and dried over anhydrous sodium sulfate. At last, the solvent was removed under vacuum, and the crude product was purified by flash column chromatography (using petroleum ether, PE, as the eluent) to afford product **3a** in 88% yield.

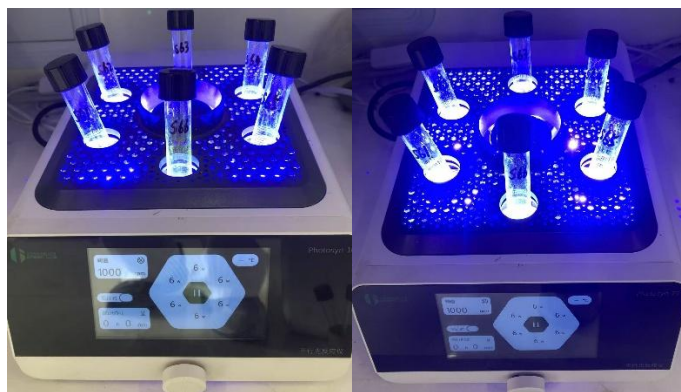
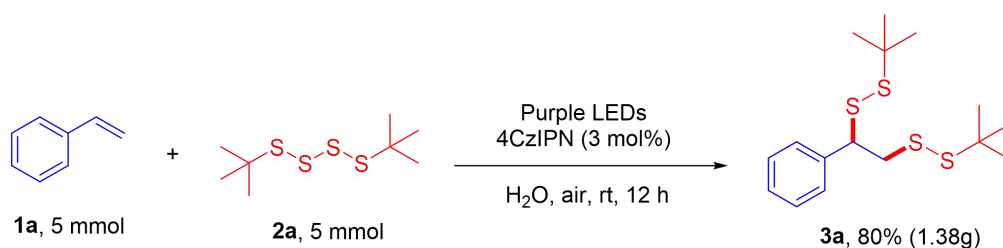


Figure S1. Irradiation of purple LEDs (6 W, 390-395 nm).

2.2 Gram Scale for the Synthesis of **3a**



In a sealed tube, **1a** (0.51 g, 5 mmol, 1.0 equiv.), **2a** (1.21 g, 5 mmol, 1.0 equiv.) and 4CzIPN (120 mg, 3.0 mol%) were dissolved in H₂O (5 mL) at room temperature under an

air atmosphere. The reaction mixture was irradiated with purple LEDs (6 W, 390-395 nm) for 12 hours. Upon complete consumption of compound **2a** (as monitored by TLC), the reaction was quenched by adding water, and the organic phase was extracted with ethyl acetate. The organic layer was subsequently washed with brine and dried over anhydrous sodium sulfate. At last, the solvent was removed under vacuum, and the crude product was purified by flash column chromatography (using petroleum ether, PE, as the eluent) to afford product **3a** (1.38 g, 80%).

2.3 Synthesis of Tetrasulfides^[1]

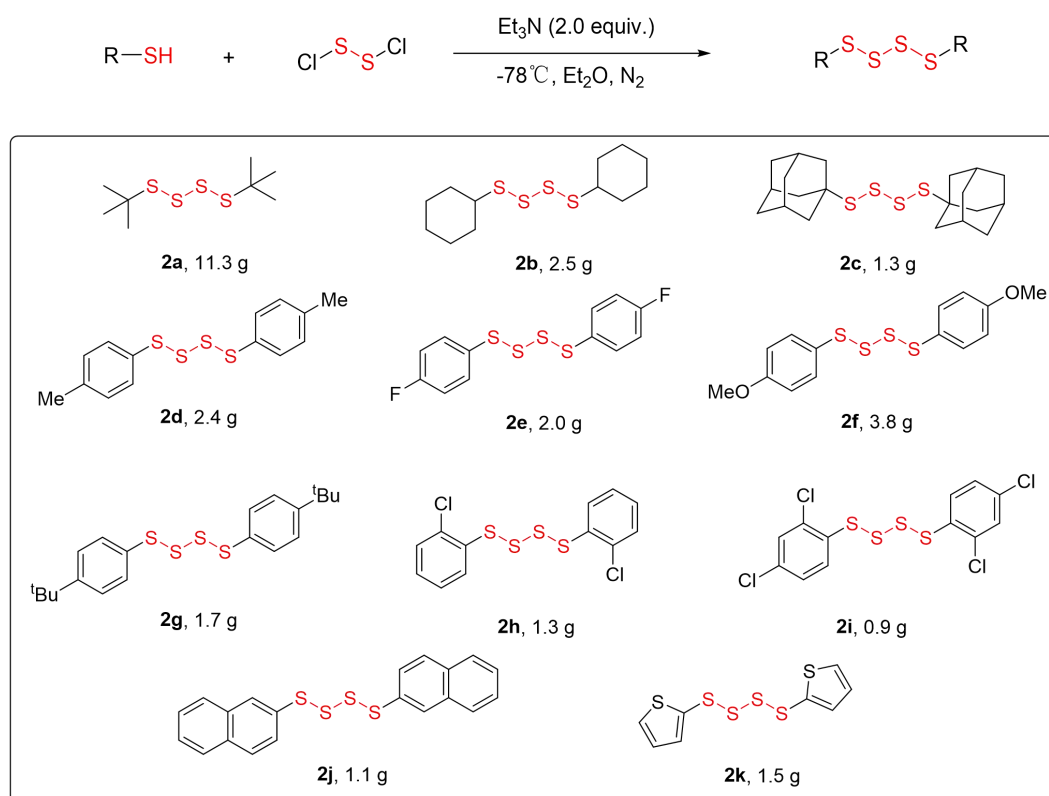


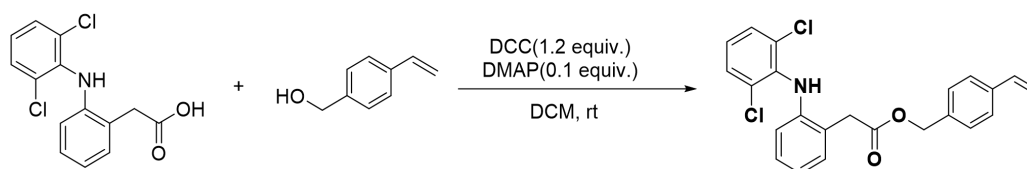
Figure S2. Synthesis of tetrasulfides **2a-2k**.

The synthesis of compound **2a-2k** was carried out according to the reported procedure^[1]. Under a nitrogen atmosphere, thiol (2.0 equiv.) and triethylamine (2.0 equiv.) were added to an oven-dried round-bottom flask, followed by the addition of 30 mL of anhydrous ethyl ether. The reaction mixture was cooled to -78 °C and maintained at this temperature for 1 h. Subsequently, sulfur monochloride (1.0 equiv.) was added dropwise. The reaction was stirred at room

temperature for 2 hours and then quenched with saturated sodium bicarbonate solution (30 mL), and the aqueous layer was discarded. The organic layer was washed sequentially with 30 mL of deionized water and 30 mL of brine. The organic phase was dried over anhydrous sodium sulfate, filtered, and the residue was purified by silica gel column chromatography using petroleum ether (PE) or a mixture of PE/ethyl acetate (PE/EA) as the eluent. The solvent was removed under reduced pressure to afford the desired tetrasulfide **2**.

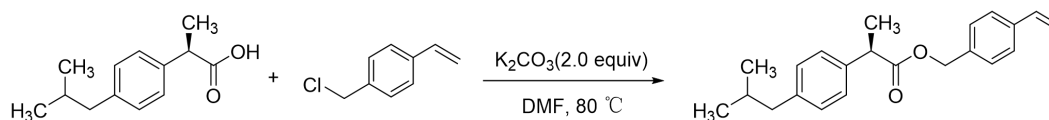
2.4 Synthesis of Pharmacophore-modified Derivatives (1p, 1q and 1r)

2.4.1 Synthesis of *Diclofenac* Derivative (1p)



The synthesis of *Diclofenac* derivative employed an esterification reaction system between hydroxyl and carboxylic acid moieties. The reaction was conducted by adding *Diclofenac* (5.0 mmol), (4-vinylphenyl)methanol (6.0 mmol), DCC (6.0 mmol), and DMAP (0.5 mmol) to a round-bottom flask containing anhydrous DCM (30 mL). The mixture was stirred at room temperature for 12 hours. Upon completion of the reaction, the solution was filtered to remove the insoluble by-products, and the crude product was purified by column chromatography using a petroleum ether/ethyl acetate (PE:EA = 20:1, v/v) solvent system to afford the target product.

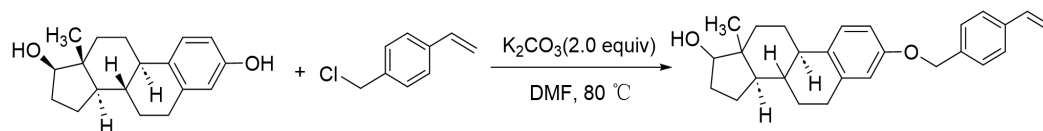
2.4.2 Synthesis of *Ibuprofen* Derivative (1q)



The synthesis of *Ibuprofen* derivatives was carried out according to the nucleophilic substitution reaction between carboxylic acids and benzyl chloride derivatives under alkaline conditions. *Ibuprofen* (5.0 mmol) and potassium carbonate (K_2CO_3 , 10.0 mmol) were added to a round-bottomed flask containing DMF (30 mL). The mixture was stirred until dissolution. 4-Vinylbenzyl chloride (6.0 mmol) was then added dropwise, and the reaction was heated to 80 °C under reflux for 12 hours. After cooling to room temperature, the reaction mixture was extracted

with ethyl acetate, washed with water, dried over anhydrous sodium sulfate (Na_2SO_4), and purified by column chromatography (PE:EA = 20:1, v/v) to afford the target product.

2.4.3 Synthesis of *Estradiol* Derivative (1r) ^[2]



The synthesis of *Estradiol* derivative was carried out according to the reported procedure ^[2]. *Estradiol* (5.0 mmol) and potassium carbonate (K_2CO_3 , 10.0 mmol) were added to a round-bottomed flask containing DMF (30 mL). The mixture was stirred until dissolution. 4-Vinylbenzyl chloride (6.0 mmol) was then added dropwise, and the reaction was heated to $80\text{ }^\circ\text{C}$ under reflux for 12 hours. After cooling to room temperature, the reaction mixture was extracted with ethyl acetate, washed with water, dried over anhydrous sodium sulfate (Na_2SO_4), and purified by column chromatography (PE:EA = 20:1, v/v) to afford the target product.

3. Conditions Optimization^[3]

Table S1. Optimization of reaction conditions ^a.

Entry	Variations from standard conditions	Yield of 3a (%)
1	None	88
2	DCM instead of H ₂ O	75
3	EA instead of H ₂ O	68
4	MeCN instead of H ₂ O	Trace
5	Ir(ppy) ₃ instead of 4CzIPN	66
6	[Ir(dF(CF ₃)ppy) ₂ (bpy)]PF ₆	75
7	Eosin Y instead of 4CzIPN	55
8	430 nm instead of 390 nm	74
9	460 nm instead of 390 nm	65
10	480 nm instead of 390 nm	Trace
11	Ratio of 1a and 2a (1.5:1)	78
12	Ratio of 1a and 2a (1:1.5)	60
13	Without photocatalyst	ND
14	In the dark	ND

4CzIPN

Ir(ppy)₃

[Ir(dF(CF₃)ppy)₂(bpy)]PF₆

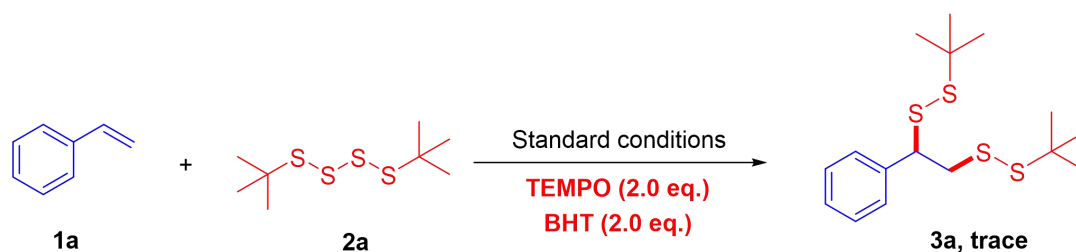
Eosin Y

^a Reaction conditions: **1a** (0.4 mmol), **2a** (0.4 mmol), photocatalyst (1 mol %) and H₂O (1 mL) were added in a 10 mL test tube at room temperature under an air atmosphere, while being stirred and irradiated by purple LEDs (6 W, 390-395 nm) for 6 h, with the isolated yields of the desired product.

Initially, we employed styrene (**1a**) and 1,4-di-*tert*-butyltetrasulfane (**2a**) as starting materials with a ratio of 1:1 and the mixture were added in aqueous phase, followed by irradiation with 390 nm visible light for 6 hours using 4CzIPN as the photosensitizer, the target product was obtained with an optimal yield of 88% (Table 1, entry 1). Considering the solvent effect and solubility, different solvents were screened. It was discovered that when dichloromethane, acetonitrile or ethyl acetate was used, lower yields of product were achieved, compared with aqueous-phase reaction (Entries 2-4). Based on several literatures^[3], we supposed that the “on-water effect” of this aqueous-phase reaction make the water-oil interface serve as a highly reactive surface, which significantly improve reaction kinetics and selectivity through synergistic interactions with water. Therefore, H₂O was ultimately determined to be the optimal solvent. During the screening of photosensitizers, we found that under 390 nm visible-light irradiation, the yield with 4CzIPN was significantly higher than that with Ir(ppy)₃, [Ir(dF(CF₃)ppy)₂(bpy)]PF₆ or Eosin Y (Entries 5-10). Adjusting the ratios of **1a** to **2a** could not further improve the yield (Entries 11-12). In addition, in the absence of the photocatalyst or purple LEDs, no desired product was detected. Control experiments demonstrated that both the photocatalyst and the light source were indispensable for this reaction (Entries 13-14).

4. Mechanistic Studies

4.1 Radical Quenching Experiments



All reactions were operated under standard conditions with the addition of 2,2,6,6-tetramethyl-1-piperinedinyloxy (TEMPO, 2.0 equiv.) or 2,6-di-tert-butyl-4-methylphenol (BHT, 2.0 equiv.). The yields were collected by isolating, only trace amounts of the target product were detected.

4.2 UV-vis Absorption Experiments

Prior to each measurement, the sample of interest was dissolved in spectroscopic-grade acetonitrile to prepare a solution with a concentration of 1×10^{-5} M. The mixture was thoroughly vortexed or sonicated to ensure complete homogeneity. Subsequently, the solution was transferred into a quartz cuvette for spectroscopic analysis. Ultraviolet-visible absorption spectra were obtained with Shimadzu UV-2600i spectrophotometer.

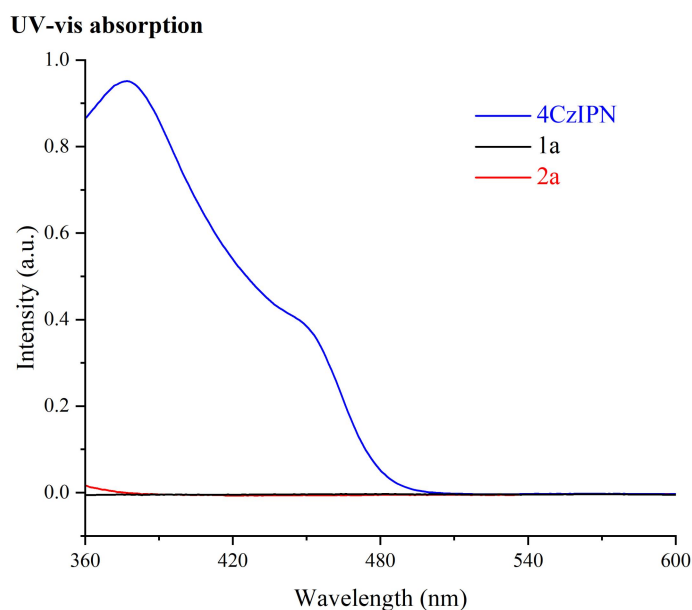


Figure S3. UV-vis absorption of 4CzIPN, 1a and 2a.

4.3 Stern-Volmer Quenching Experiment^[4]

Prior to each measurement, the photo redox catalyst was combined with varying concentrations of the quencher in spectroscopic-grade acetonitrile solution. After thorough mixing, the solution was transferred to a quartz cuvette. For the emission quenching study of 4CzIPN, the catalyst concentration was set to 1×10^{-4} M, and the solution was excited at 395 nm. Fluorescence quenching studies were performed using a Thermo Scientific Lumina Fluorescence spectrophotometer.

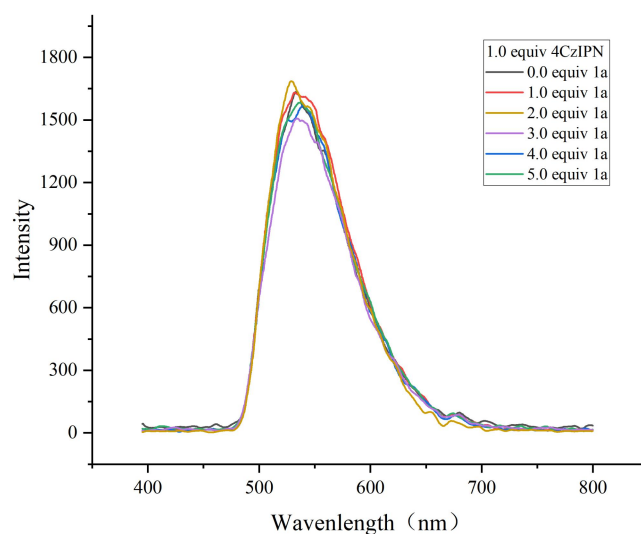


Figure S4. Fluorescence quenching of 4CzIPN with **1a**.

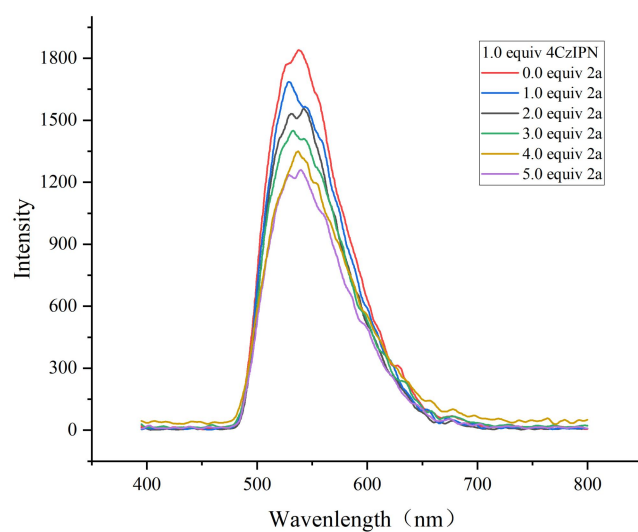


Figure S5. Fluorescence quenching of 4CzIPN with **2a**.

Stern-Volmer quenching

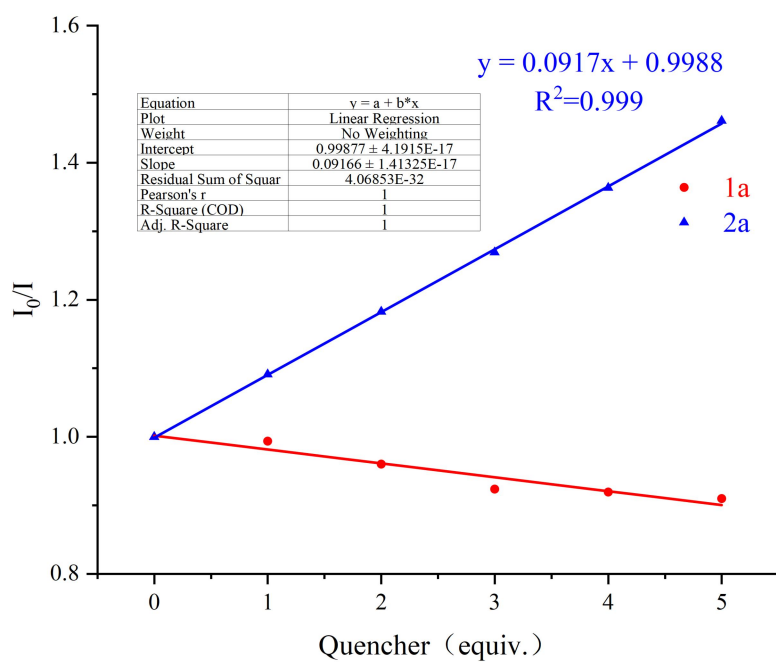


Figure S6. Stern-Volmer Plot of Fluorescence Quenching Experiments^[4]

4.4 Raman Shift Experiments^[5]

Raman shift were performed with DXR3xi Raman Imaging Microscope.

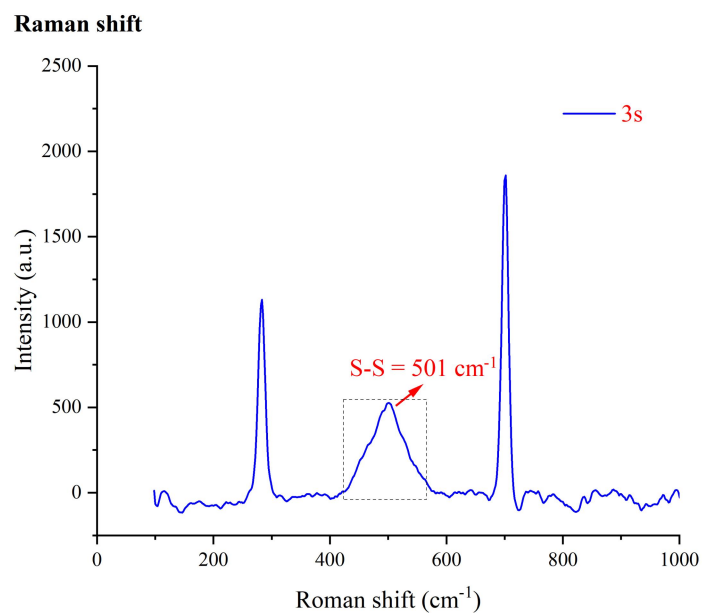


Figure S7. Raman shift of 3s^[5]

4.5 Light On-Off Experiments

During the photoreaction process, Light On-Off experiments were designed by controlling the Photosyn-10 photoreactor (On-Off cycles) to irradiate the reaction mixture every hour until the reaction was complete. The yields were collected by isolating the products.

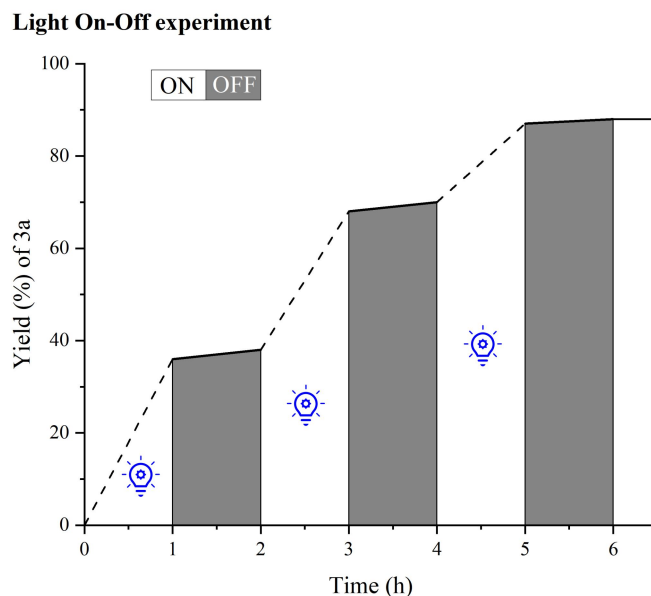


Figure S8. Light On-Off Experiments of **3a**.

4.6 Quantum Yield Measurements^[6-7]

All experimental procedures were carried out in accordance with the methods described in the literature^[6].

4.6.1 Photon Flux Detection

A ferrioxalate actinometer solution was prepared by following the Hammond variation of the Hatchard and Parker procedure outlined in Handbook of Photochemistry^[7]. The ferrioxalate actinometer solution measures the decomposition of ferric ions to ferrous ions, which are complexed by 1,10-phenanthroline and monitored by UV/Vis absorbance at 390 nm. The moles of iron-phenanthroline complex formed are related to moles of photons absorbed.

Firstly, the solutions were prepared and stored in a dark laboratory: **A**: Potassium ferrioxalate solution: 589.5 mg of potassium ferrioxalate and 278 μ L of sulfuric acid (95% - 98%) were added to a 100 mL volumetric flask, and filled to the mark with

water (HPLC grade). **B:** Phenantroline solution: 0.2% by weight of 1,10-phenanthroline in water (200 mg in 100 mL volumetric flask). **C:** Buffer solution: to a 100 mL volumetric flask, 4.94 g of NaOAc and 1 mL of sulfuric acid (95% - 98%) were added and filled to the mark with water (HPLC grade).

Secondly, 1 mL of the actinometer solution, whose quantum yield is being measured, were added to a standard 25 mL Schlenk tube. The tube was placed in parallel photoreactor irradiated without stirring by purple light (390 nm) who worked at 10W. This procedure was repeated 2 times, quenching the reactions after different time intervals: 1, 2, 3, 4, and 5 seconds.

Subsequently, The actinometer measurements were done as follows: 1) After irradiation, the actinometer solution was removed and placed in a 10 mL volumetric flask containing 0.5 mL of 1,10-phenanthroline solution and 2 mL of buffer solution. This flask was filled to the mark with water (HPLC grade). 2) The UV-vis spectra of the complexed actinometer samples were recorded for each time interval. The absorbance of the complexed actinometer solution was monitored at 390 nm. The moles of Fe^{2+} formed for each sample are determined according to the Beer's Law (eq. S1):

$$\text{moles}(\text{Fe}^{2+}) = \frac{V1 \cdot V3 \cdot \Delta A (390\text{nm})}{10^3 \cdot V2 \cdot l \cdot \epsilon (390\text{nm})} \quad \text{eq. S1}$$

where V1 is the irradiated volume (1 mL), V2 is the aliquot of the irradiated solution taken for the determination of the ferrous ions (1 mL), V3 is the final volume after complexation with phenanthroline (10 mL), l is the optical path-length of the irradiation cell (1 cm), $\Delta A (390 \text{ nm})$ the optical difference in absorbance between the irradiated solution and the one stored in the dark, $\epsilon (390 \text{ nm})$ is that of the complex $\text{Fe}(\text{phen})_3^{2+}$ ($12500 \text{ L} \cdot \text{mol}^{-1} \cdot \text{cm}^{-1}$). The moles of Fe^{2+} formed (x) are plotted as a function of time (t) (Figure S9). The slope of this line was correlated to the moles of incident photons by unit of time ($q_{n,p}^0$) by the use of the following eq. S2:

$$\Phi(\lambda) = \frac{dx/dt}{q_{n,p}^0 [1 - 10^{-A(\lambda)}]} \quad \text{eq. S2}$$

where dx/dt is the rate of change of a measurable quantity (spectral or any other

property), the quantum yield (Φ) for Fe^{2+} at 390 nm is 0.8, and $A(\lambda)$ is the absorbance of the actinometer at the wavelength used to carry out the experiments (390 nm). The absorbance at 390 nm $A(390)$ was measure using a GENESYS 180 UV-Vis spectrophotometer in 1 mm path quartz cuvettes in the presence of the bandpass filter of 390 nm employed to run the measurements, obtaining an absorbance of 0.15. ($q_{n,p}^0$), which is the photon flux, was determined to be $3.36 \times 10^{-9} \text{ einstein} \cdot \text{s}^{-1}$.

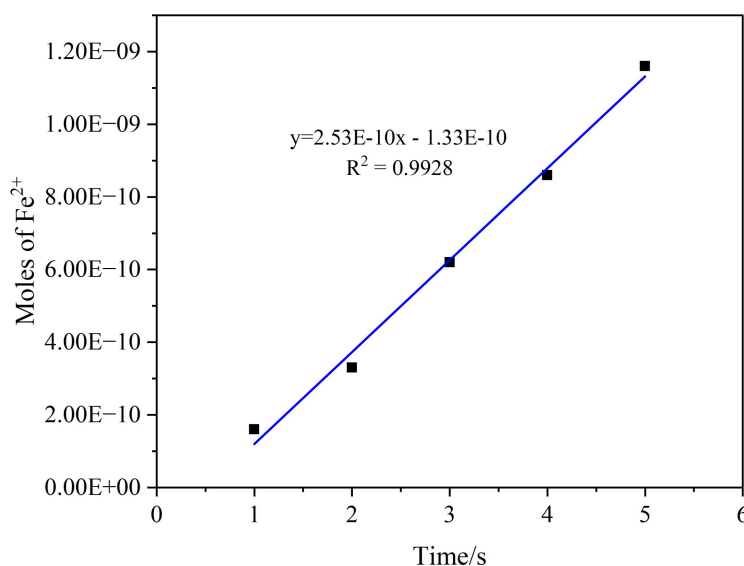


Figure S9. The profile between the moles of Fe^{2+} (y axis) and time (x axis).

4.6.2 Quantum Yield Calculation

According to the Stark-Einstein law, the quantum yield is defined as:

$$\Phi = \frac{\text{Moles of product formed}}{\text{Photons absorbed of sample}} \quad \text{eq. S3}$$

If the transmittance of photons at the purple LEDs wavelength (390 nm) is sufficiently small, it can be assumed that all of the photons which pass through the cell are absorbed. The above equation may be then written as:

$$\Phi = \frac{\text{Moles of product formed}}{\text{Photon flux} \cdot \text{time}} = \frac{\text{Moles of product formed}}{\text{Photons}} \quad \text{eq. S4}$$

According to this relationship, the quantum yield was determined by the slop. The experiment procedure is as follows: For six clean tubes, according to the general procedure, the 0.2 mmol scale model reaction solution was irradiated with 10 W

purple LEDs (390 nm) for specified time intervals (0 min, 20 min, 40 min, 60 min, 80 min, and 100 min). The moles of products formed were determined by GC yield with Polysulfide as reference standard.

Based on the data, we got the graph (Figure S10). The number of moles of products (y axis) per unit time is related to the number of photons (x axis, calculated from Photon Flux * Time). The slope gives the quantum yield (Φ) of the photoreaction as 0.69.

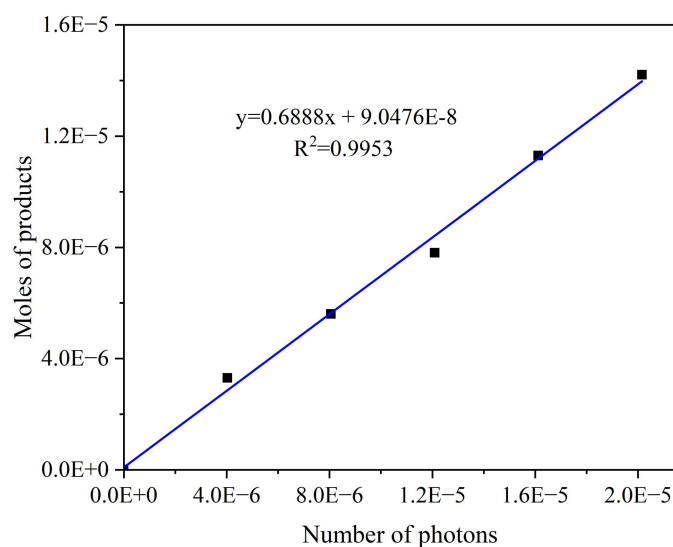


Figure S10. The quantum yield (Φ) of the photoreaction.

5. Electrochemical Analysis

Initially, a 0.5 M sample was prepared as a catholyte and introduced into a binder-free carbon nanotube (CNT) paper, also known as Buckypaper (BP), serving as the current collector. A Celgard 2400 separator was then placed atop the BP electrode, followed by the addition of lithium foil and a nickel foam spacer to complete the cell assembly. The coin cell was subsequently crimped and removed from the glovebox for electrochemical evaluation. The CNT paper current collector provides efficient pathways for both electron and ion conduction, while the catholyte is confined within the nanoscale spaces of the CNT network, minimizing outward diffusion. Additionally, the aromatic groups in the catholyte exhibit intermolecular interactions with the CNTs via π - π stacking, further suppressing the shuttle effect of soluble species during battery cycling^[6].

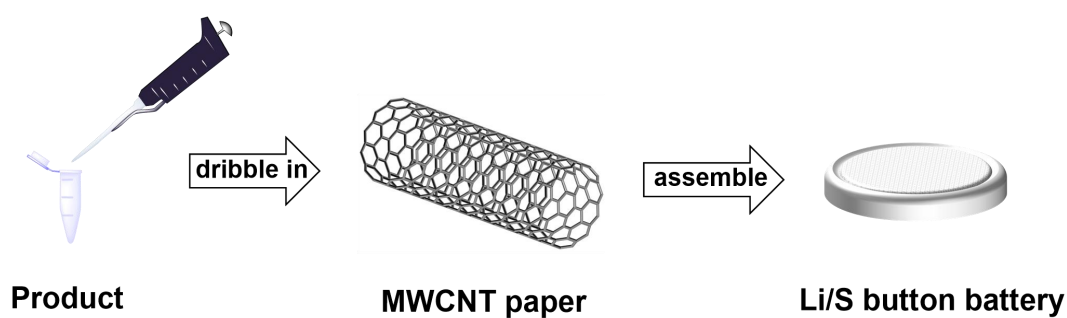


Figure S11. Assemble of the Li/S cell^[6].

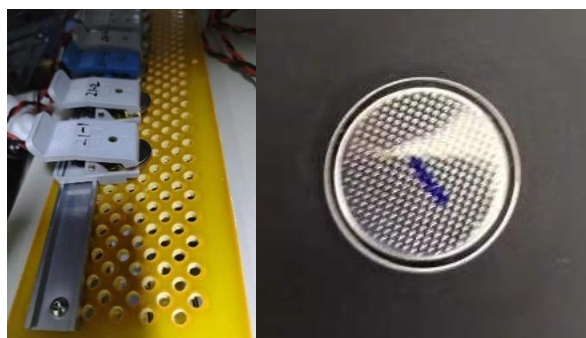


Figure S12. Real object picture of the coin cell.

5.1 Cyclic Voltammetry (CV)^[6]

Cyclic voltammetry (CV) was performed on a Bio-Logic VSP potentiostat. The potential was swept from the open-circuit voltage (OCV) of 2.35 V to 0 V at a scan rate of 0.05 V s⁻¹, followed by sweeping back to 4.0 V. The electrode was then allowed to rest for 5 minutes, and this cycle

was repeated 3 times.

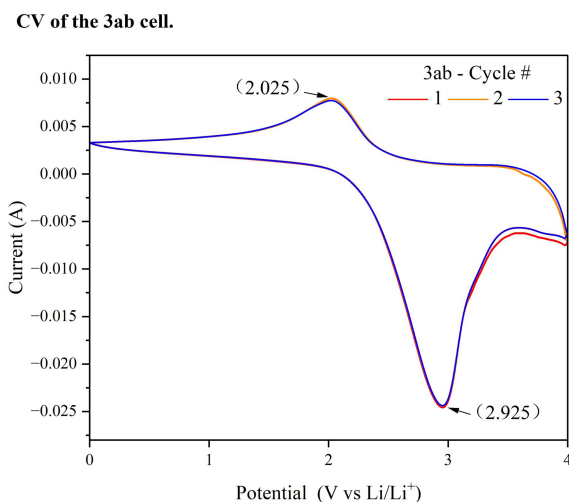


Figure S13. CV of the **3ab** cell.

5.2 Voltage-capacity Profile^[6]

The battery was subjected to galvanostatic cycling at various C-rates on an Arbin BT 2000 multi-function battery testing system, with a cut-off voltage of 3.8 V. The charging protocol included a constant current (CC) step at 0.1 C to 3.8 V, followed by a constant voltage (CV) step at 3.8 V until the current reached 0.01 C, and then a 10-minute rest period. The battery was subsequently discharged at C/10 rate to 1.5 V, with a discharging protocol involving a constant current (CC) step at 0.1 C to 1.5 V. The voltage-capacity curve for the first cycle at a 0.1 C discharge rate was plotted.

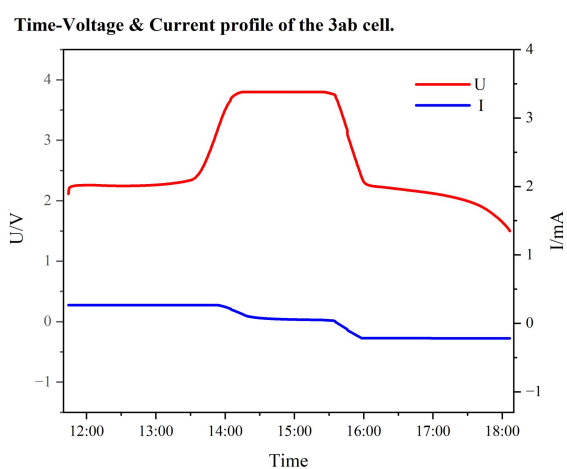


Figure S14. Time-Voltage & Current profile of the **3ab** cell.

Voltage–capacity profile of the cell in the first cycle at C/10 rate.

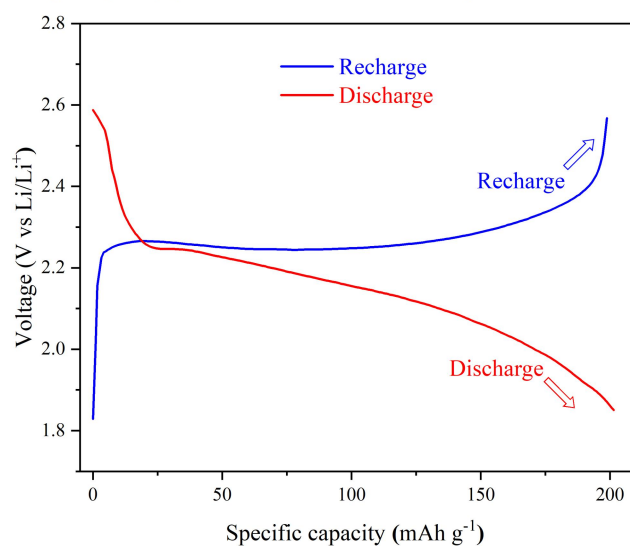


Figure S15. Voltage-capacity profile of the cell in the first cycle at C/10 rate.

5.3 Cycling Performance and Coulombic Efficiency (CE)^[6]

After completing the first discharge, the battery was subjected to subsequent discharging at C/10 (a discharging protocol of 0.1 C to 1.5 V), followed by a 10-minute rest period. This cycle was repeated 5 times. The cycling performance and Coulombic efficiency were evaluated by calculating the specific capacity retention over these cycles.

Cycling performance and Coulombic efficiency (CE) of the cell at C/10 rate.

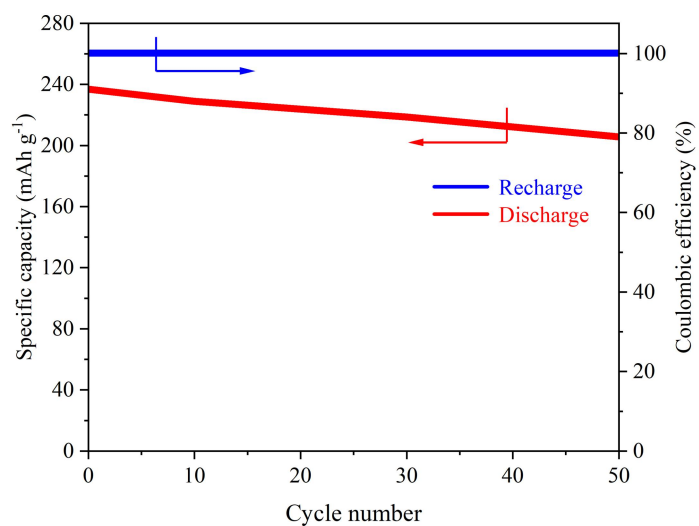
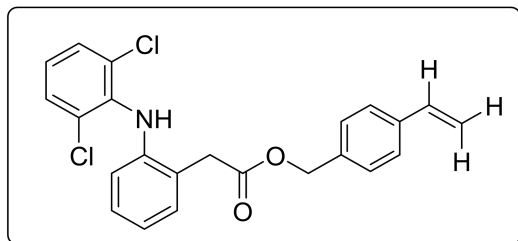


Figure S16. Cycling performance and Coulombic efficiency (CE) of the cell at C/10 rate.

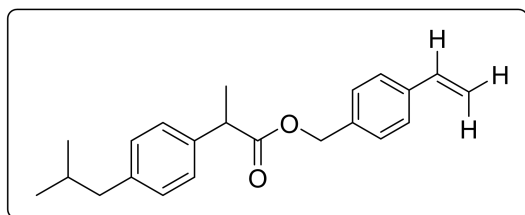
6. Characterization of Products

4-vinylbenzyl 2-((2,6-dichlorophenyl)amino)phenylacetate (1p)



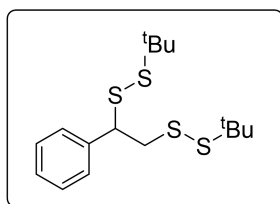
White oily liquid (1.40 g, 68%); TLC, R_f = 0.40 (PE:EA = 20:1, v/v); **^1H NMR** (400 MHz, CDCl_3) δ 7.36 (d, J = 8.2 Hz, 2H), 7.29 (d, J = 8.1 Hz, 3H), 7.21 (dd, J = 7.5, 1.7 Hz, 1H), 7.11 (td, J = 7.6, 1.7 Hz, 1H), 6.96-6.88 (m, 3H), 6.68 (dd, J = 17.6, 10.9 Hz, 1H), 6.54 (d, J = 7.9 Hz, 1H), 5.73 (d, J = 16.6 Hz, 1H), 5.24 (d, J = 11.7 Hz, 1H), 5.14 (s, 2H), 3.84 (s, 2H). **^{13}C NMR** (101 MHz, CDCl_3) δ 172.2, 142.8, 137.8, 137.8, 136.4, 135.0, 131.0, 129.5, 128.9, 128.7, 128.1, 126.5, 124.3, 124.1, 122.1, 118.4, 114.5, 66.9, 38.7. HRMS (ESI-TOF) m/z calcd for $\text{C}_{23}\text{H}_{19}\text{Cl}_2\text{NO}_2$ [M^+]: 411.0793, found 411.0795.

4-vinylbenzyl 2-(4-isobutylphenyl)propanoate (1q)



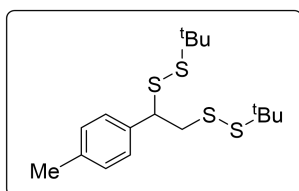
White oily liquid (1.16 g, 72%); TLC, R_f = 0.50 (PE:EA = 20:1, v/v); **^1H NMR** (400 MHz, CDCl_3) δ 7.34 (d, J = 8.2 Hz, 2H), 7.22-7.07 (m, 6H), 6.69 (dd, J = 17.6, 11.0 Hz, 1H), 5.74 (d, J = 17.6 Hz, 1H), 5.25 (d, J = 10.9 Hz, 1H), 5.09 (d, J = 2.7 Hz, 2H), 3.75 (q, J = 7.2 Hz, 1H), 2.45 (d, J = 7.2 Hz, 2H), 1.84 (dq, J = 13.7, 6.8 Hz, 1H), 1.51 (d, J = 7.2 Hz, 3H), 0.90 (d, J = 6.6 Hz, 6H). **^{13}C NMR** (101 MHz, CDCl_3) δ 174.7, 140.7, 137.7, 137.5, 136.5, 135.7, 129.5, 128.2, 127.4, 126.4, 114.3, 66.2, 45.2, 45.2, 30.4, 22.5, 18.5. HRMS (ESI-TOF) m/z calcd for $\text{C}_{22}\text{H}_{26}\text{O}_2$ [M^+]: 322.1933, found 322.1932.

2,2'-(1-phenylethane-1,2-diyl)bis(1-(*tert*-butyl)disulfane) (3a)



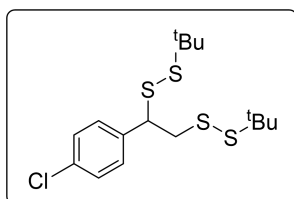
Yellow oily liquid (121.8 mg, 88%); TLC, R_f = 0.40 (PE:EA = 50:1, v/v); ^1H NMR (400 MHz, CDCl_3) δ 7.35 (d, J = 6.9 Hz, 2H), 7.30 (dd, J = 6.7, 3.2 Hz, 3H), 4.19 (dd, J = 10.9, 4.5 Hz, 1H), 3.51 (dd, J = 13.1, 4.5 Hz, 1H), 3.20 (dd, J = 13.1, 11.0 Hz, 1H), 1.36 (s, 9H), 1.35 (s, 9H). ^{13}C NMR (101 MHz, CDCl_3) δ 138.8, 128.9, 128.4, 128.3, 55.3, 48.4, 48.0, 45.4, 30.3, 30.2. HRMS (GC/TOF) m/z calcd for $\text{C}_{16}\text{H}_{26}\text{S}_4$ [M^+]: 346.0917, found 346.0919.

2,2'-(1-(*p*-tolyl)ethane-1,2-diyl)bis(1-(*tert*-butyl)disulfane) (3b)



Yellow oily liquid (123.9 mg, 86%); TLC, R_f = 0.40 (PE:EA = 50:1, v/v); ^1H NMR (400 MHz, CDCl_3) δ 7.18 (d, J = 4.8 Hz, 4H), 4.17 (dd, J = 11.1, 4.5 Hz, 1H), 3.50 (dd, J = 13.0, 4.5 Hz, 1H), 3.20 (dd, J = 13.0, 11.1 Hz, 1H), 2.35 (s, 3H), 1.37 (s, 9H), 1.35 (s, 9H). ^{13}C NMR (101 MHz, CDCl_3) δ 138.1, 135.6, 129.6, 128.2, 55.0, 48.4, 48.0, 45.5, 30.3, 30.2, 21.4. HRMS (GC/TOF) m/z calcd for $\text{C}_{17}\text{H}_{28}\text{S}_4$ [M^+]: 360.1074, found 360.1077.

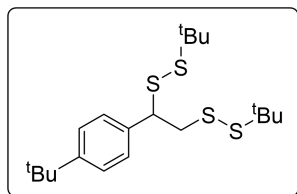
2,2'-(1-(4-chlorophenyl)ethane-1,2-diyl)bis(1-(*tert*-butyl)disulfane) (3c)



Yellow oily liquid (129.2 mg, 85%); TLC, R_f = 0.40 (PE:EA = 50:1, v/v); ^1H NMR (400 MHz, CDCl_3) δ 7.32 (d, J = 8.4 Hz, 2H), 7.23 (d, J = 8.4 Hz, 2H), 4.16 (dd, J = 10.9, 4.5 Hz, 1H), 3.48 (dd, J = 13.2, 4.5 Hz, 1H), 3.11 (dd, J = 13.1, 11.0 Hz, 1H), 1.35 (s, 9H), 1.34 (s, 9H). ^{13}C NMR (101 MHz, CDCl_3) δ 137.4, 133.9, 129.8, 129.0, 54.6, 48.5, 48.1, 45.1, 30.2, 30.2. HRMS

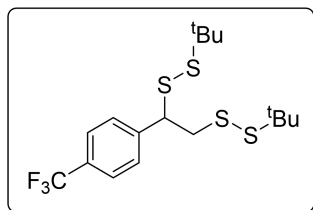
(GC/TOF) m/z calcd for $C_{16}H_{25}ClS_4$ $[M^+]$: 380.0528, found 380.0529.

2,2'-(1-(4-(*tert*-butyl)phenyl)ethane-1,2-diyl)bis(1-(*tert*-butyl)disulfane) (3d)



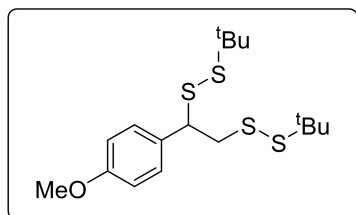
Yellow oily liquid (133.5 mg, 83%); TLC, R_f = 0.40 (PE:EA = 50:1, v/v); 1H NMR (400 MHz, $CDCl_3$) δ 7.37 (d, J = 8.4 Hz, 2H), 7.23 (d, J = 8.3 Hz, 2H), 4.19 (dd, J = 11.0, 4.4 Hz, 1H), 3.53 (dd, J = 13.1, 4.4 Hz, 1H), 3.22 (dd, J = 13.0, 11.0 Hz, 1H), 1.37 (s, 9H), 1.36 (s, 9H), 1.32 (s, 9H). ^{13}C NMR (101 MHz, $CDCl_3$) δ 150.8, 135.1, 127.6, 125.5, 54.5, 48.0, 47.6, 45.1, 34.4, 31.1, 30.0, 29.9. HRMS (GC/TOF) m/z calcd for $C_{20}H_{34}S_4$ $[M^+]$: 402.1543, found 402.1546.

2,2'-(1-(4-(trifluoromethyl)phenyl)ethane-1,2-diyl)bis(1-(*tert*-butyl)disulfane) (3e)



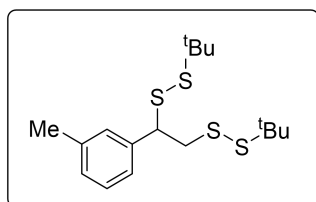
Yellow oily liquid (129.2 mg, 78%); TLC, R_f = 0.30 (PE:EA = 50:1, v/v); 1H NMR (400 MHz, $CDCl_3$) δ 7.61 (d, J = 8.2 Hz, 2H), 7.41 (d, J = 8.1 Hz, 2H), 4.23 (dd, J = 10.9, 4.6 Hz, 1H), 3.49 (dd, J = 13.3, 4.6 Hz, 1H), 3.13 (dd, J = 13.3, 10.8 Hz, 1H), 1.35 (s, 9H), 1.34 (s, 9H). ^{13}C NMR (101 MHz, $CDCl_3$) δ 143.2, 130.2 (J = 64.6 Hz), 128.8, 125.8 (J = 4.0 Hz), 125.2 (J = 267.7 Hz), 55.0, 48.6, 48.2, 44.9, 30.2, 30.2. HRMS (GC/TOF) m/z calcd for $C_{17}H_{25}F_3S_4$ $[M^+]$: 414.0791, found 414.0793.

2,2'-(1-(4-methoxyphenyl)ethane-1,2-diyl)bis(1-(*tert*-butyl)disulfane) (3f)



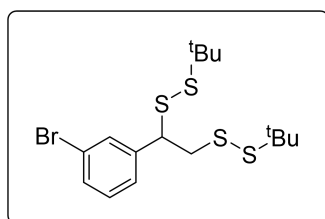
Yellow oily liquid (129.4 mg, 86%); TLC, R_f = 0.30 (PE:EA = 10:1, v/v); **¹H NMR** (400 MHz, CDCl₃) δ 7.23 (d, J = 8.7 Hz, 2H), 6.89 (d, J = 8.7 Hz, 2H), 4.16 (dd, J = 11.2, 4.4 Hz, 1H), 3.80 (s, 3H), 3.51 (dd, J = 13.0, 4.3 Hz, 1H), 3.17 (dd, J = 13.0, 11.2 Hz, 1H), 1.36 (s, 9H), 1.35 (s, 9H). **¹³C NMR** (101 MHz, CDCl₃) δ 159.5, 130.5, 129.5, 114.3, 55.4, 54.5, 48.3, 48.0, 45.5, 30.3, 30.2. HRMS (GC/TOF) m/z calcd for C₁₇H₂₈OS₄ [M⁺]: 376.1023, found 376.1025.

2,2'-(1-(*m*-tolyl)ethane-1,2-diyl)bis(1-(*tert*-butyl)disulfane) (3g)



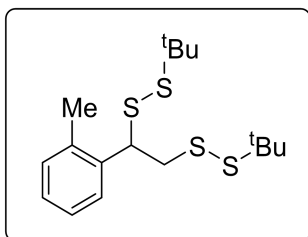
Yellow oily liquid (108.0 mg, 75%); TLC, R_f = 0.40 (PE:EA = 50:1, v/v); **¹H NMR** (400 MHz, CDCl₃) δ 7.23 (d, J = 7.6 Hz, 1H), 7.11 (d, J = 7.6 Hz, 3H), 4.15 (dd, J = 11.0, 4.4 Hz, 1H), 3.50 (dd, J = 13.1, 4.4 Hz, 1H), 3.20 (dd, J = 13.0, 11.0 Hz, 1H), 2.36 (s, 3H), 1.37 (s, 9H), 1.35 (s, 9H). **¹³C NMR** (101 MHz, CDCl₃) δ 138.6, 138.5, 129.1, 129.0, 128.7, 125.4, 55.3, 48.4, 48.0, 45.5, 30.3, 30.2, 21.6. HRMS (GC/TOF) m/z calcd for C₁₇H₂₈S₄ [M⁺]: 360.1074, found 360.1078.

2,2'-(1-(3-bromophenyl)ethane-1,2-diyl)bis(1-(*tert*-butyl)disulfane) (3h)



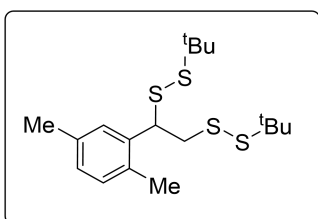
Yellow oily liquid (127.2 mg, 75%); TLC, R_f = 0.40 (PE:EA = 50:1, v/v); **¹H NMR** (400 MHz, CDCl₃) δ 7.44-7.40 (m, 2H), 7.23-7.20 (m, 2H), 4.13 (dd, J = 10.8, 4.6 Hz, 1H), 3.46 (dd, J = 13.3, 4.6 Hz, 1H), 3.10 (dd, J = 13.2, 10.8 Hz, 1H), 1.35 (s, 9H), 1.34 (s, 9H). **¹³C NMR** (101 MHz, CDCl₃) δ 141.3, 131.5, 131.3, 130.4, 127.1, 122.8, 54.8, 48.5, 48.2, 45.0, 30.3, 30.2. HRMS (GC/TOF) m/z calcd for C₁₆H₂₅BrS₄ [M⁺]: 424.0022, found 424.0024.

2,2'-(1-(*o*-tolyl)ethane-1,2-diyl)bis(1-(*tert*-butyl)disulfane) (3i)



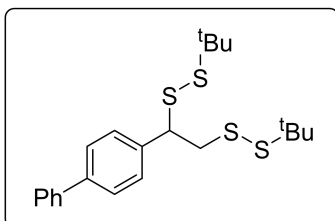
Yellow oily liquid (105.4 mg, 73%); TLC, R_f = 0.40 (PE:EA = 50:1, v/v); **^1H NMR** (400 MHz, CDCl_3) δ 7.28 (d, J = 6.8 Hz, 1H), 7.23-7.20 (m, 1H), 7.19-7.17 (m, 2H), 4.50 (dd, J = 11.1, 4.3 Hz, 1H), 3.57 (dd, J = 13.1, 4.2 Hz, 1H), 3.21 (dd, J = 13.1, 11.1 Hz, 1H), 2.45 (s, 3H), 1.37 (s, 9H), 1.35 (s, 9H). **^{13}C NMR** (101 MHz, CDCl_3) δ 137.3, 136.9, 130.8, 128.0, 127.0, 126.6, 50.0, 48.1, 48.0, 45.4, 30.3, 30.2, 20.2. HRMS (ESI-TOF) m/z calcd for $\text{C}_{17}\text{H}_{28}\text{S}_4$ [M^+]: 361.1152, found 361.1156.

2,2'-(1-(2,5-dimethylphenyl)ethane-1,2-diyl)bis(1-(tert-butyl)disulfane) (3j)



Yellow oily liquid (117.0 mg, 78%); TLC, R_f = 0.30 (PE:EA = 50:1, v/v); **^1H NMR** (400 MHz, CDCl_3) δ 7.07 (d, J = 7.8 Hz, 2H), 7.00 (d, J = 7.7 Hz, 1H), 4.48 (dd, J = 11.1, 4.2 Hz, 1H), 3.57 (dd, J = 13.1, 4.2 Hz, 1H), 3.21 (dd, J = 13.1, 11.1 Hz, 1H), 2.40 (s, 3H), 2.32 (s, 3H), 1.38 (s, 9H), 1.36 (s, 9H). **^{13}C NMR** (101 MHz, CDCl_3) δ 136.6, 136.0, 134.1, 130.7, 128.8, 127.6, 50.0, 48.1, 48.0, 45.4, 30.3, 30.2, 21.3, 19.7. HRMS (ESI-TOF) m/z calcd for $\text{C}_{18}\text{H}_{30}\text{S}_4$ [M^+]: 375.1309, found 375.1307.

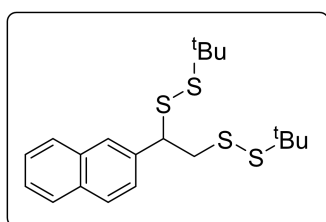
2,2'-(1-([1,1'-biphenyl]-4-yl)ethane-1,2-diyl)bis(1-(tert-butyl)disulfane) (3k)



Brown oily liquid (135.1 mg, 80%); TLC, R_f = 0.30 (PE:EA = 50:1, v/v); **^1H NMR** (400 MHz,

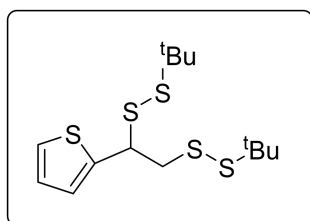
CDCl₃) δ 7.61-7.58 (m, 4H), 7.44 (t, J = 7.5 Hz, 3H), 7.38 (d, J = 8.1 Hz, 2H), 4.25 (dd, J = 11.0, 4.5 Hz, 1H), 3.55 (dd, J = 13.1, 4.5 Hz, 1H), 3.24 (dd, J = 13.1, 11.0 Hz, 1H), 1.39 (s, 9H), 1.37 (s, 9H). ¹³C NMR (101 MHz, CDCl₃) δ 141.1, 140.8, 137.7, 128.9, 128.8, 127.6, 127.5, 127.2, 55.0, 48.5, 48.1, 45.3, 30.3, 30.2. HRMS (GC/TOF) m/z calcd for C₂₂H₃₀S₄ [M⁺]: 422.1230, found 422.1232.

2,2'-(1-(naphthalen-2-yl)ethane-1,2-diyl)bis(1-(*tert*-butyl)disulfane) (3l)



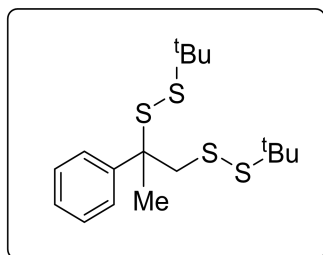
Yellow oily liquid (114.1 mg, 72%); TLC, R_f = 0.60 (PE:EA = 30:1, v/v); ¹H NMR (400 MHz, CDCl₃) δ 7.83 (d, J = 4.4 Hz, 3H), 7.74 (s, 1H), 7.48-7.45 (m, 3H), 4.19 (dd, J = 11.0, 4.8 Hz, 1H), 3.46 (dd, J = 12.6, 4.8 Hz, 1H), 3.22 (dd, J = 12.6, 11.0 Hz, 1H), 1.37 (s, 9H), 1.34 (s, 9H). ¹³C NMR (101 MHz, CDCl₃) δ 136.6, 133.4, 133.3, 128.7, 128.2, 127.9, 127.5, 126.3, 126.2, 125.9, 57.0, 48.5, 43.4, 33.4, 31.1, 30.2. HRMS (GC/TOF) m/z calcd for C₂₀H₂₈S₄ [M⁺]: 396.1074, found 396.1074.

2-(1,2-bis(*tert*-butyldisulfaneyl)ethyl)thiophene (3m)



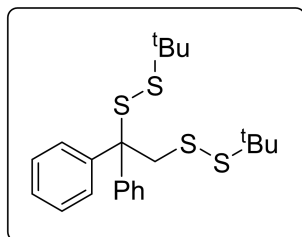
Yellow oily liquid (95.8 mg, 68%); TLC, R_f = 0.30 (PE:EA = 50:1, v/v); ¹H NMR (400 MHz, CDCl₃) δ 7.25 (d, J = 1.3 Hz, 1H), 7.02-7.00 (m, 1H), 6.96 (dd, J = 5.0, 3.5 Hz, 1H), 4.29 (dd, J = 10.8, 4.5 Hz, 1H), 3.40 (dd, J = 12.8, 4.5 Hz, 1H), 3.06 (dd, J = 12.8, 10.8 Hz, 1H), 1.36 (s, 9H), 1.34 (s, 9H). ¹³C NMR (101 MHz, CDCl₃) δ 142.7, 127.0, 126.4, 125.4, 52.2, 48.7, 43.6, 35.0, 31.1, 30.2. HRMS (GC/TOF) m/z calcd for C₁₄H₂₄S₅ [M⁺]: 352.0482, found 352.0479.

2,2'-(2-phenylpropane-1,2-diyl)bis(1-(*tert*-butyl)disulfane) (3n)



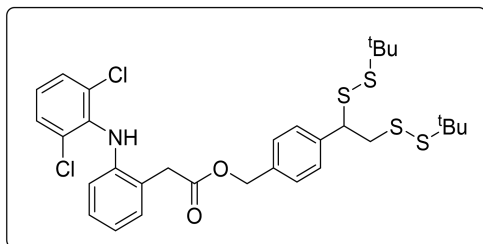
White oily liquid (93.9 mg, 65%); TLC, R_f = 0.40 (PE:EA = 50:1, v/v); $^1\text{H NMR}$ (400 MHz, CDCl_3) δ 7.48 (d, J = 7.3 Hz, 2H), 7.39-7.31 (m, 3H), 3.82 (d, J = 12.6 Hz, 1H), 3.30 (d, J = 13.6 Hz, 1H), 1.89 (s, 3H), 1.31 (s, 9H), 1.16 (s, 9H). $^{13}\text{C NMR}$ (101 MHz, CDCl_3) δ 141.8, 128.4, 127.7, 127.4, 55.5, 55.1, 48.0, 47.4, 30.6, 30.0, 24.5. HRMS (ESI-TOF) m/z calcd for $\text{C}_{17}\text{H}_{28}\text{S}_4$ [M^+]: 361.1152, found 361.1153.

2,2'-(1,1-diphenylethane-1,2-diyl)bis(1-(*tert*-butyl)disulfane) (3o)



Yellow oily liquid (126.6 mg, 75%); TLC, R_f = 0.30 (PE:EA = 50:1, v/v); $^1\text{H NMR}$ (400 MHz, CDCl_3) δ 7.50 (d, J = 8.3 Hz, 4H), 7.33 (d, J = 1.2 Hz, 4H), 7.28 (d, J = 1.2 Hz, 2H), 3.57 (s, 2H), 1.17 (s, 9H), 1.00 (s, 9H). $^{13}\text{C NMR}$ (101 MHz, CDCl_3) δ 143.2, 129.9, 127.6, 127.2, 63.7, 47.8, 42.9, 40.1, 30.7, 30.3. HRMS (GC/TOF) m/z calcd for $\text{C}_{22}\text{H}_{30}\text{S}_4$ [M^+]: 422.1230, found 422.1233.

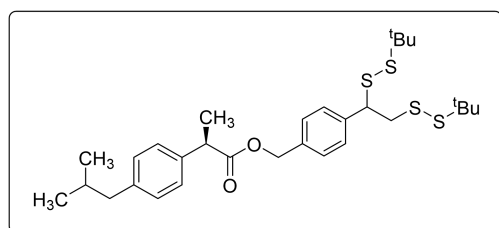
4-(1,2-bis(*tert*-butyldisulfaneyl)ethyl)benzyl 2-(2-((2,6-dichlorophenyl)amino)phenyl)acetate (3p)



Yellow oily liquid (143.9 mg, 55%); TLC, R_f = 0.40 (PE:EA = 20:1, v/v); $^1\text{H NMR}$ (400 MHz, CDCl_3) δ 7.32 (d, J = 8.1 Hz, 6H), 7.13 (s, 1H), 6.99-6.94 (m, 3H), 6.55 (d, J = 7.0 Hz, 1H), 5.16

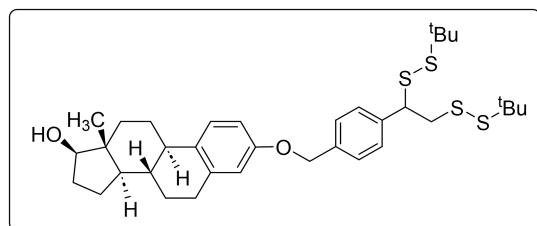
(s, 2H), 4.18 (dd, $J = 10.9, 4.6$ Hz, 1H), 3.86 (s, 2H), 3.49 (dd, $J = 13.1, 4.5$ Hz, 1H), 3.16 (dd, $J = 13.2, 10.9$ Hz, 1H), 1.34 (d, $J = 3.9$ Hz, 18H). ^{13}C NMR (101 MHz, CDCl_3) δ 172.3, 142.8, 139.1, 137.9, 135.4, 131.0, 129.6, 129.0, 128.8, 128.6, 128.2, 124.3, 124.1, 122.2, 118.5, 66.9, 55.0, 48.4, 48.1, 45.2, 38.7, 30.2, 30.2. HRMS (ESI-TOF) m/z calcd for $\text{C}_{31}\text{H}_{37}\text{Cl}_2\text{NO}_2\text{S}_4$ [M^+]: 654.1162, found 654.1166.

4-(1,2-bis(*tert*-butyldisulfaneyl)ethyl)benzyl (2*R*)-2-(4-isobutylphenyl)propanoate (3q)



Yellow oily liquid (135.7 mg, 60%); TLC, $R_f = 0.40$ (PE:EA = 20:1, v/v); ^1H NMR (400 MHz, CDCl_3) δ 7.22-7.20 (m, 5H), 7.11 (s, 3H), 5.10 (d, $J = 2.7$ Hz, 2H), 4.17 (dd, $J = 10.9, 4.5$ Hz, 1H), 3.77 (s, 1H), 3.49 (dd, $J = 13.1, 4.5$ Hz, 1H), 3.19-3.12 (m, 1H), 2.47 (s, 2H), 1.86 (s, 1H), 1.52 (s, 3H), 1.35 (d, $J = 3.8$ Hz, 18H). ^{13}C NMR (101 MHz, CDCl_3) δ 174.6, 140.7, 138.6, 137.7, 136.0, 129.5, 128.5, 128.3, 127.3, 66.0, 55.0, 48.4, 48.0, 45.2, 45.2, 35.0, 31.6, 30.3, 30.2, 22.5, 18.6. HRMS (ESI-TOF) m/z calcd for $\text{C}_{30}\text{H}_{44}\text{O}_2\text{S}_4$ [M^+]: 565.2302, found 565.2304.

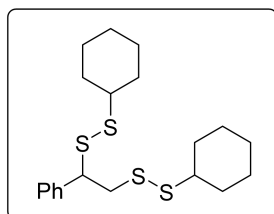
(8*S*,9*R*,13*R*,14*R*,17*R*)-3-((4-(1,2-bis(*tert*-butyldisulfaneyl)ethyl)benzyl)oxy)-13-methyl-7,8,9,11,12,13,14,15,16,17-decahydro-6*H*-cyclopenta[*a*]phenanthren-17-ol (3r)



Yellow oily liquid (146.5 mg, 58%); TLC, $R_f = 0.40$ (PE:EA = 20:1, v/v); ^1H NMR (400 MHz, CDCl_3) δ 7.23 (d, $J = 4.3$ Hz, 5H), 7.11 (s, 2H), 5.10 (d, $J = 2.4$ Hz, 2H), 4.18 (dd, $J = 10.9, 4.5$ Hz, 1H), 3.76 (q, $J = 7.2$ Hz, 2H), 3.50 (dd, $J = 13.1, 4.5$ Hz, 1H), 3.20-3.10 (m, 1H), 2.46 (d, $J = 7.1$ Hz, 3H), 1.87 (p, $J = 6.7$ Hz, 2H), 1.52 (d, $J = 7.2$ Hz, 6H), 1.36 (d, $J = 3.8$ Hz, 18H), 0.93 (s, 6H). ^{13}C NMR (101 MHz, CDCl_3) δ 174.6, 140.7, 138.6, 137.7, 136.0, 129.5, 128.4, 128.2, 127.3,

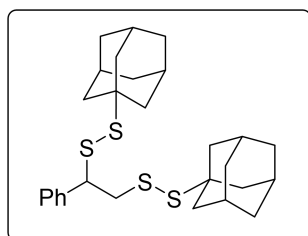
119.2, 114.3, 66.0, 54.9, 48.4, 48.0, 45.2, 45.1, 31.6, 31.5, 30.3, 30.2, 30.2, 30.1, 30.0, 22.5, 18.6, 18.5. HRMS (ESI-TOF) m/z calcd for $C_{35}H_{50}O_2S_4$ [M^+]: 631.2772, found 631.2775.

2,2'-(1-phenylethane-1,2-diyl)bis(1-cyclohexyldisulfane) (3s)



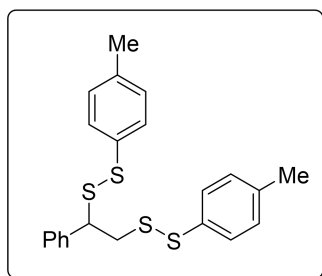
Yellow oily liquid (135.7 mg, 85%); TLC, R_f = 0.40 (PE:EA = 50:1, v/v); 1H NMR (400 MHz, $CDCl_3$) δ 7.32 (q, J = 6.8 Hz, 5H), 4.19 (dd, J = 10.5, 5.1 Hz, 1H), 3.48 (dd, J = 13.3, 5.0 Hz, 1H), 3.21 (dd, J = 13.3, 10.4 Hz, 1H), 2.65 (td, J = 10.8, 3.8 Hz, 1H), 2.41-2.33 (m, 1H), 2.03-1.91 (m, 4H), 1.81-1.72 (m, 4H), 1.64-1.57 (m, 2H), 1.32-1.18 (m, 10H). ^{13}C NMR (101 MHz, $CDCl_3$) δ 139.1, 128.7, 128.5, 128.1, 54.7, 49.6, 49.6, 44.5, 33.0, 33.0, 32.8, 26.2, 25.8, 25.7. HRMS (ESI-TOF) m/z calcd for $C_{20}H_{30}S_4$ [M^+]: 399.1309, found 399.1306.

2,2'-(1-phenylethane-1,2-diyl)bis(1-((3*s*,5*s*,7*s*)-adamantan-1-yl)disulfane) (3t)



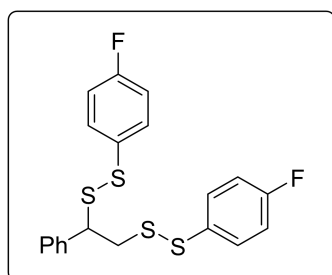
White oily liquid (157.0 mg, 78%); TLC, R_f = 0.40 (PE:EA = 50:1, v/v); 1H NMR (400 MHz, $CDCl_3$) δ 7.35-7.32 (m, 5H), 4.16 (dd, J = 10.9, 4.5 Hz, 1H), 3.50 (dd, J = 13.0, 4.4 Hz, 1H), 3.16 (dd, J = 13.0, 11.0 Hz, 1H), 2.09 (s, 6H), 1.89 (s, 7H), 1.70 (s, 6H). ^{13}C NMR (101 MHz, $CDCl_3$) δ 138.9, 128.8, 128.4, 128.1, 55.6, 49.9, 49.6, 45.8, 42.9, 42.8, 36.2, 36.2, 30.0, 29.9. HRMS (ESI-TOF) m/z calcd for $C_{28}H_{38}S_4$ [M^+]: 503.1935, found 503.1933.

2,2'-(1-phenylethane-1,2-diyl)bis(1-(*p*-tolyl)disulfane) (3u)



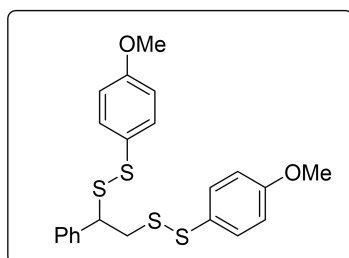
Yellow oily liquid (129.5 mg, 78%); TLC, R_f = 0.40 (PE:EA = 50:1, v/v); $^1\text{H NMR}$ (400 MHz, CDCl_3) δ 7.36 (t, J = 7.8 Hz, 5H), 7.32-7.27 (m, 4H), 7.14 (t, J = 8.1 Hz, 4H), 4.12 (dd, J = 10.8, 4.5 Hz, 1H), 3.82 (dd, J = 13.6, 4.5 Hz, 1H), 3.40 (dd, J = 13.5, 10.8 Hz, 1H), 2.40 (d, J = 5.9 Hz, 6H). $^{13}\text{C NMR}$ (101 MHz, CDCl_3) δ 138.2, 137.4, 136.7, 133.8, 131.6, 130.8, 129.8, 129.8, 128.9, 128.8, 128.5, 128.2, 54.1, 39.1, 21.2, 21.2. HRMS (ESI-TOF) m/z calcd for $\text{C}_{22}\text{H}_{22}\text{S}_4$ [M^+]: 415.0683, found 415.0681.

2,2'-(1-phenylethane-1,2-diyl)bis(1-(4-fluorophenyl)disulfane) (3v)



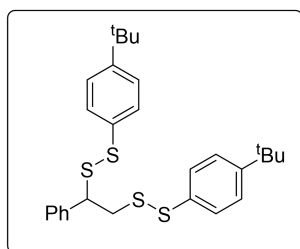
Yellow oily liquid (128.6 mg, 76%); TLC, R_f = 0.40 (PE:EA = 50:1, v/v); $^1\text{H NMR}$ (400 MHz, CDCl_3) δ 7.40 (ddt, J = 6.8, 4.4, 2.1 Hz, 7H), 7.33-7.30 (m, 2H), 7.09-7.04 (m, 4H), 4.11 (dd, J = 10.6, 4.8 Hz, 1H), 3.77 (dd, J = 13.7, 4.8 Hz, 1H), 3.50-3.44 (m, 1H). $^{13}\text{C NMR}$ (101 MHz, CDCl_3) δ 163.5 (J = 16.2 Hz), 161.1 (J = 15.2 Hz), 137.9, 133.5 (d, J = 8.1 Hz), 132.2 (J = 4.0 Hz), 130.9 (J = 8.1 Hz), 130.1 (J = 3.1 Hz), 128.8, 128.4, 128.1, 116.3 (J = 3.0 Hz), 116.1 (J = 4.0 Hz), 54.4, 39.9. HRMS (ESI-TOF) m/z calcd for $\text{C}_{20}\text{H}_{16}\text{OS}_4$ [M^+]: 423.0181, found 423.0183.

2,2'-(1-phenylethane-1,2-diyl)bis(1-(4-methoxyphenyl)disulfane) (3w)



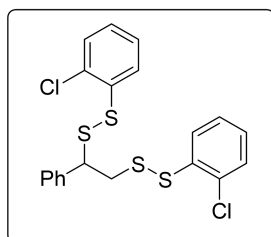
Yellow oily liquid (148.4 mg, 83%); TLC, R_f = 0.40 (PE:EA = 10:1, v/v); **^1H NMR** (400 MHz, CDCl_3) δ 7.46-7.39 (m, 3H), 7.36-7.27 (m, 7H), 6.93-6.82 (m, 3H), 4.63 (dd, J = 9.7, 3.4 Hz, 1H), 3.81 (s, 6H), 3.22-3.18 (m, 1H), 3.00-2.95 (m, 1H). **^{13}C NMR** (101 MHz, CDCl_3) δ 159.5, 142.2, 134.1, 128.6, 128.0, 126.0, 124.8, 114.9, 71.4, 55.5, 46.2. HRMS (ESI-TOF) m/z calcd for $\text{C}_{22}\text{H}_{22}\text{O}_2\text{S}_4$ [M^+]: 447.0581, found 447.0580.

2,2'-(1-phenylethane-1,2-diyl)bis(1-(4-(*tert*-butyl)phenyl)disulfane) (3x)



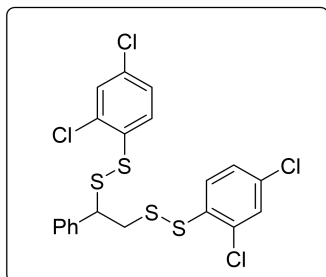
Yellow oily liquid (145.8 mg, 73%); TLC, R_f = 0.30 (PE:EA = 50:1, v/v); **^1H NMR** (400 MHz, CDCl_3) δ 7.34-7.26 (m, 5H), 7.24 (d, J = 3.3 Hz, 2H), 7.22 (dd, J = 5.0, 3.3 Hz, 6H), 4.09 (dd, J = 10.9, 4.5 Hz, 1H), 3.77 (dd, J = 13.6, 4.5 Hz, 1H), 3.34 (dd, J = 13.4, 10.9 Hz, 1H), 1.28 (s, 9H), 1.27 (s, 9H). **^{13}C NMR** (101 MHz, CDCl_3) δ 150.5, 149.7, 138.2, 133.8, 131.9, 131.3, 130.0, 128.7, 128.4, 128.2, 126.1, 126.1, 54.3, 38.8, 34.6, 34.5, 31.4, 31.4. HRMS (ESI-TOF) m/z calcd for $\text{C}_{28}\text{H}_{34}\text{S}_4$ [M^+]: 499.1622, found 499.1623.

2,2'-(1-phenylethane-1,2-diyl)bis(1-(2-chlorophenyl)disulfane) (3y)



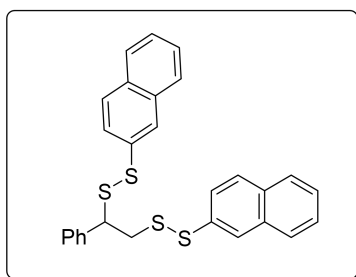
Yellow oily liquid (143.8 mg, 79%); TLC, R_f = 0.40 (PE:EA = 50:1, v/v); **^1H NMR** (400 MHz, CDCl_3) δ 7.64 (dd, J = 7.9, 1.6 Hz, 1H), 7.34-7.28 (m, 7H), 7.25-7.19 (m, 2H), 7.16-7.07 (m, 3H), 4.09 (dd, J = 10.6, 4.6 Hz, 1H), 3.79 (dd, J = 13.6, 4.6 Hz, 1H), 3.47 (dd, J = 13.5, 10.7 Hz, 1H). **^{13}C NMR** (101 MHz, CDCl_3) δ 137.6, 135.5, 134.7, 134.5, 132.0, 130.8, 130.0, 129.8, 129.6, 129.0, 128.7, 128.3, 127.8, 127.4, 127.3, 127.2, 54.1, 37.3. HRMS (ESI-TOF) m/z calcd for $\text{C}_{20}\text{H}_{16}\text{Cl}_2\text{S}_4$ [M^+]: 454.9590, found 454.9592.

2,2'-(1-phenylethane-1,2-diyl)bis(1-(2,4-dichlorophenyl)disulfane) (3z)



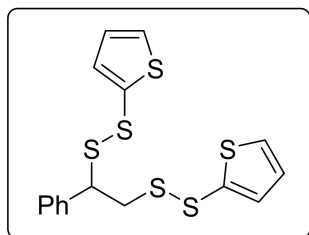
Yellow oily liquid (146.4 mg, 70%); TLC, R_f = 0.40 (PE:EA = 50:1, v/v); $^1\text{H NMR}$ (400 MHz, CDCl_3) δ 7.41 (d, J = 2.2 Hz, 1H), 7.37 (s, 1H), 7.28 (d, J = 5.6 Hz, 5H), 7.19 (d, J = 8.3 Hz, 1H), 7.11-7.07 (m, 3H), 4.39 (dd, J = 9.5, 5.4 Hz, 1H), 3.48-3.38 (m, 2H). $^{13}\text{C NMR}$ (101 MHz, CDCl_3) δ 138.6, 138.1, 136.2, 135.2, 134.6, 133.3, 133.0, 132.1, 131.8, 130.0, 129.9, 128.9, 128.4, 128.1, 127.6, 127.5, 51.6, 39.0. HRMS (ESI-TOF) m/z calcd for $\text{C}_{20}\text{H}_{14}\text{Cl}_4\text{S}_4$ [M^+]: 522.8811, found 522.8814.

2,2'-(1-phenylethane-1,2-diyl)bis(1-(naphthalen-2-yl)disulfane) (3aa)



Yellow oily liquid (128.6 mg, 66%); TLC, R_f = 0.40 (PE:EA = 50:1, v/v); $^1\text{H NMR}$ (400 MHz, CDCl_3) δ 7.80-7.59 (m, 7H), 7.52-7.41 (m, 7H), 7.31 (d, J = 5.3 Hz, 4H), 7.24 (s, 1H), 4.41 (dd, J = 10.3, 4.7 Hz, 1H), 3.65 (dd, J = 13.8, 4.7 Hz, 1H), 3.46 (dd, J = 13.8, 10.3 Hz, 1H). $^{13}\text{C NMR}$ (101 MHz, CDCl_3) δ 139.6, 133.8, 133.7, 132.8, 132.6, 132.0, 131.9, 131.7, 130.1, 128.8, 128.7, 128.6, 128.3, 128.1, 128.0, 128.0, 127.8, 127.8, 127.7, 127.3, 126.7, 126.6, 126.5, 126.0, 52.4, 39.6. HRMS (ESI-TOF) m/z calcd for $\text{C}_{28}\text{H}_{22}\text{S}_4$ [M^+]: 487.0683, found 487.0684.

2,2'-(1-phenylethane-1,2-diyl)bis(disulfanediyl)dithiophene (3ab)



Yellow oily liquid (95.7 mg, 60%); TLC, R_f = 0.40 (PE:EA = 50:1, v/v); **^1H NMR** (400 MHz, CDCl_3) δ 7.35-7.32 (m, 3H), 7.30 (t, J = 2.3 Hz, 2H), 7.19 (dd, J = 7.7, 1.8 Hz, 2H), 7.00 (dd, J = 3.5, 1.2 Hz, 1H), 6.97-6.90 (m, 3H), 4.15 (dd, J = 9.8, 5.6 Hz, 1H), 3.42 (dd, J = 13.5, 5.6 Hz, 1H), 3.32 (dd, J = 13.4, 9.9 Hz, 1H). **^{13}C NMR** (101 MHz, CDCl_3) δ 139.0, 136.0, 134.2, 133.4, 131.5, 130.8, 129.8, 128.6, 128.3, 128.0, 127.6, 127.6, 54.9, 43.4. HRMS (ESI-TOF) m/z calcd for $\text{C}_{16}\text{H}_{14}\text{S}_6$ [M^+]: 398.9498, found 398.9498.

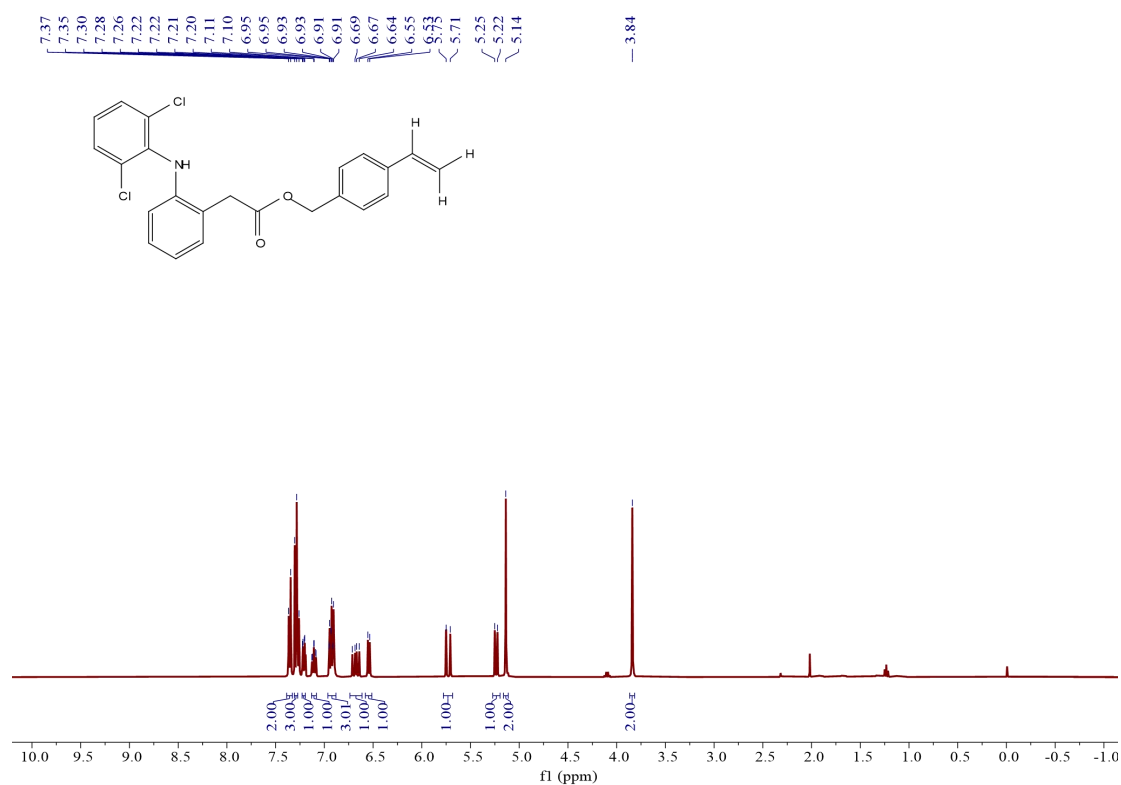
7. References

- [1] (a) Harpp, D. N.; Derbesy, G. A simple method to prepare unsymmetrical di- tri- and tetrasulfides. *Tetrahedron Lett.* **1994**, *35*, 5381-5384. (b) Zysman-Colman, E.; Harpp, D. N. Optimization of the synthesis of symmetric aromatic tri- and tetrasulfides. *J. Org. Chem.* **2003**, *68*, 2487-2489. (c) Wu, Z.; Pratt, D. A. Radical Substitution Provides a Unique Route to Disulfides. *J. Am. Chem. Soc.* **2020**, *142*, 10284-10290.
- [2] Curran, D. T.; Szydło, M.; Müller-Bunz, H.; Nikitin, K. and Byrne, P. A. Direct synthesis of ethers from alcohols & aldehydes enabled by an oxocarbenium ion interception strategy. *Chem. Sci.* **2025**, *16*, 6991-7003.
- [3] (a) Li, X. H.; Cui, W. W.; Deng, Q. R.; Song, X. Y.; Lv, J. and Yang, D. S. Three-component reaction access to S-alkyl dithiocarbamates under visible-light irradiation conditions in water. *Green Chem.* **2022**, *24*, 1302-1307. (b) Xu, J.; Liu, L.; Yan, Z.-C.; Liu, Y.; Qin, L.; Deng, N. and Xu, H.-J. Photocatalyzed hydroxyalkylation of N-heteroaromatics with aldehydes in the aqueous phase. *Green Chem.* **2023**, *25*, 2268-2273. (c) Tian, Y. M.; Silva, W.; Gschwind, R. M.; König, B. Accelerated photochemical reactions at oil-water interface exploiting melting point depression. *Science.* **2024**, *16*, 750-756. (d) Kim, S. B.; Kim D. H. & Bae, H. Y. “On-Water” accelerated dearomative cycloaddition via aquaphotocatalysis. *Nat. Commun.* **2024**, *8*, 3876. (e) Meng, J. I.; Jia, Y. X.; Li, C. L. and Jiang, X. F. From Aldehyde to Ketone via Water-Accelerated Molybdenum-Photocatalysis. *ChemCatChem.* **2024**, *16*, NO. e202400723.
- [4] Dong, Q.-R.; Wang, Y.-S.; Zhang, J.; Chang, H.-H.; Tian, J. and Gao, W.-C. Synthesis of Unsymmetrical Disulfides via Photocatalytic Hydrodisulfuration. *ACS Catal.* **2024**, *14*, 18237-18246.
- [5] Wang, F.; Chen, Y.; Rao, W. D.; Ackermann, L. & Wang, S.-Y. Efficient preparation of unsymmetrical disulfides by nickel-catalyzed reductive coupling strategy. *Nat Commun.* **2022**, *13*, 2588.
- [6] Jiang, Y.-X.; Tang, S.-B.; Luo, Y.-Y.; Wang, Z.-X.; Li, Z.-K. and Su, J. Photocatalytic cleavage of unactivated C(sp³)–H bonds via the uranyl cation: enabling the allylation of alkanes. *Org. Chem. Front.*, **2025**, *12*, 5844.

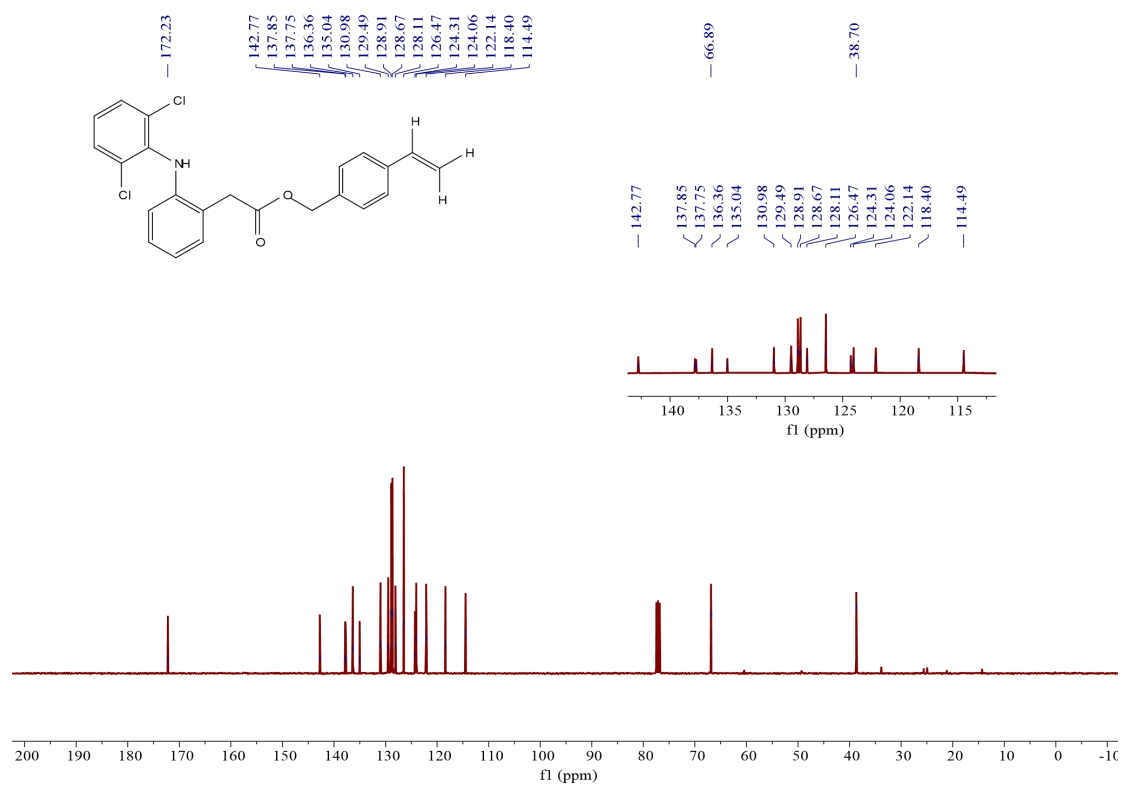
- [7] Montalti, M.; Credi, A.; Prodi, L.; Gandolfi, M. T. Handbook of Photochemistry. *CRC Press*, Taylor & Francis Group: **2006**.
- [8] (a) Wu, M.; Bhargav, A.; Cui, Y.; Siegel, A.; Agarwal, M.; Ma, Y. and Fu, Y. Z. Highly Reversible Diphenyl Trisulfide Catholyte for Rechargeable Lithium Batteries. *ACS Energy Lett.* **2016**, *1*, 1221-1226. (b) Bhargav, A.; Bell, M. E.; Karty, J.; Cui, Y. and Fu, Y. Z. A Class of Organopolysulfides As Liquid Cathode Materials for High-Energy-Density Lithium Batteries. *ACS Appl. Mater. Interfaces.* **2018**, *10*, 21084-21090. (c) Wang, D.-Y.; Si, Y. B.; Guo W. & Fu, Y. Z. Electrosynthesis of 1,4-bis(diphenylphosphanyl) tetrasulfide via sulfur radical addition as cathode material for rechargeable lithium battery. *Nat. Commun.* **2021**, *12*, 322.

NMR Spectra

8. NMR Spectra

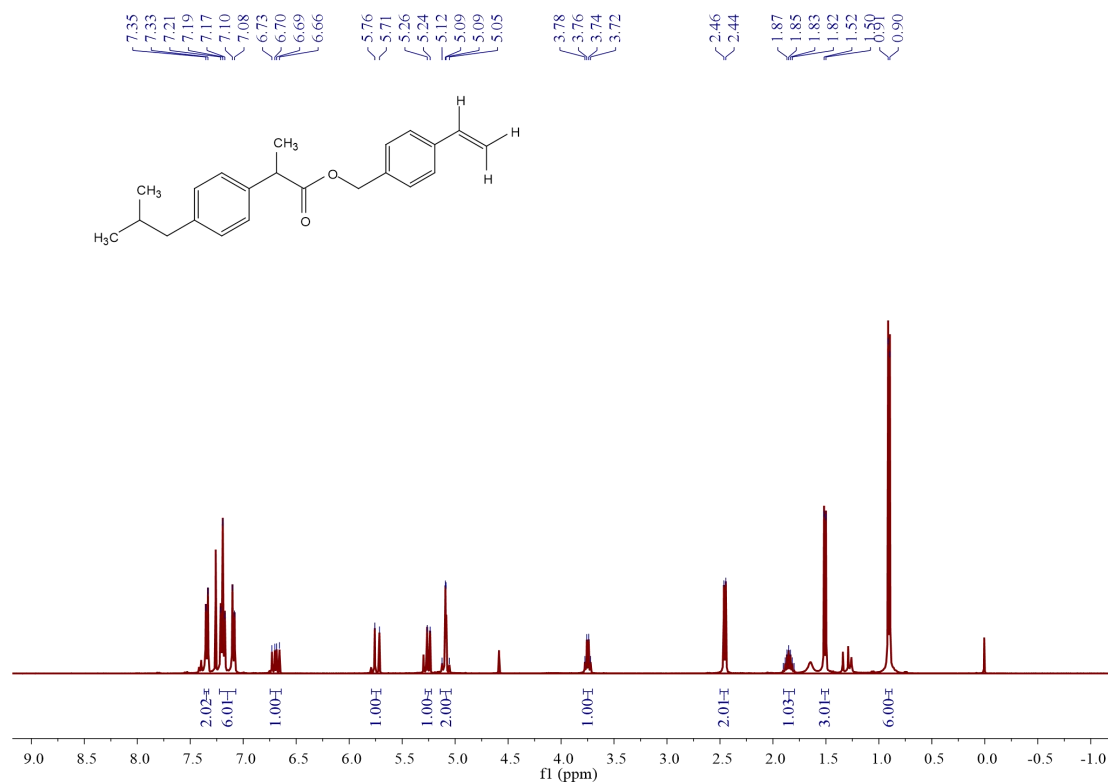


¹H NMR spectra of 1p (400 MHz, CDCl₃)

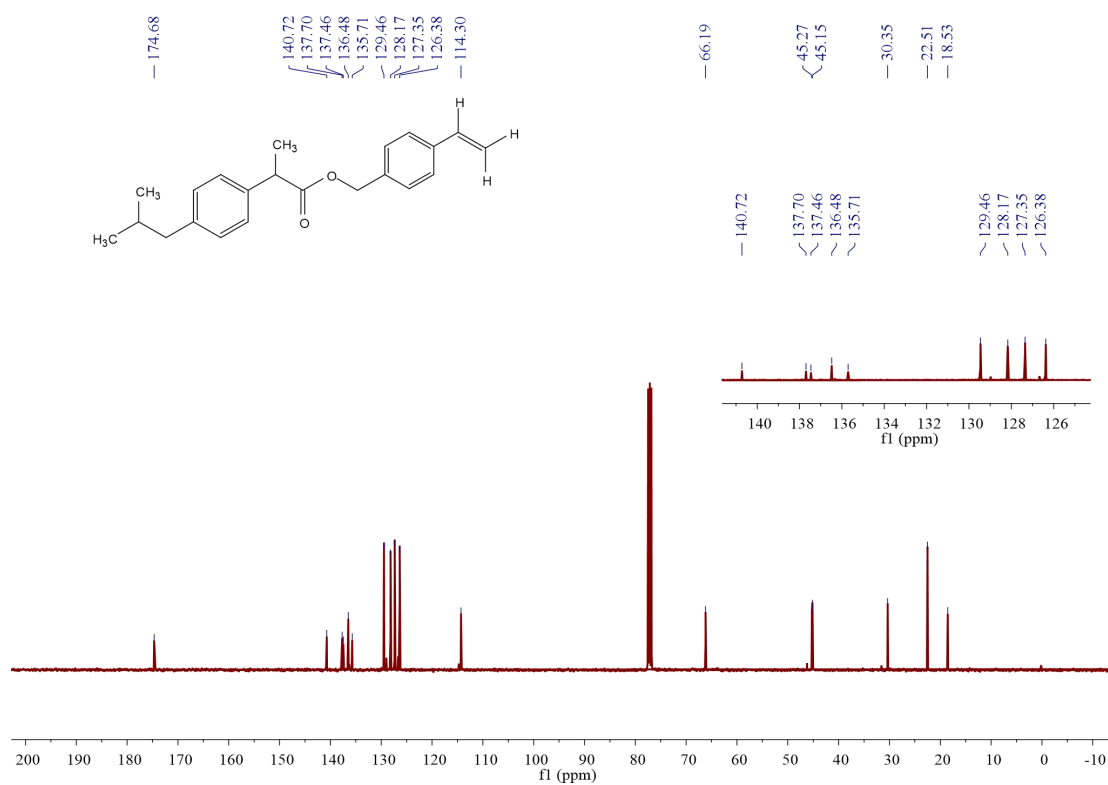


¹³C NMR spectra of 1p (101 MHz, CDCl₃)

NMR Spectra

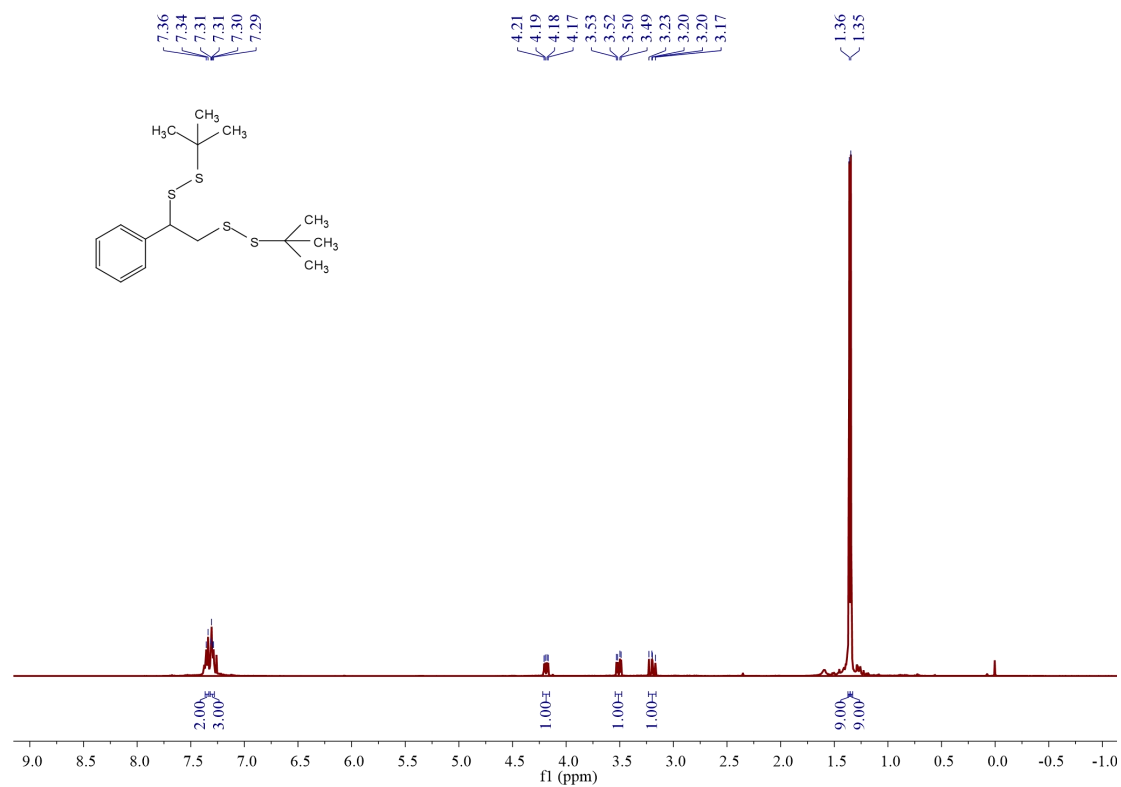


¹H NMR spectra of 1q (400 MHz, CDCl₃)

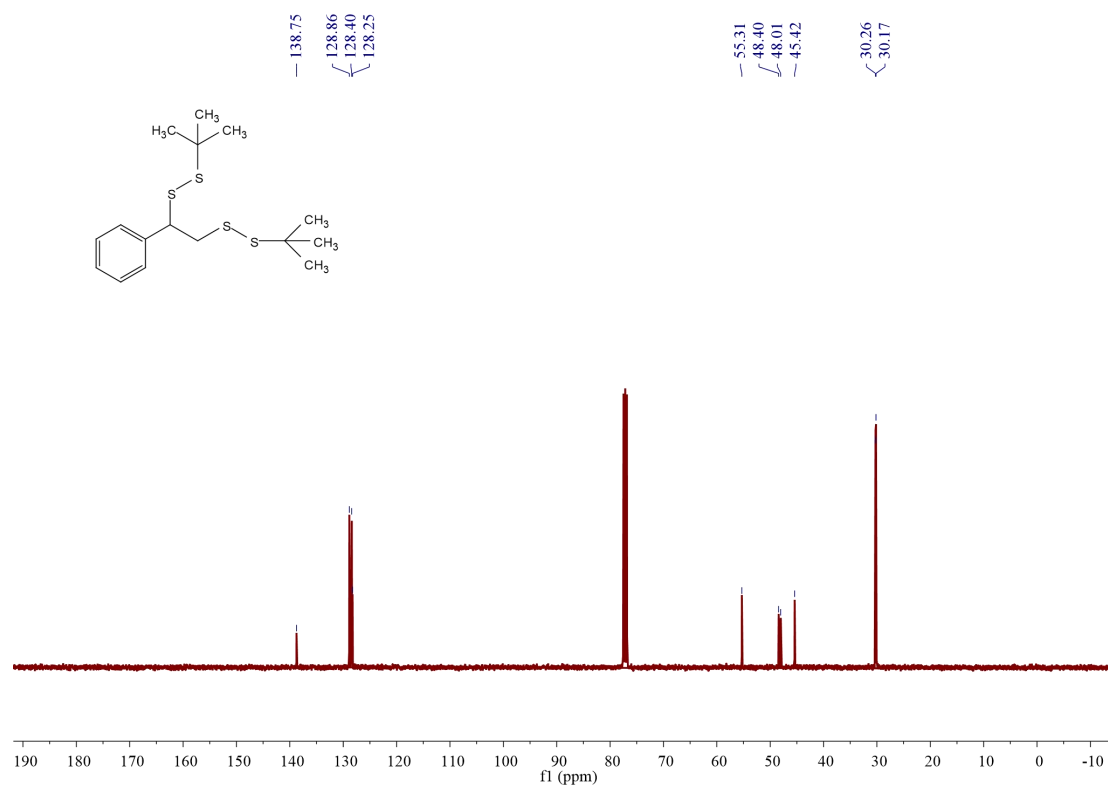


¹³C NMR spectra of 1q (101 MHz, CDCl₃)

NMR Spectra

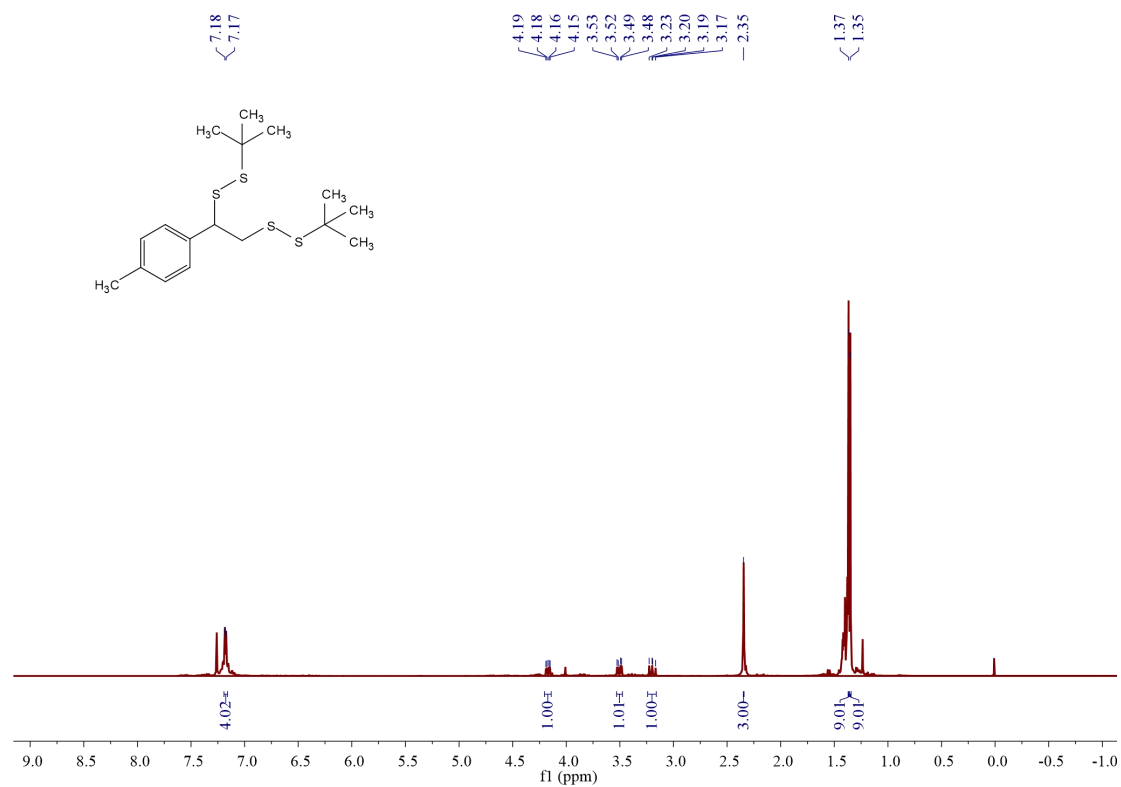


¹H NMR spectra of 3a (400 MHz, CDCl₃)

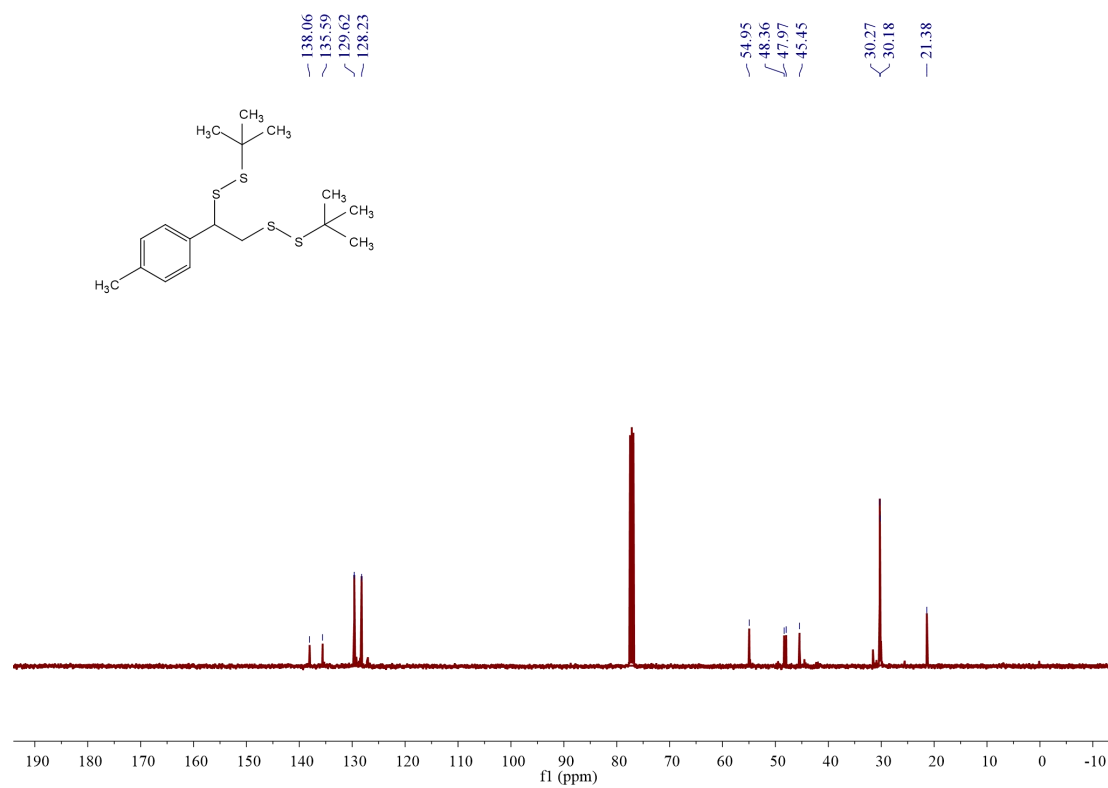


¹³C NMR spectra of 3a (101 MHz, CDCl₃)

NMR Spectra

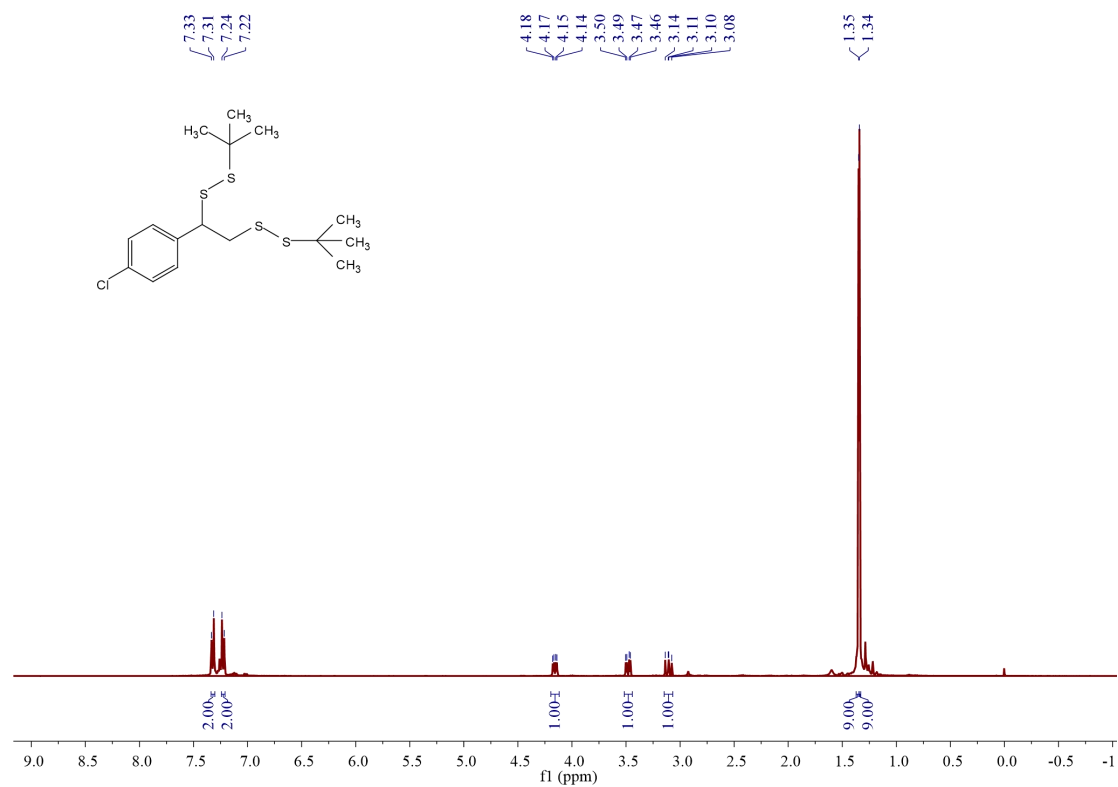


^1H NMR spectra of 3b (400 MHz, CDCl_3)

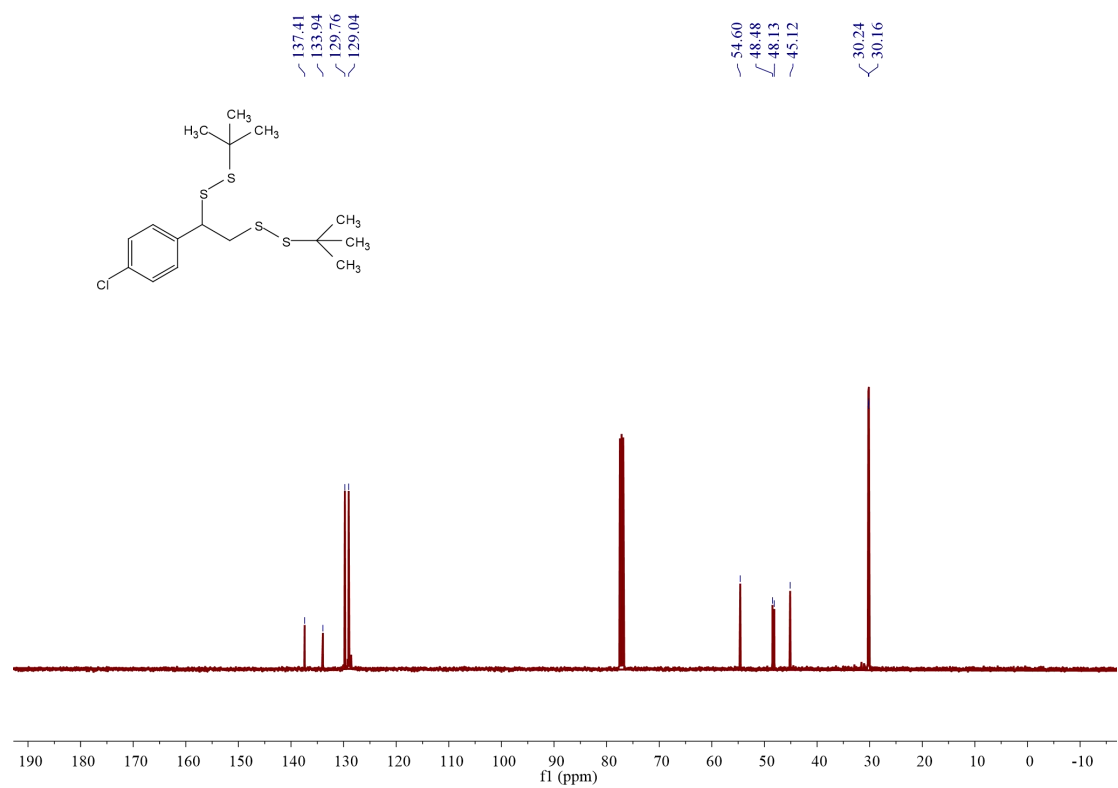


^{13}C NMR spectra of 3b (101 MHz, CDCl_3)

NMR Spectra

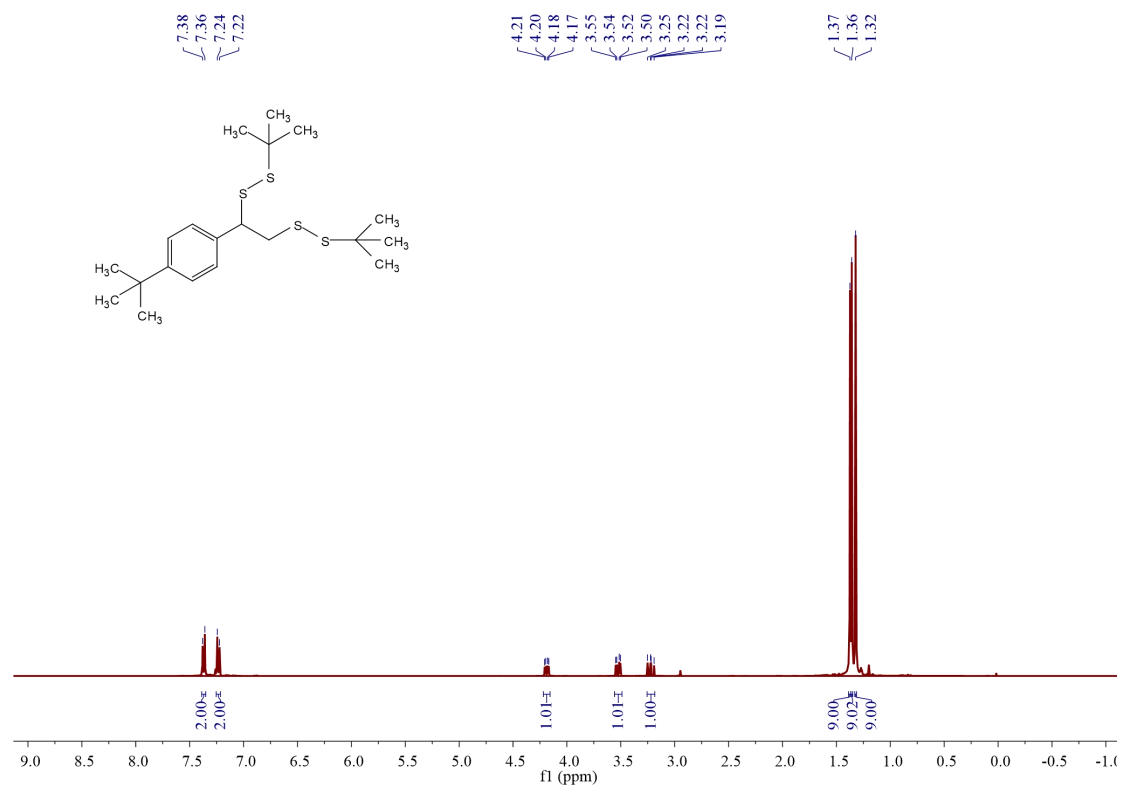


¹H NMR spectra of 3c (400 MHz, CDCl₃)

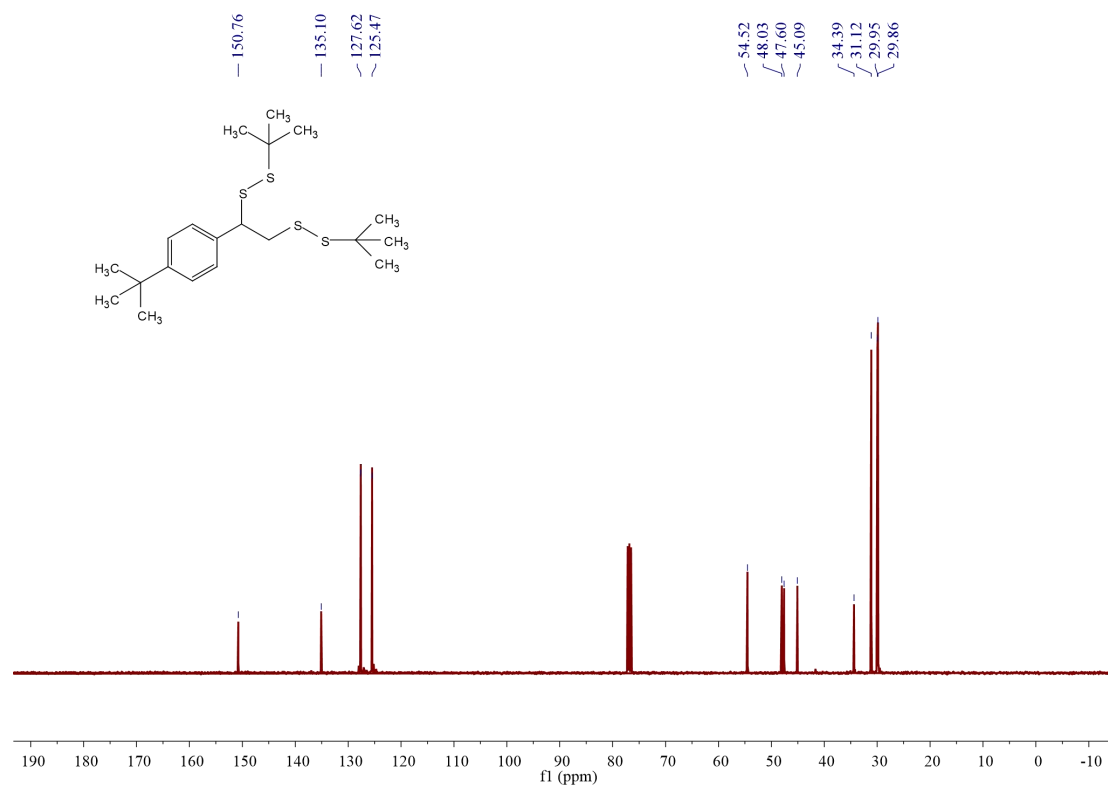


¹³C NMR spectra of 3c (101 MHz, CDCl₃)

NMR Spectra

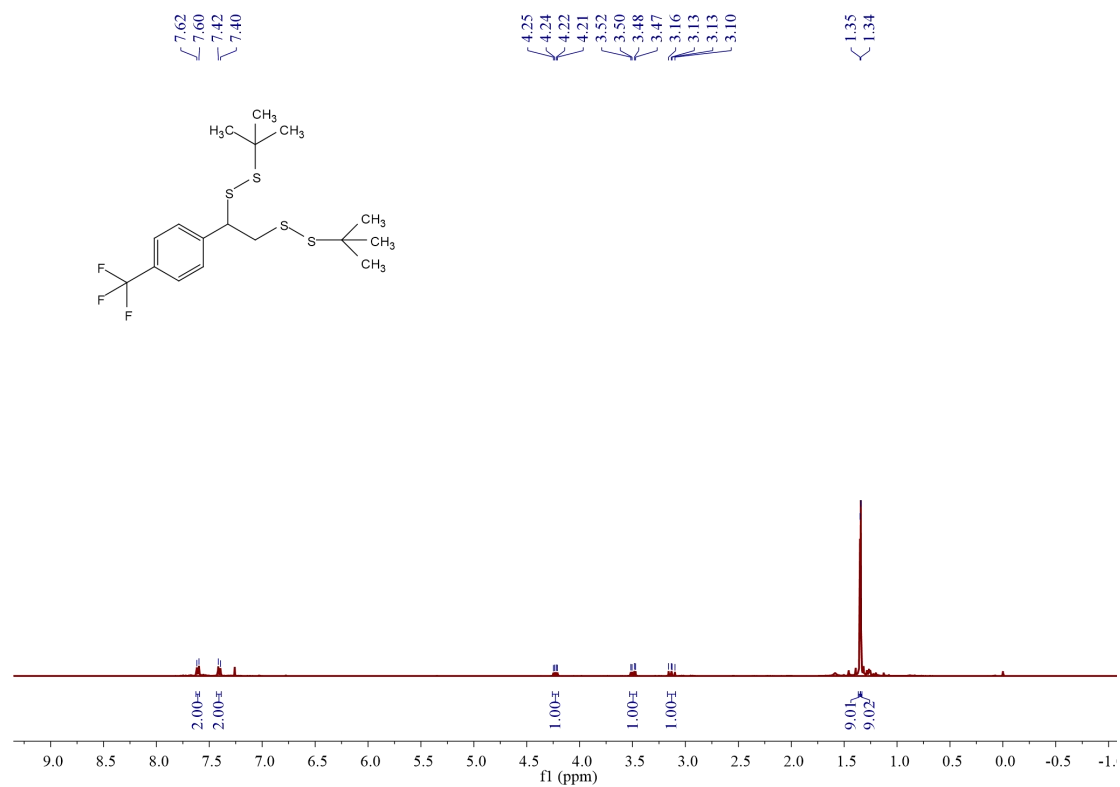


¹H NMR spectra of 3d (400 MHz, CDCl₃)

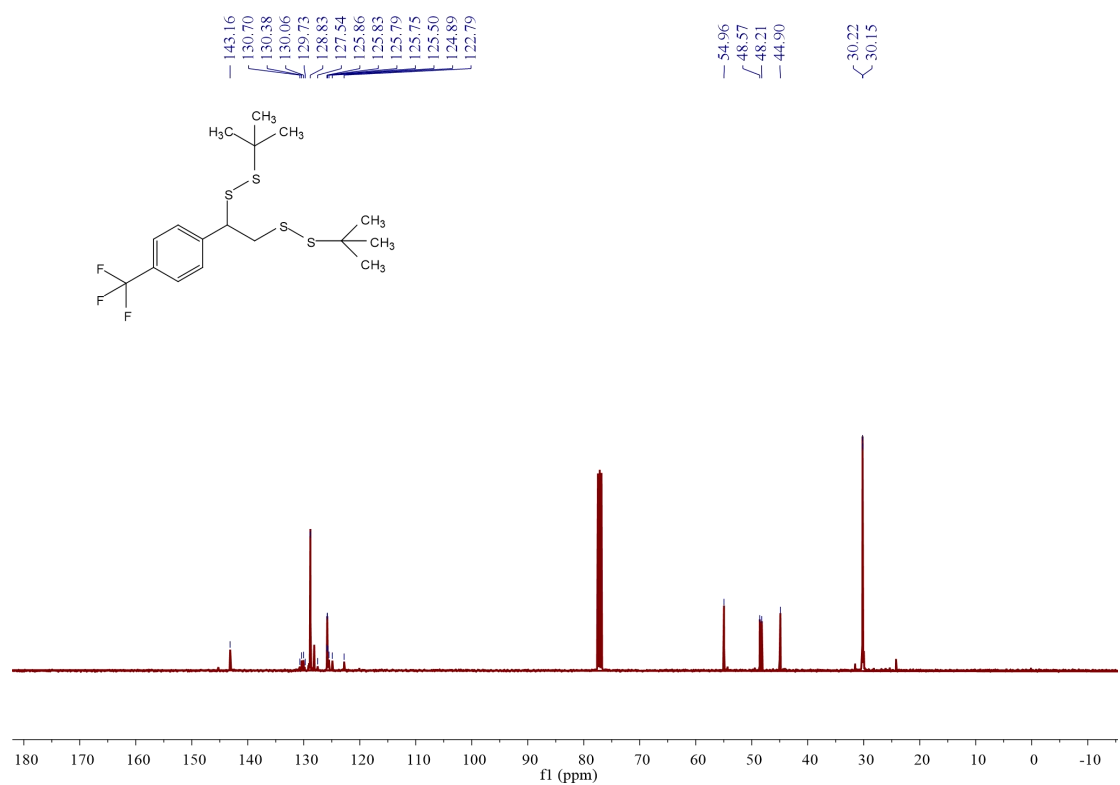


¹³C NMR spectra of 3d (101 MHz, CDCl₃)

NMR Spectra

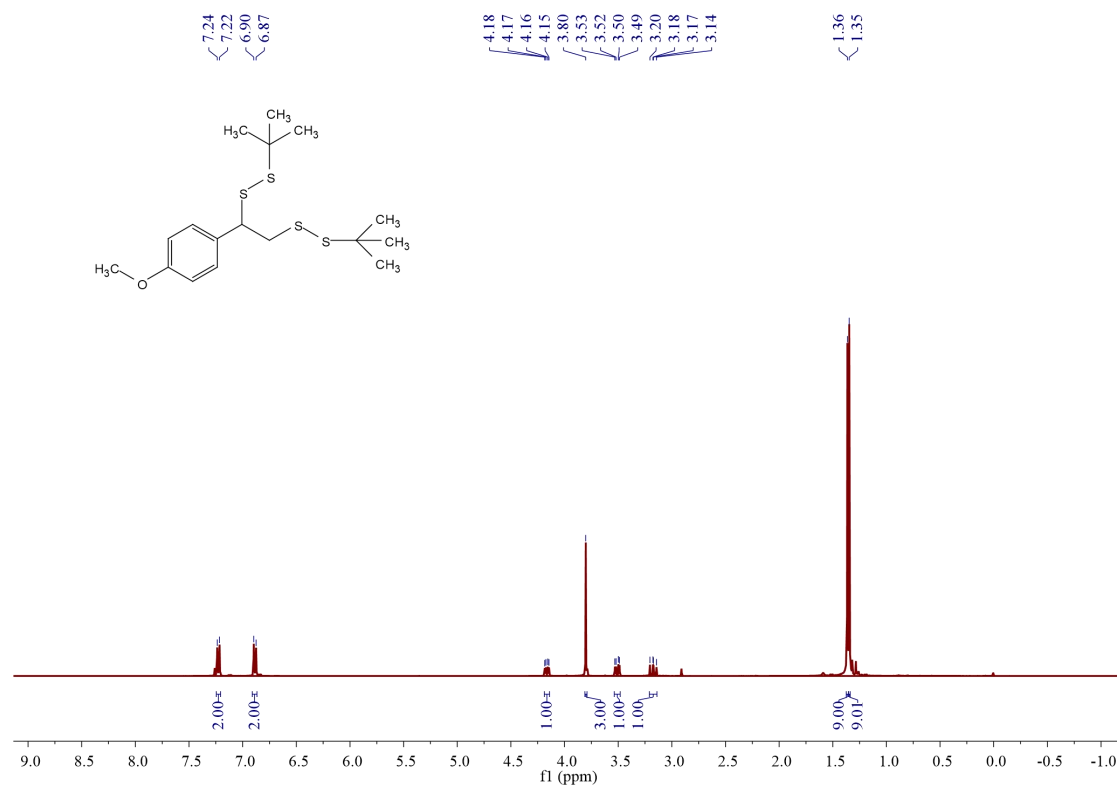


^1H NMR spectra of **3e** (400 MHz, CDCl_3)

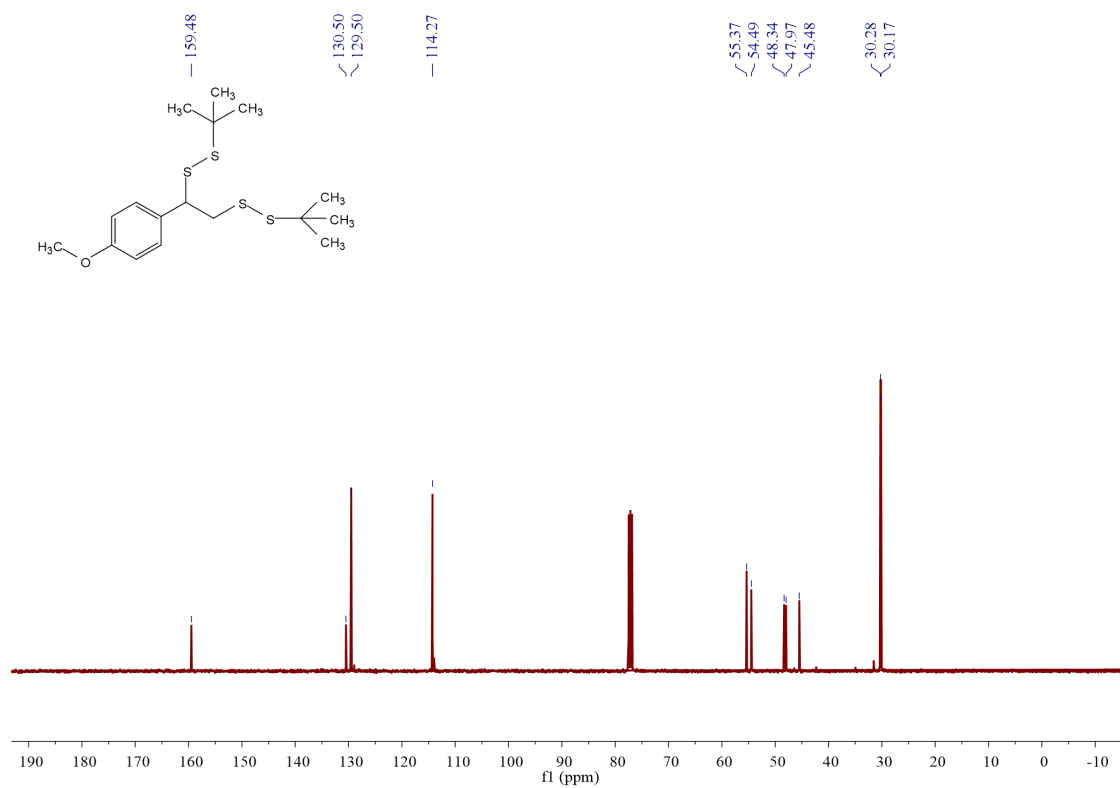


^{13}C NMR spectra of **3e** (101 MHz, CDCl_3)

NMR Spectra

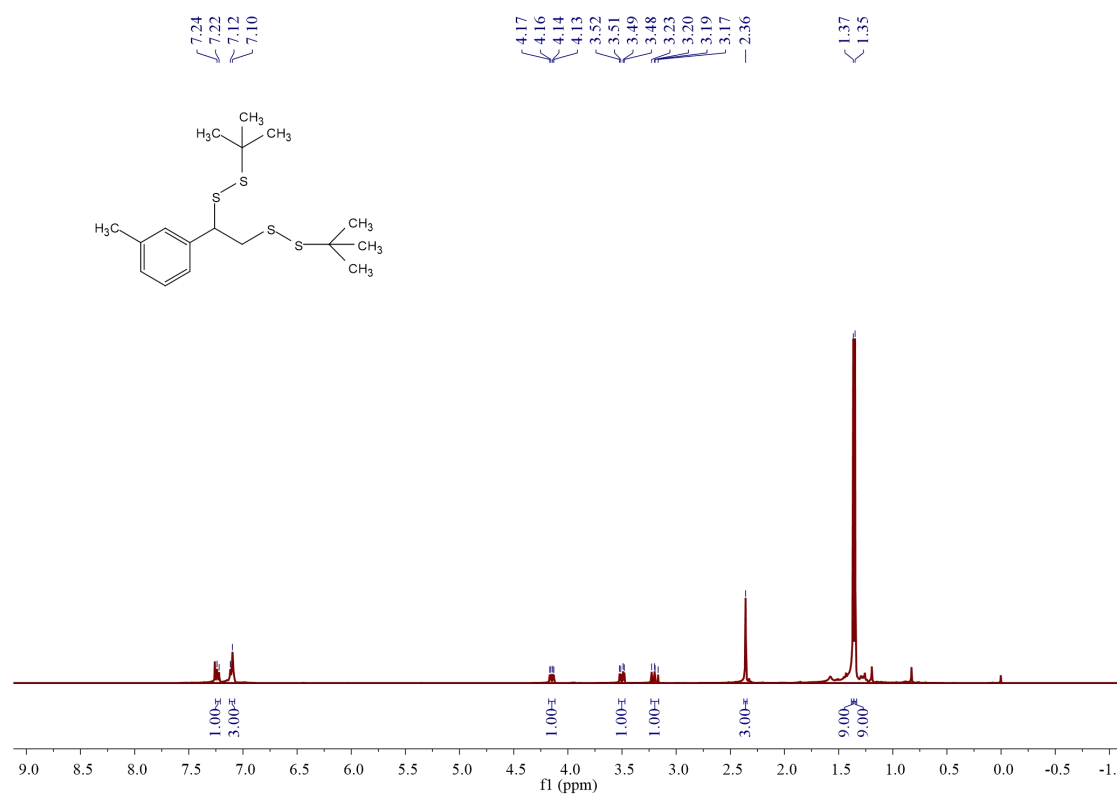


¹H NMR spectra of 3f (400 MHz, CDCl₃)

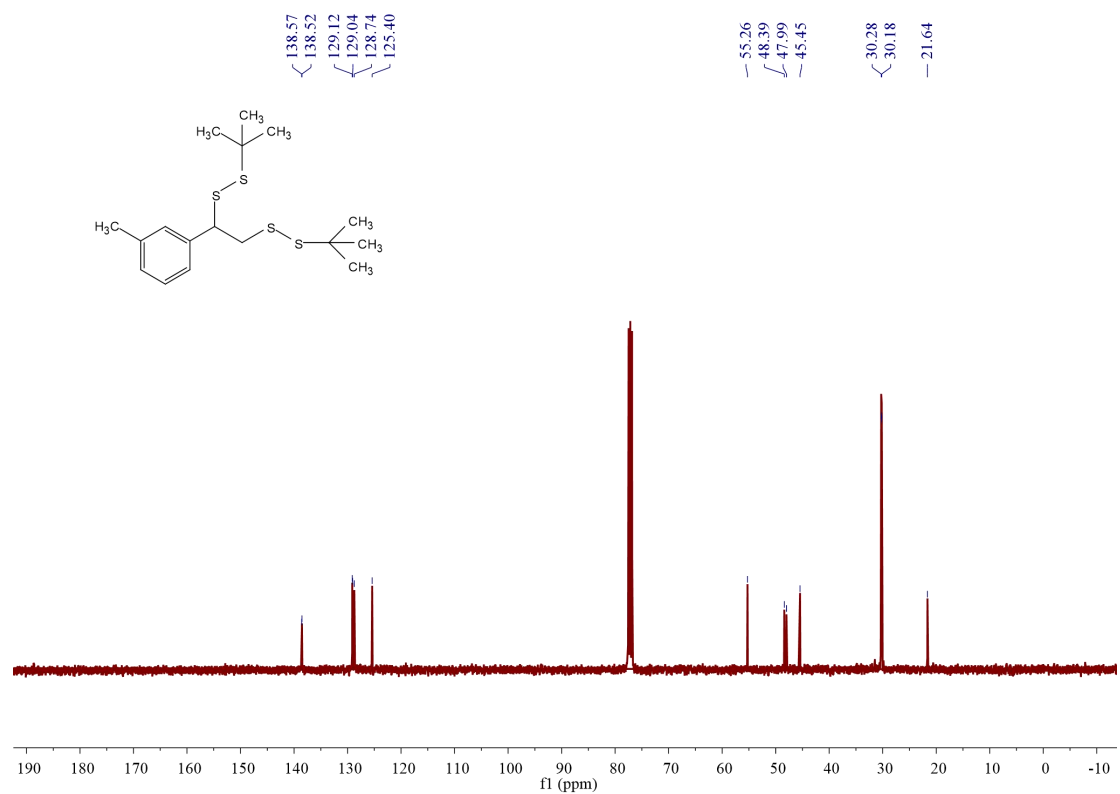


¹³C NMR spectra of 3f (101 MHz, CDCl₃)

NMR Spectra

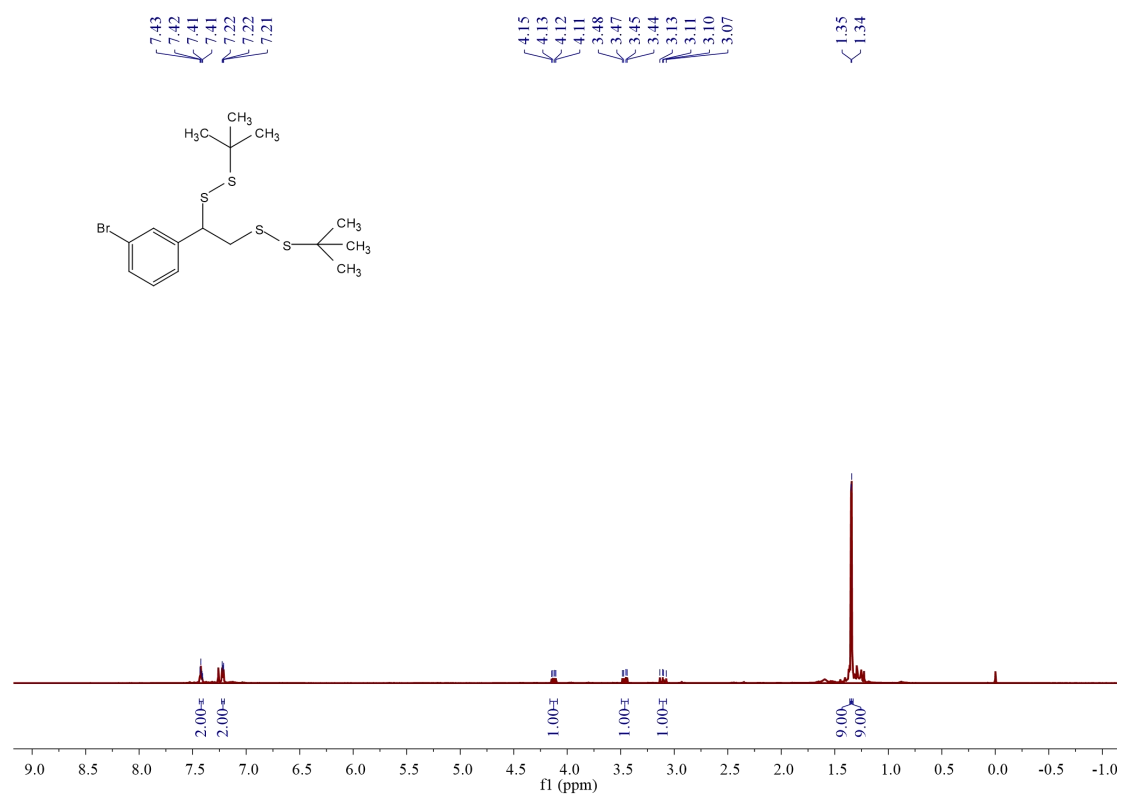


¹H NMR spectra of 3g (400 MHz, CDCl₃)

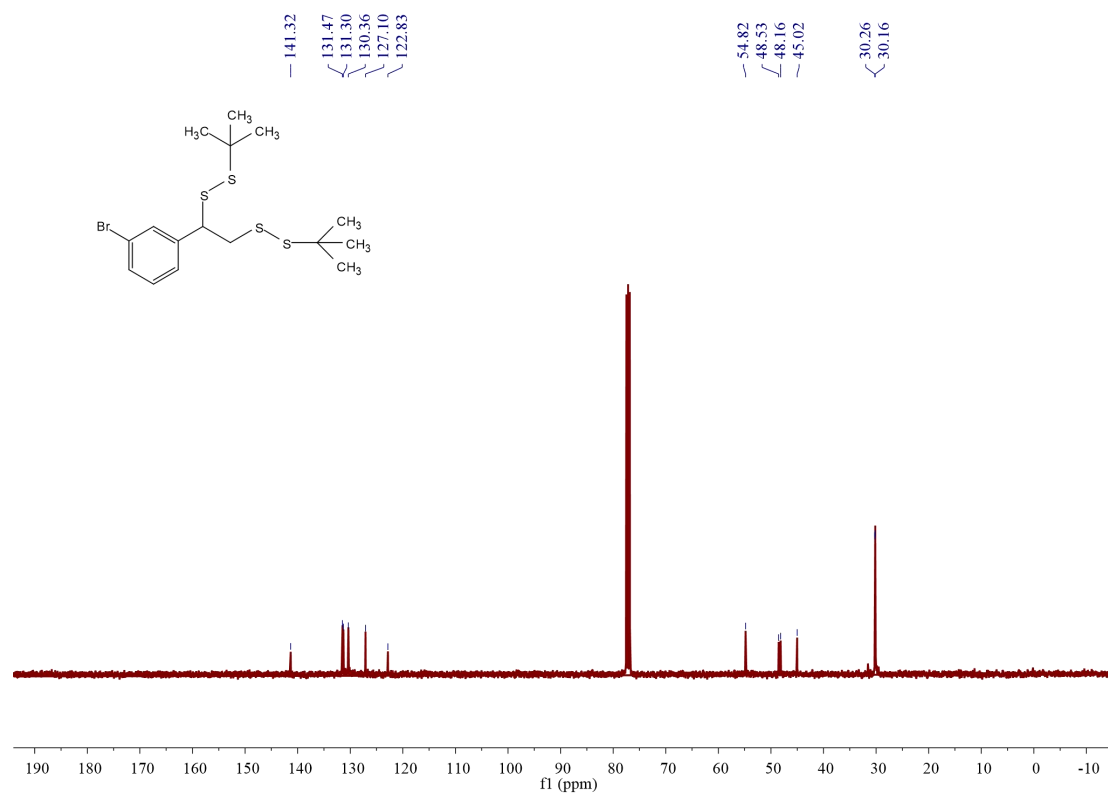


¹³C NMR spectra of 3g (101 MHz, CDCl₃)

NMR Spectra

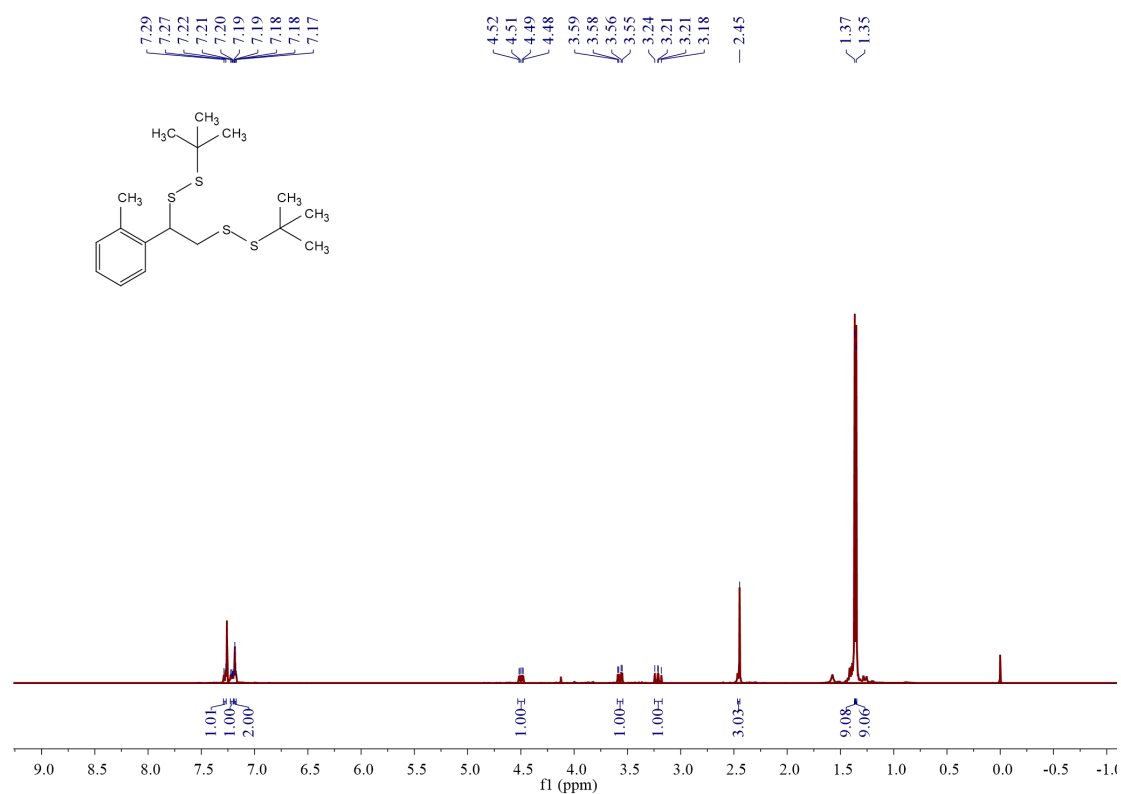


¹H NMR spectra of 3h (400 MHz, CDCl₃)

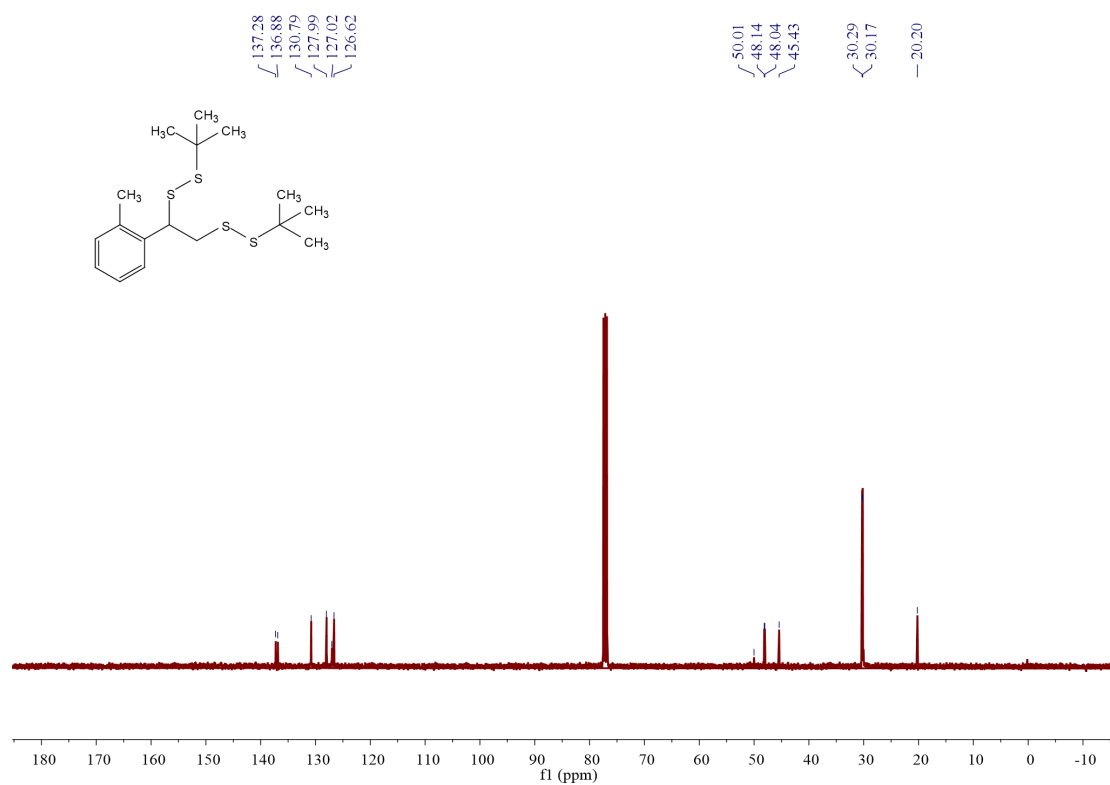


¹³C NMR spectra of 3h (101 MHz, CDCl₃)

NMR Spectra

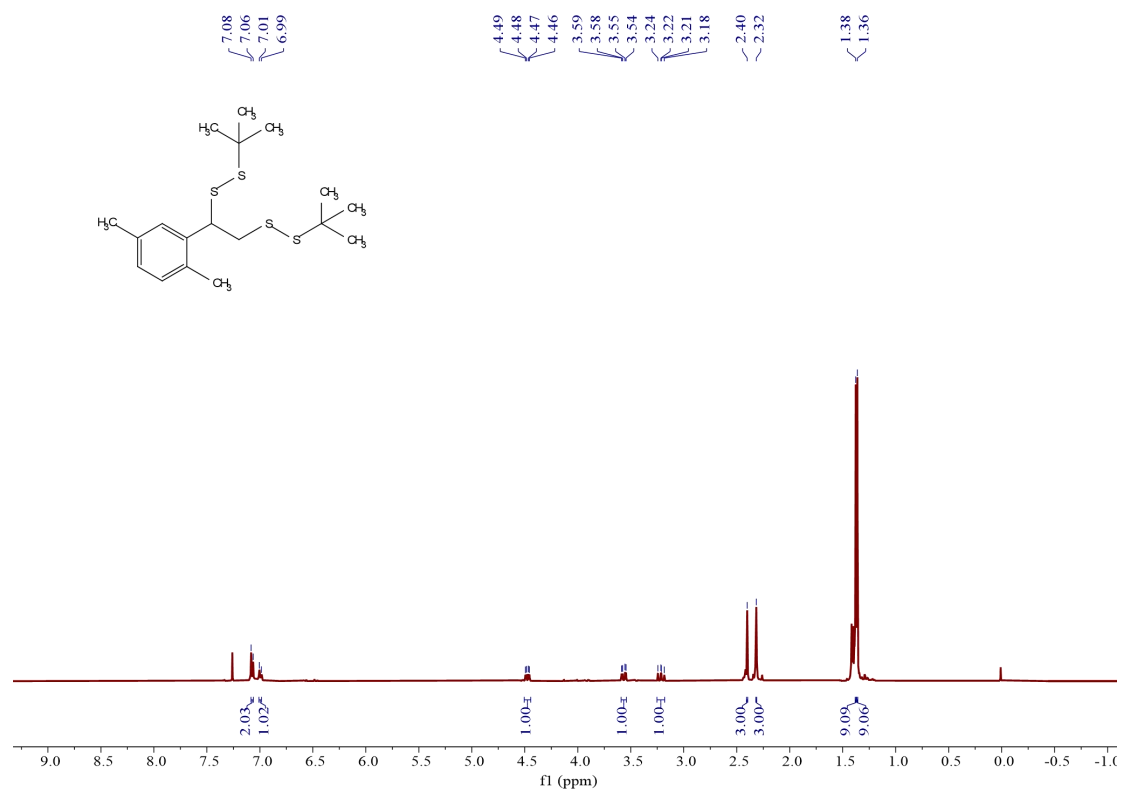


¹H NMR spectra of 3i (400 MHz, CDCl₃)

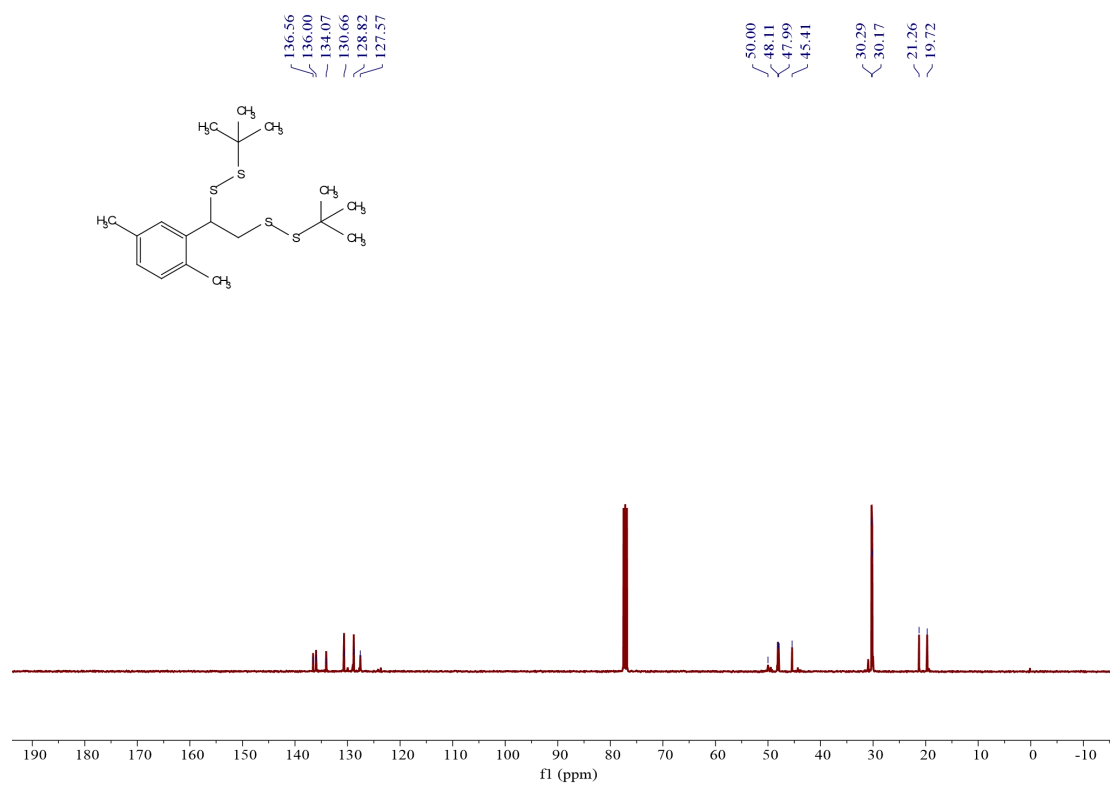


¹³C NMR spectra of 3i (101 MHz, CDCl₃)

NMR Spectra

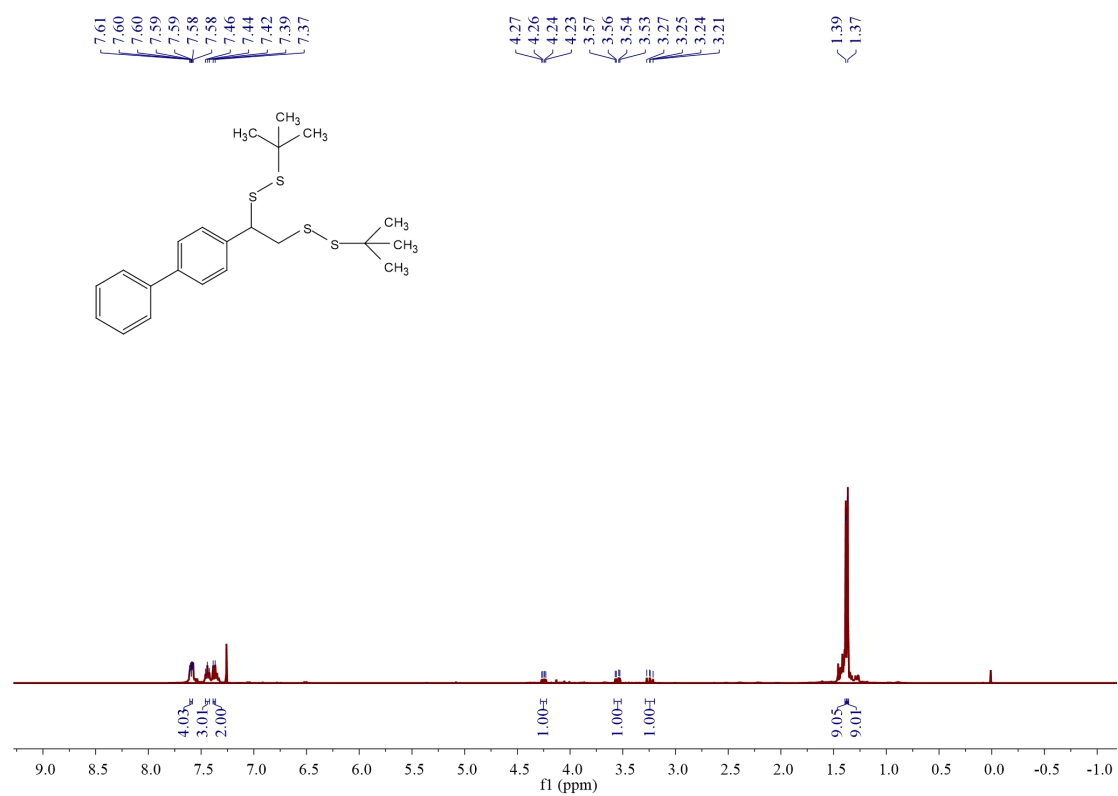


¹H NMR spectra of **3j** (400 MHz, CDCl₃)

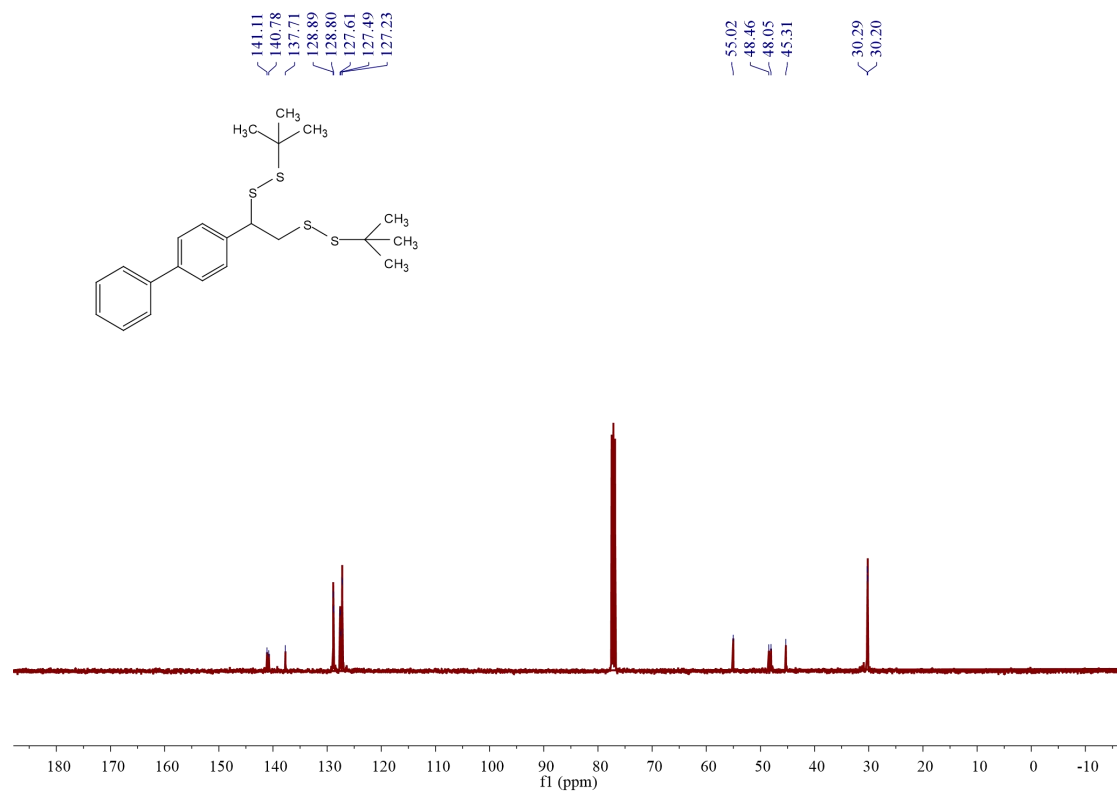


¹³C NMR spectra of **3j** (101 MHz, CDCl₃)

NMR Spectra

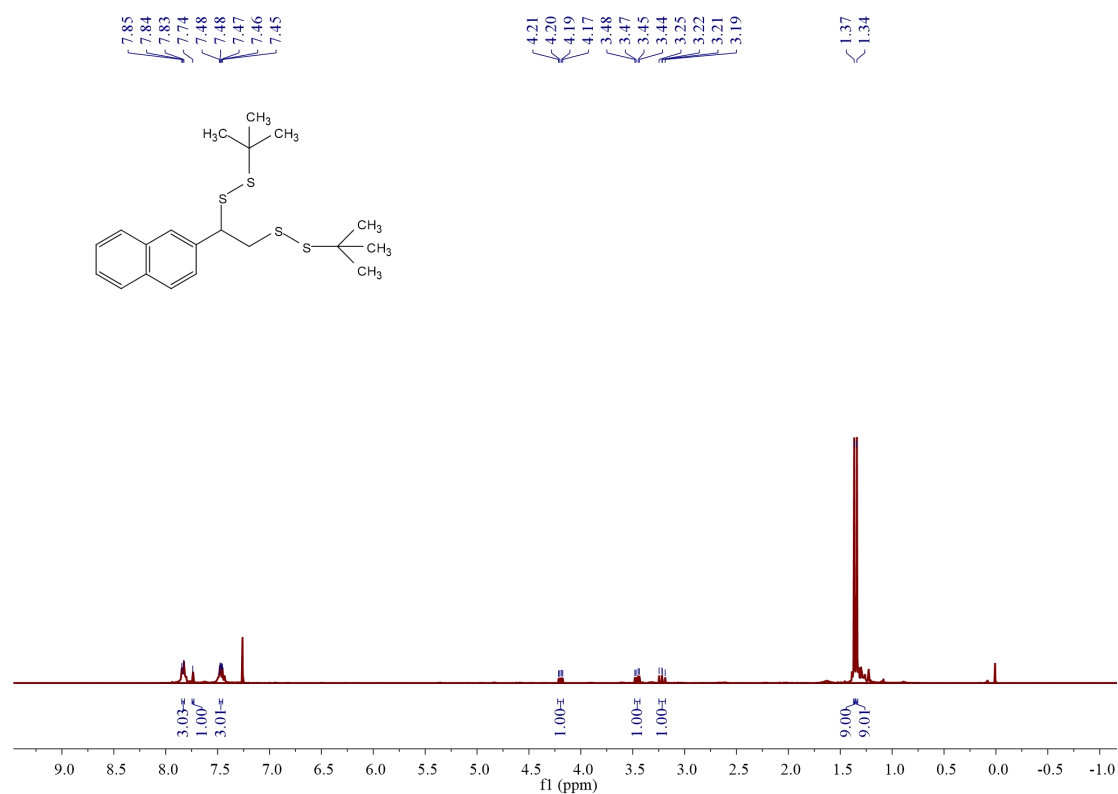


¹H NMR spectra of 3k (400 MHz, CDCl₃)

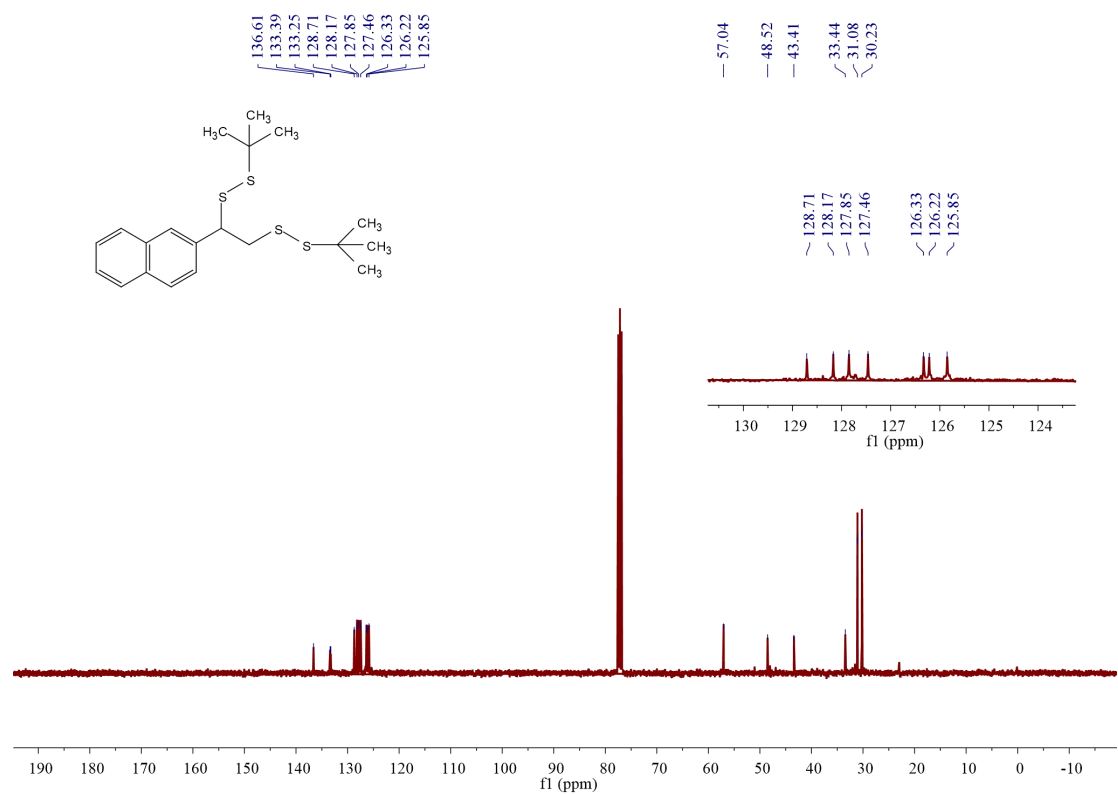


¹³C NMR spectra of 3k (101 MHz, CDCl₃)

NMR Spectra

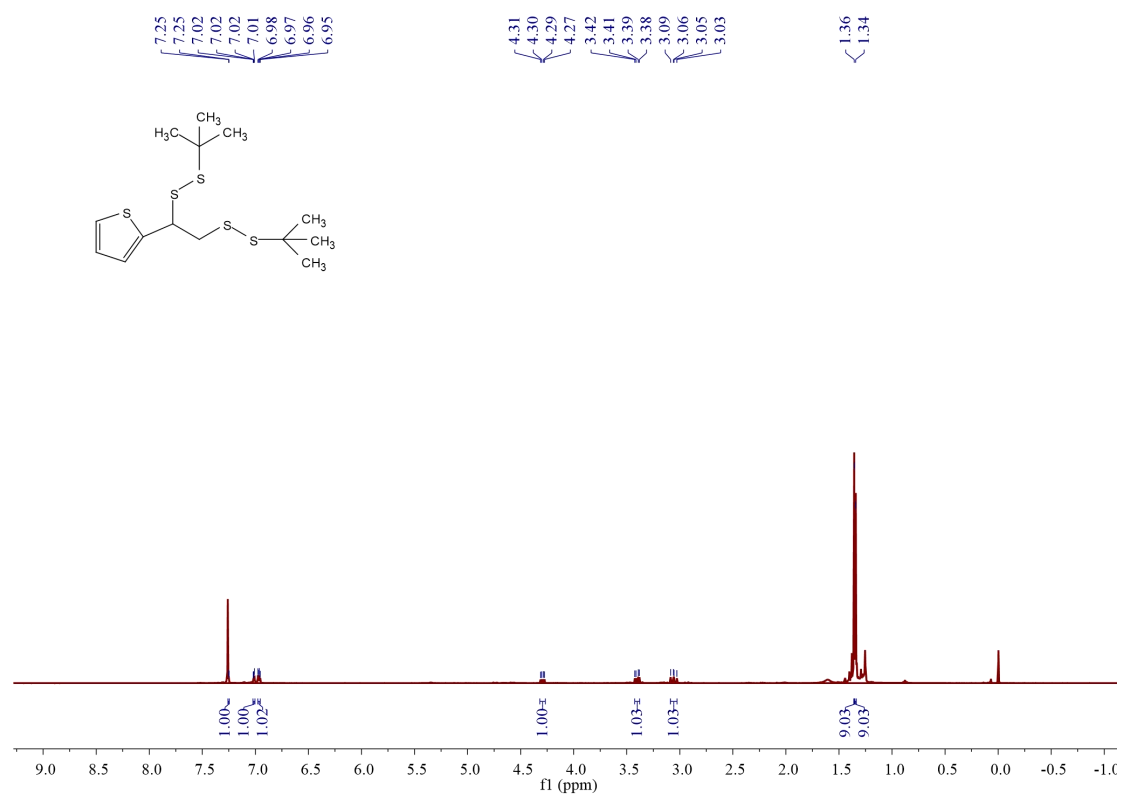


¹H NMR spectra of 3l (400 MHz, CDCl₃)

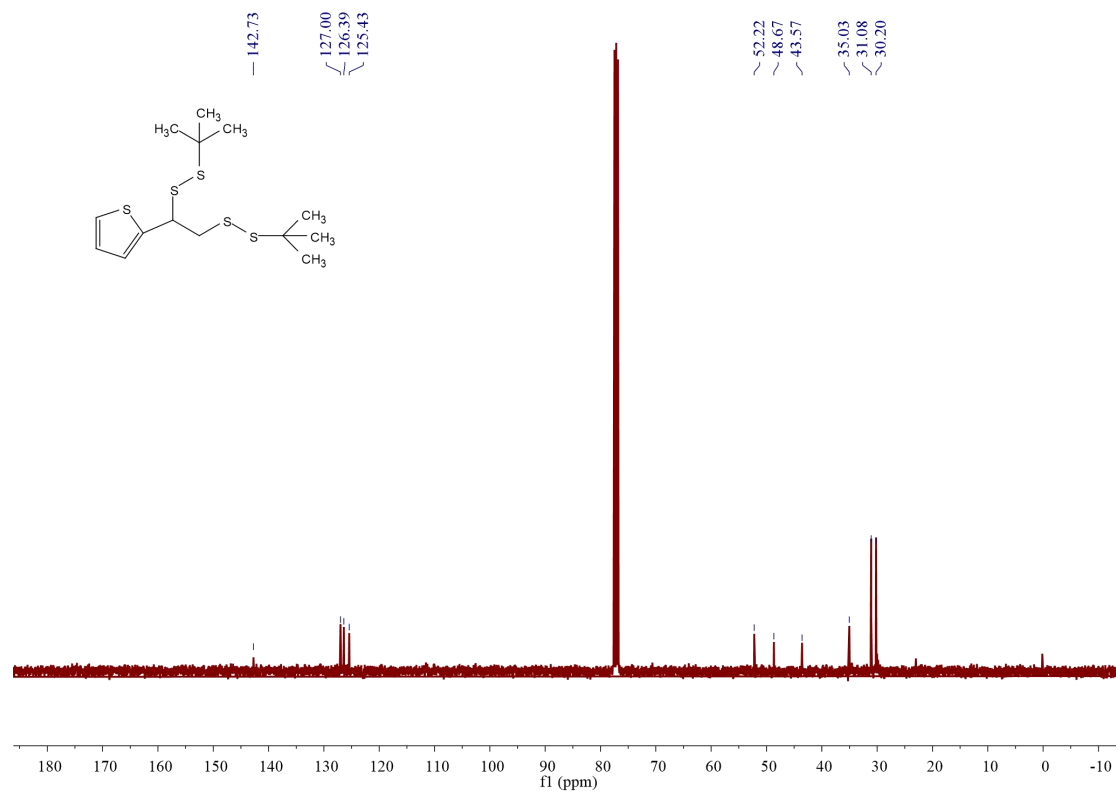


¹³C NMR spectra of 3l (101 MHz, CDCl₃)

NMR Spectra

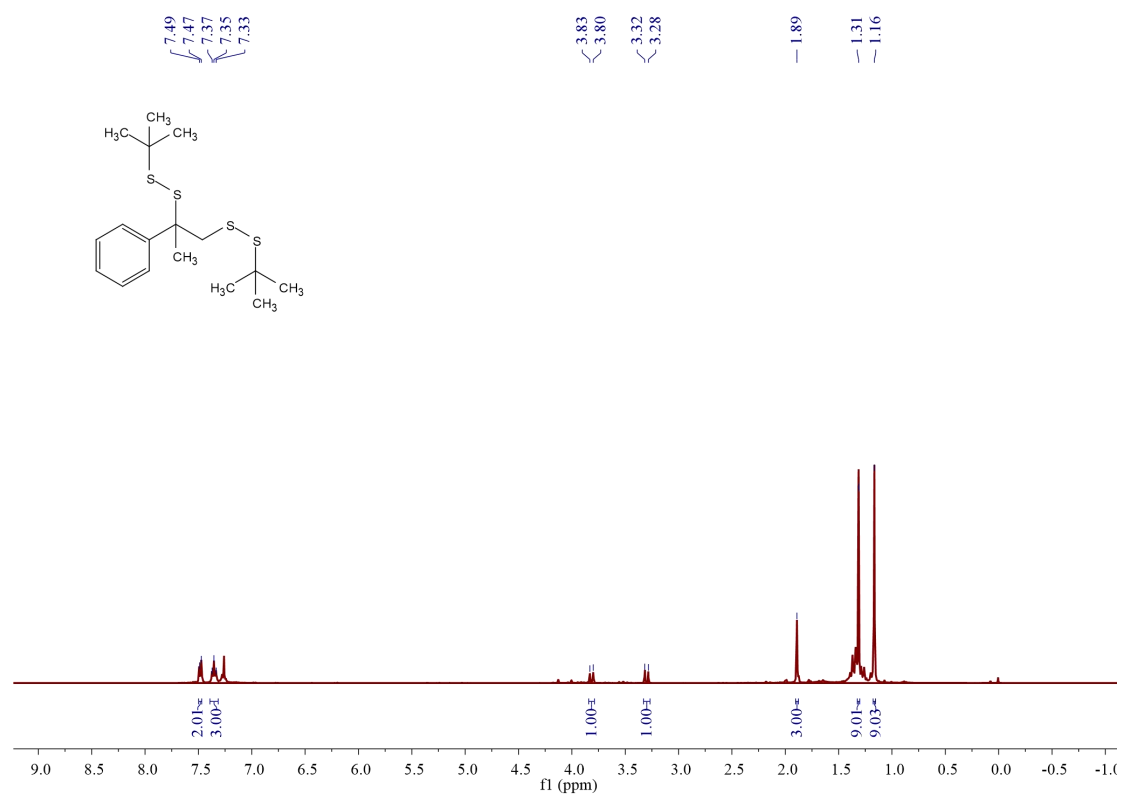


¹H NMR spectra of 3m (400 MHz, CDCl₃)

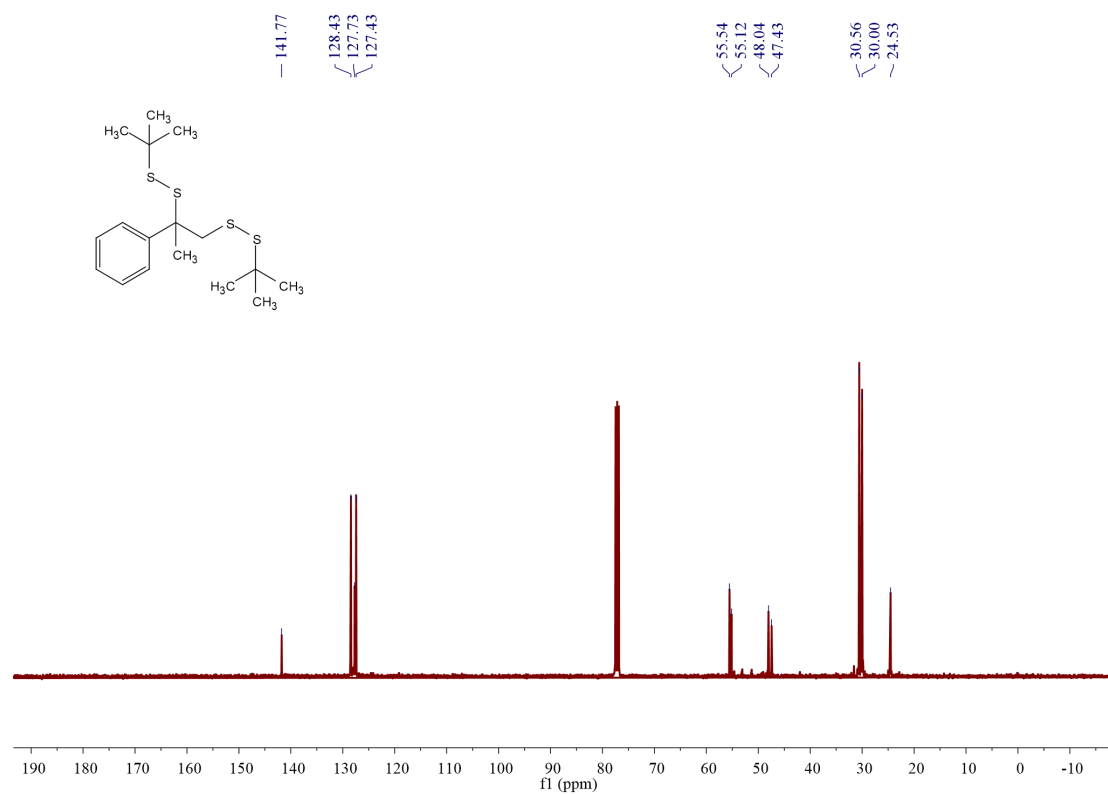


¹³C NMR spectra of 3m (101 MHz, CDCl₃)

NMR Spectra

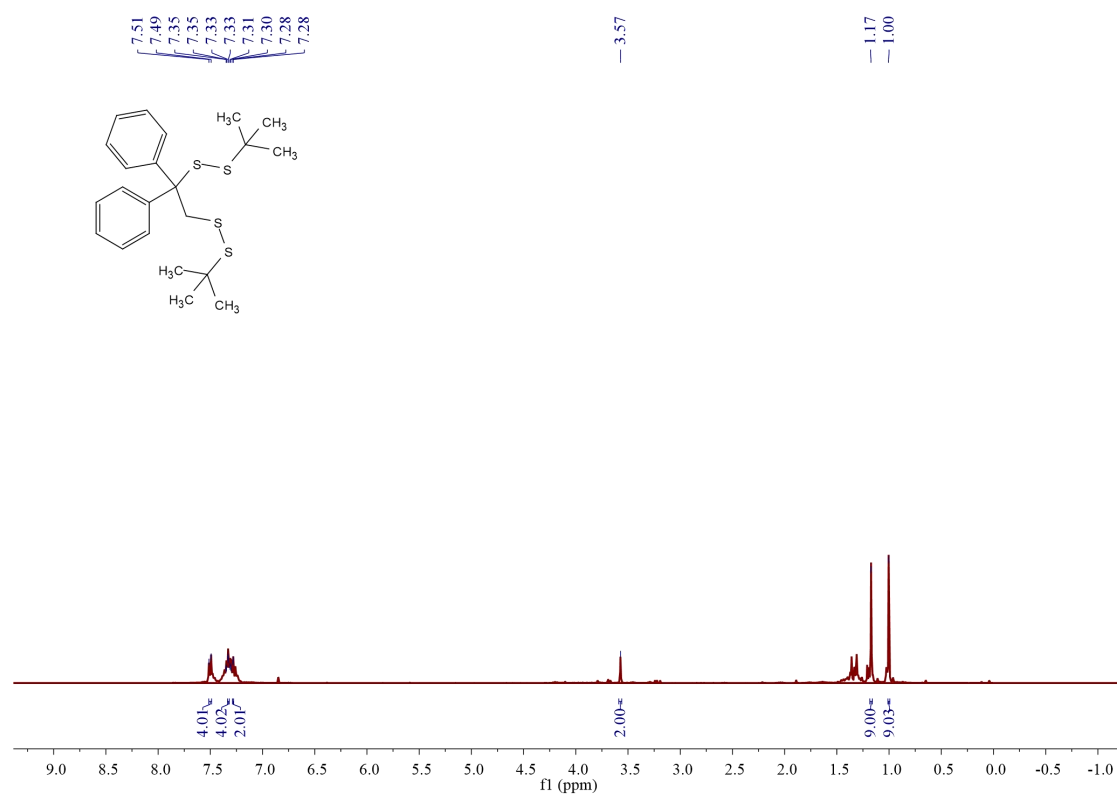


¹H NMR spectra of 3n (400 MHz, CDCl₃)

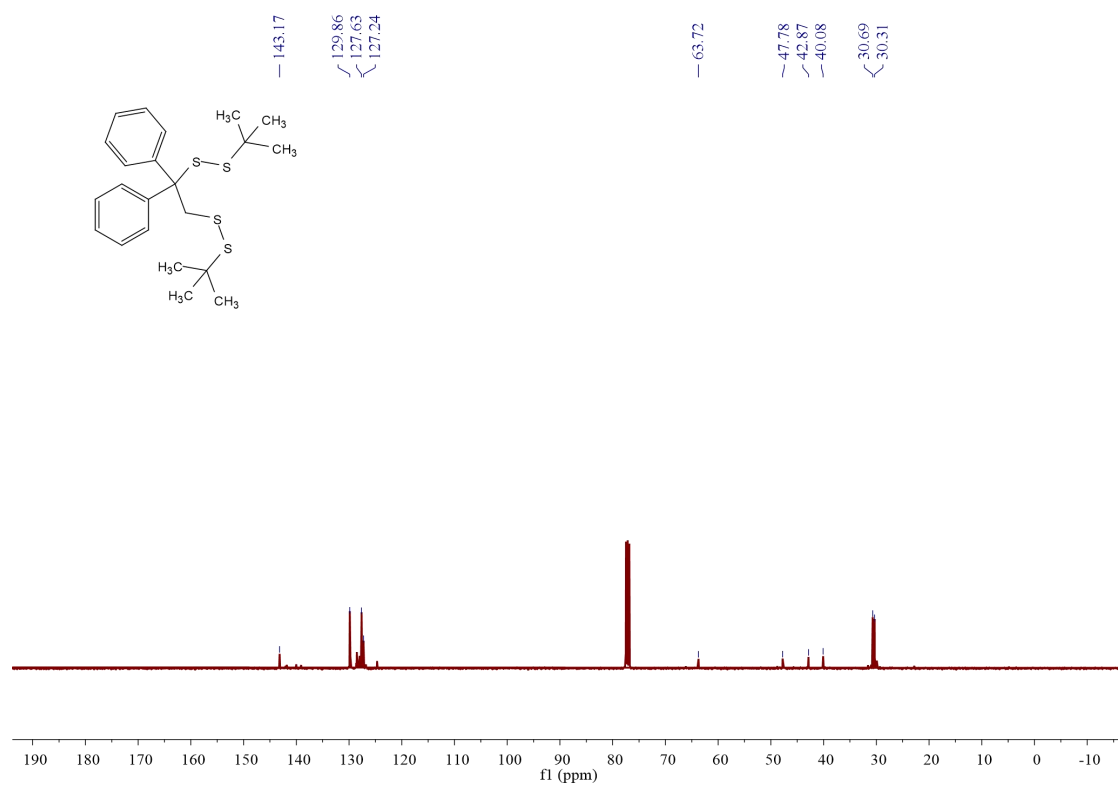


¹³C NMR spectra of 3n (101 MHz, CDCl₃)

NMR Spectra

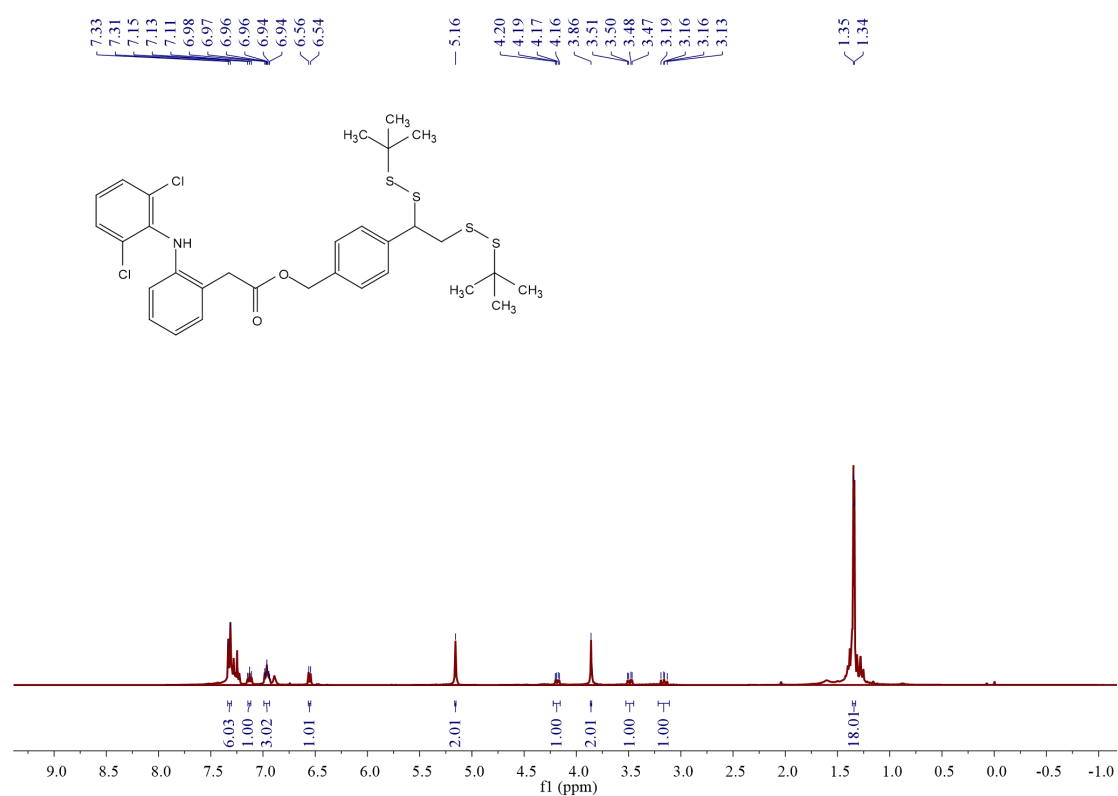


¹H NMR spectra of 3o (400 MHz, CDCl₃)

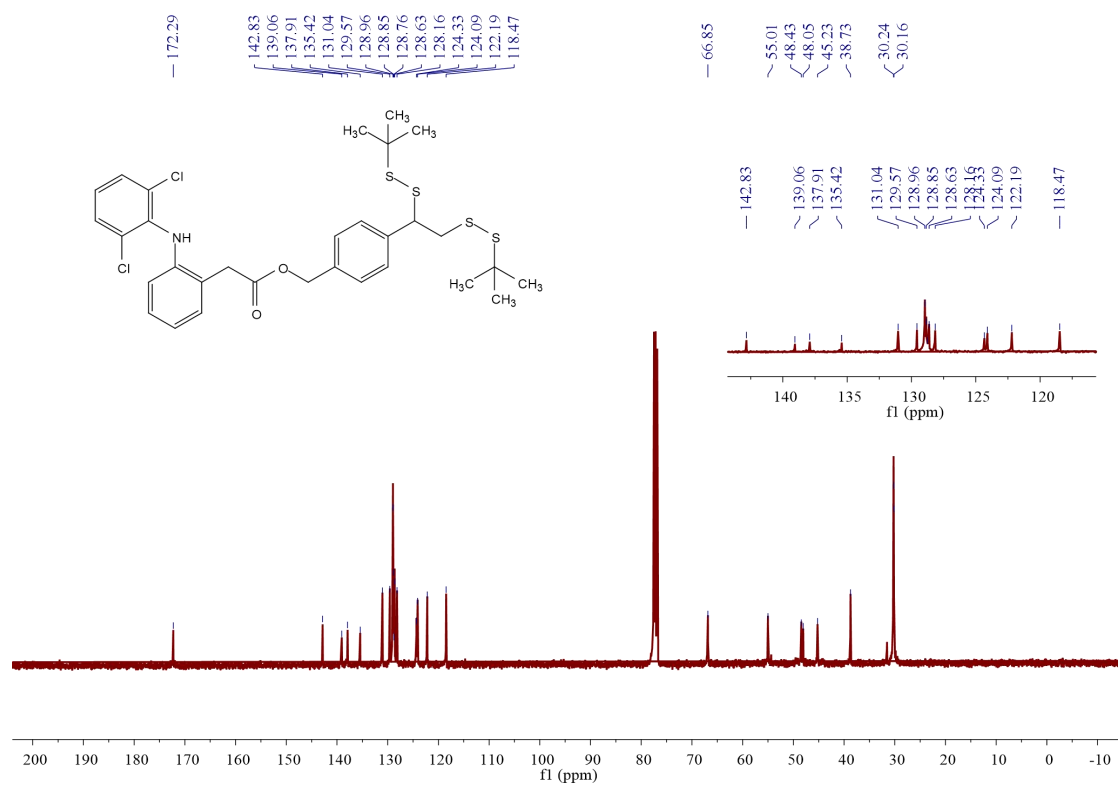


¹³C NMR spectra of 3o (101 MHz, CDCl₃)

NMR Spectra

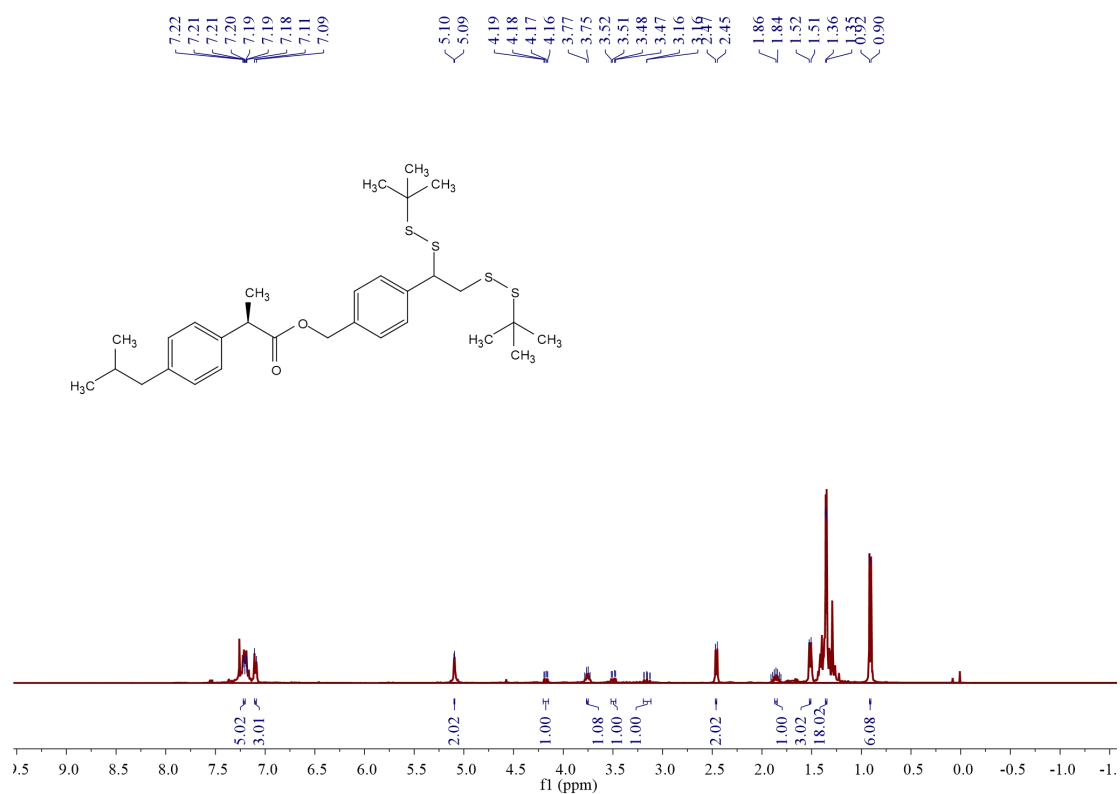


¹H NMR spectra of 3p (400 MHz, CDCl₃)

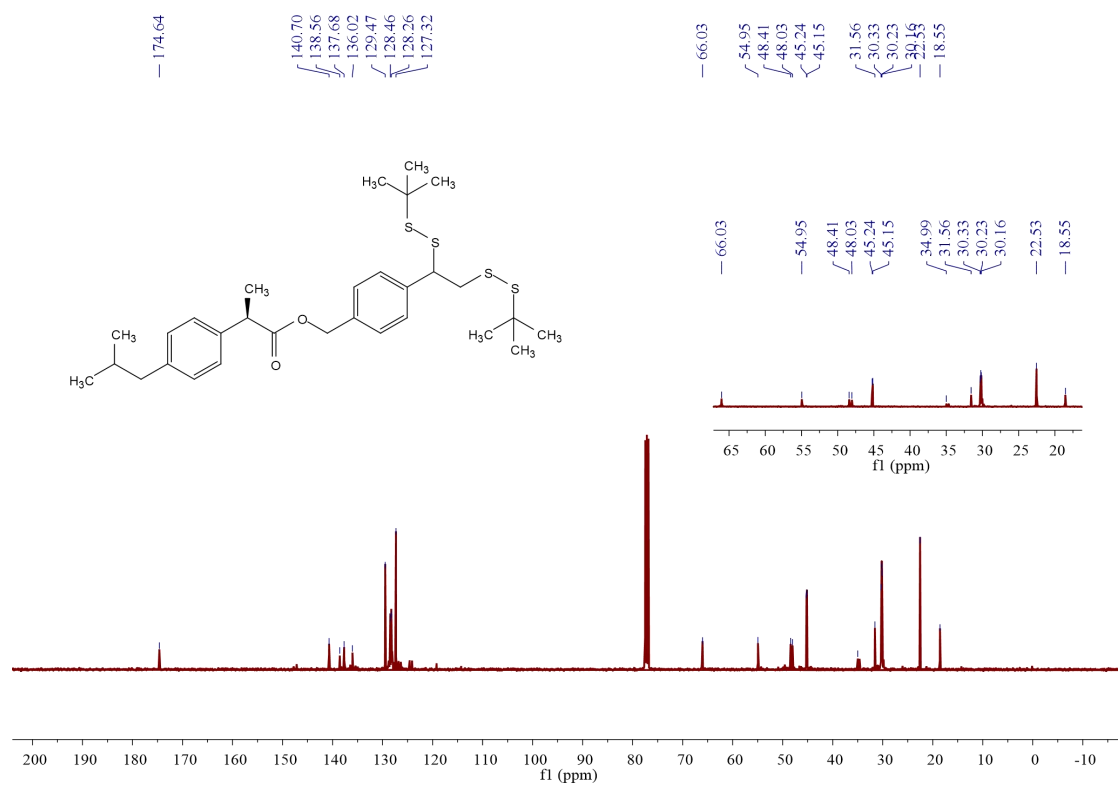


¹³C NMR spectra of 3p (101 MHz, CDCl₃)

NMR Spectra

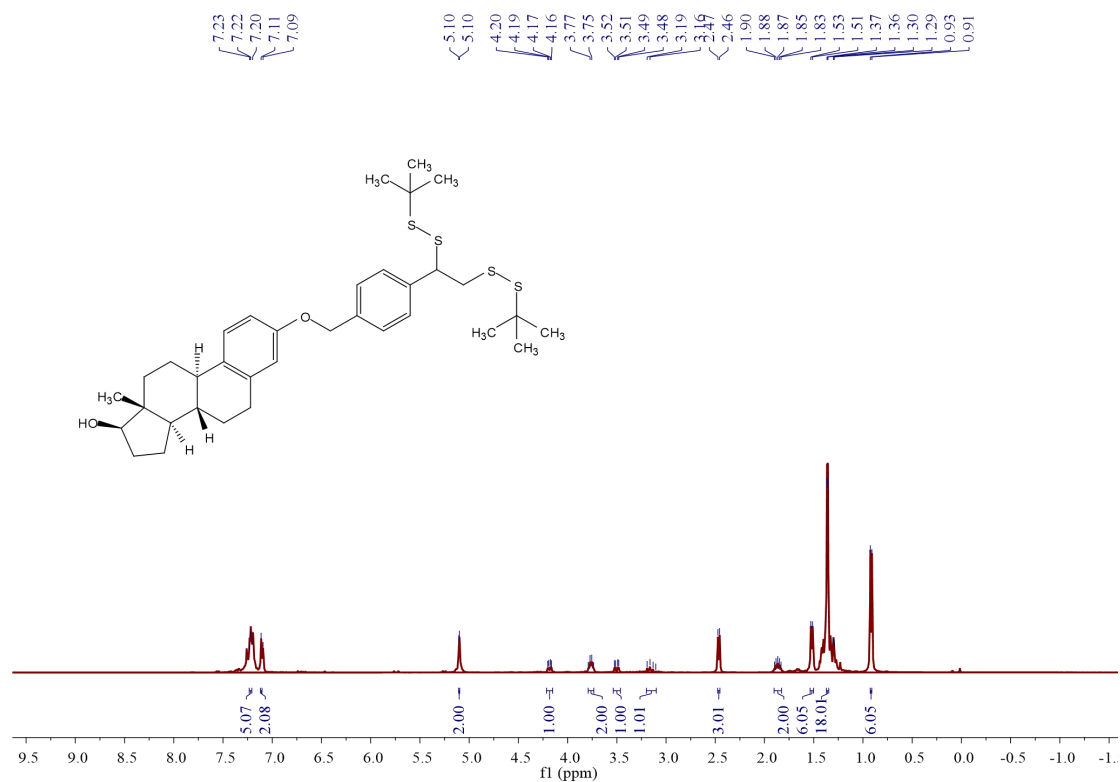


¹H NMR spectra of 3q (400 MHz, CDCl₃)

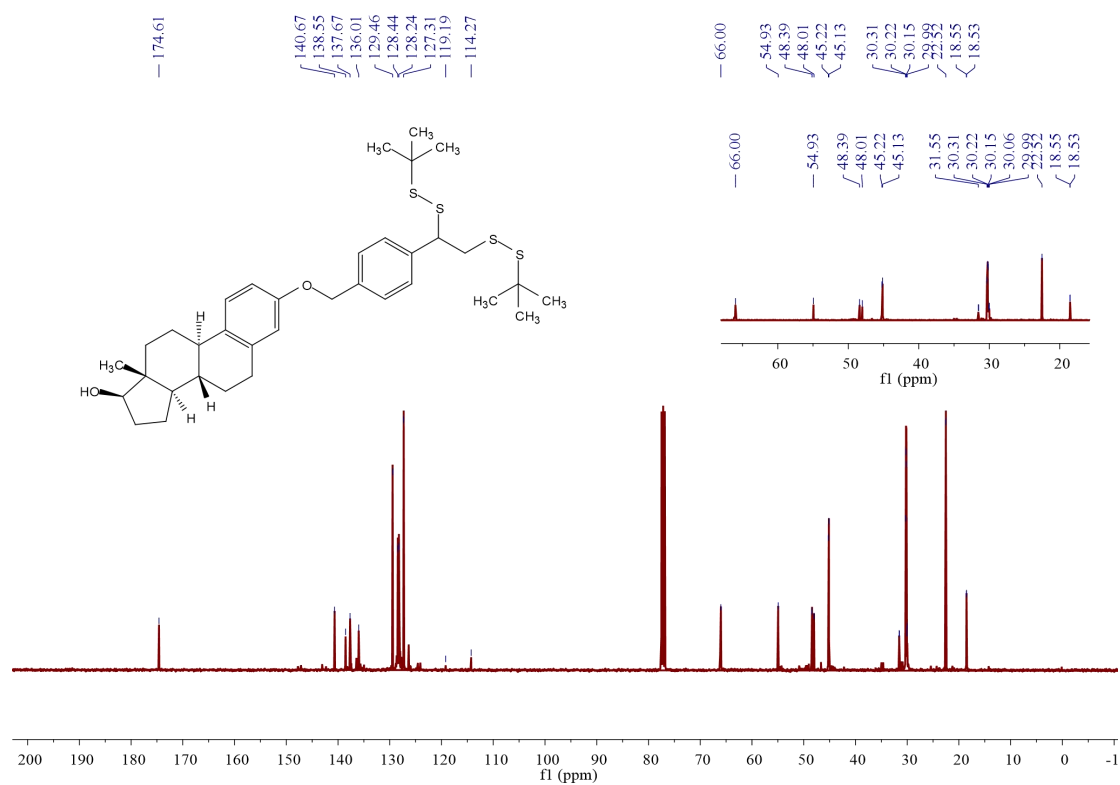


¹³C NMR spectra of 3q (101 MHz, CDCl₃)

NMR Spectra

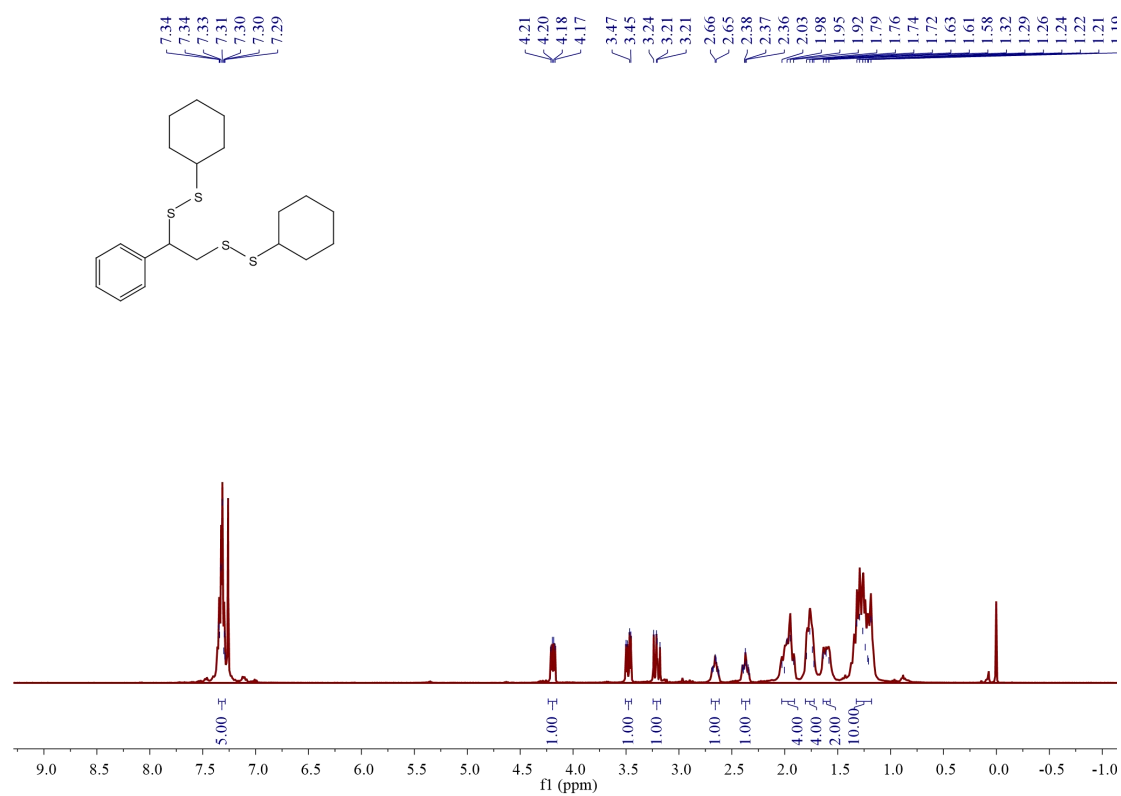


¹H NMR spectra of 3r (400 MHz, CDCl₃)

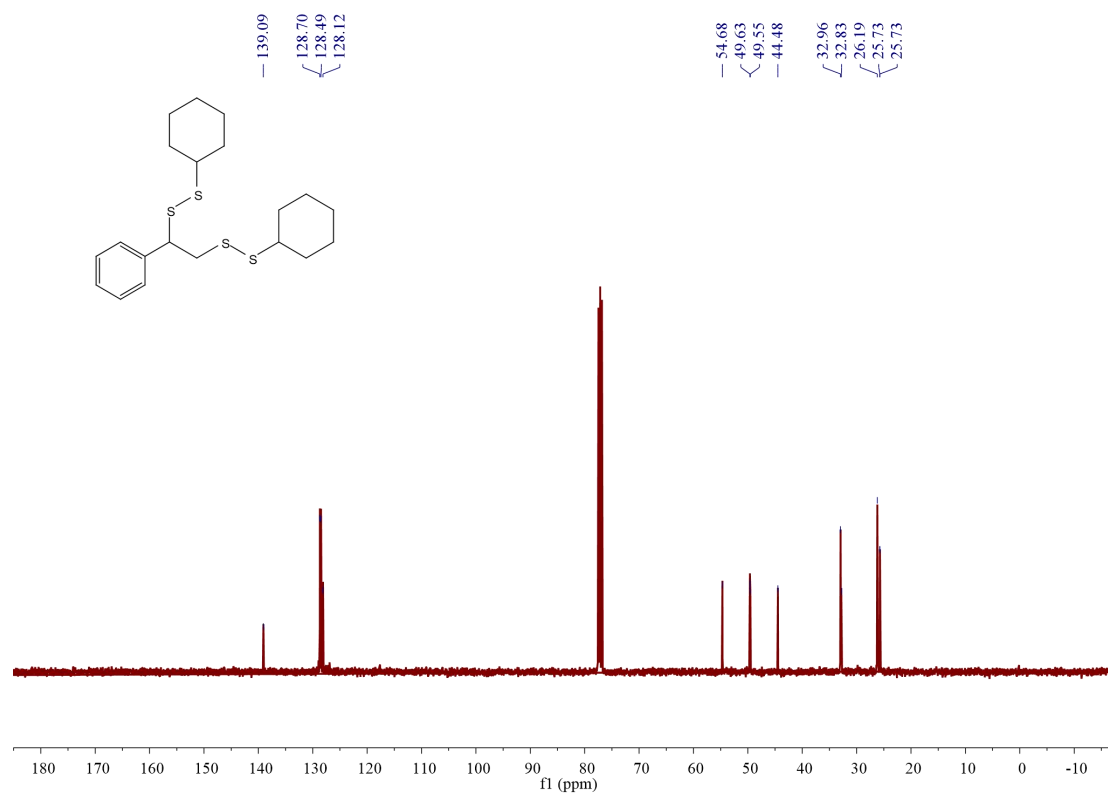


¹³C NMR spectra of 3r (101 MHz, CDCl₃)

NMR Spectra

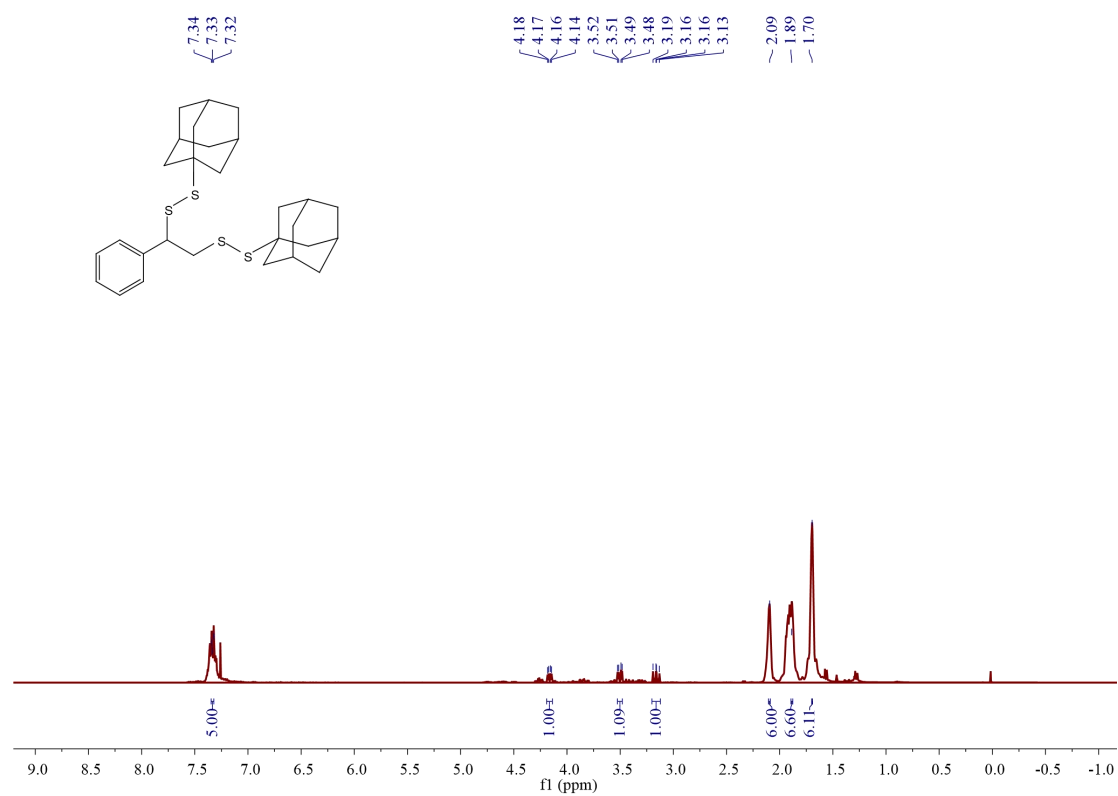


¹H NMR spectra of 3s (400 MHz, CDCl₃)

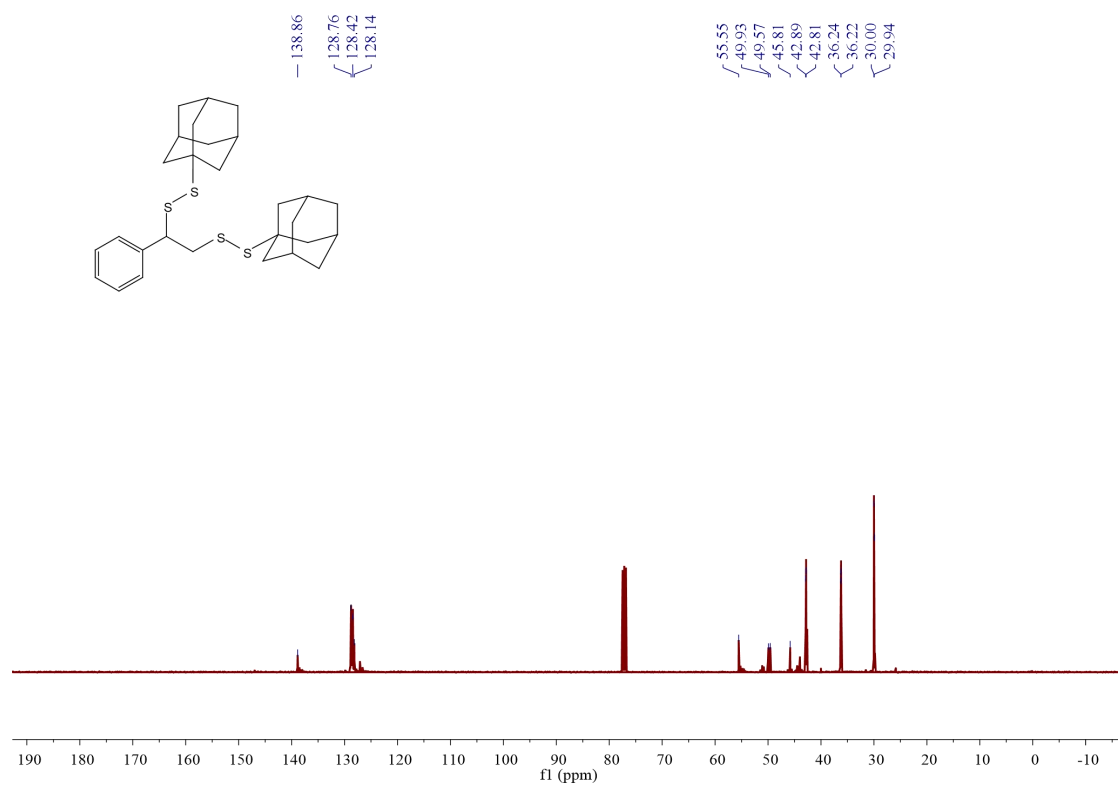


¹³C NMR spectra of 3s (101 MHz, CDCl₃)

NMR Spectra

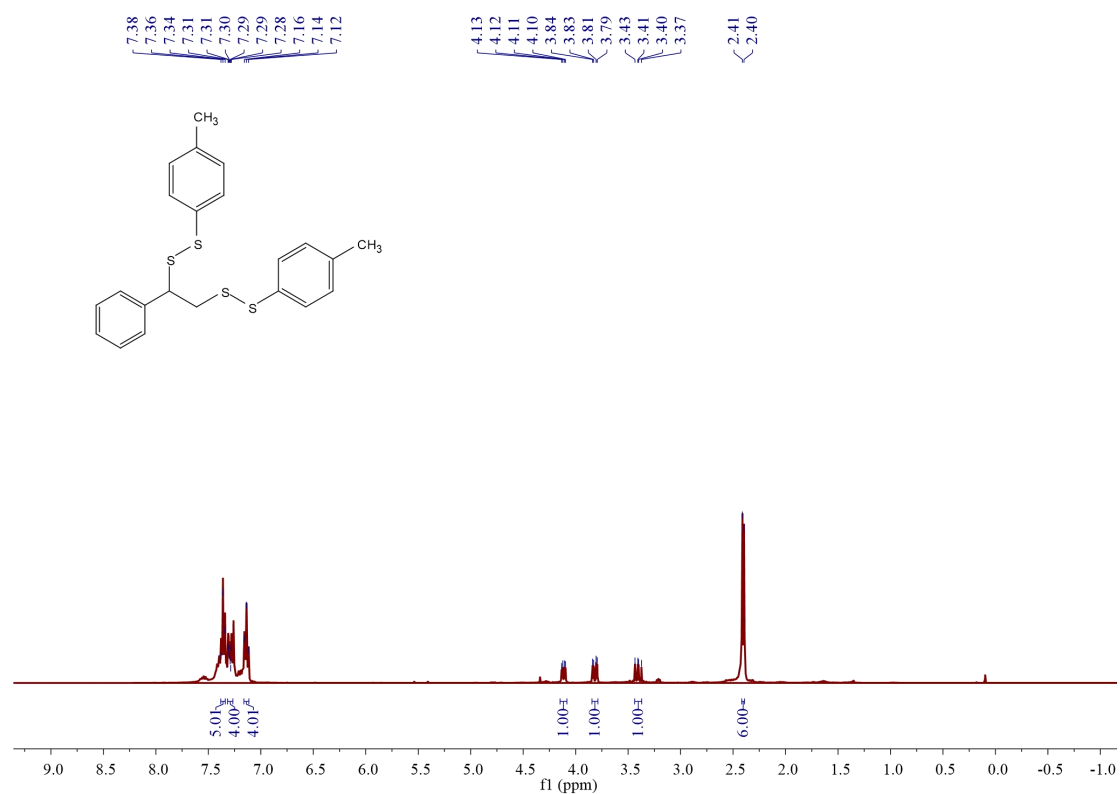


¹H NMR spectra of 3t (400 MHz, CDCl₃)

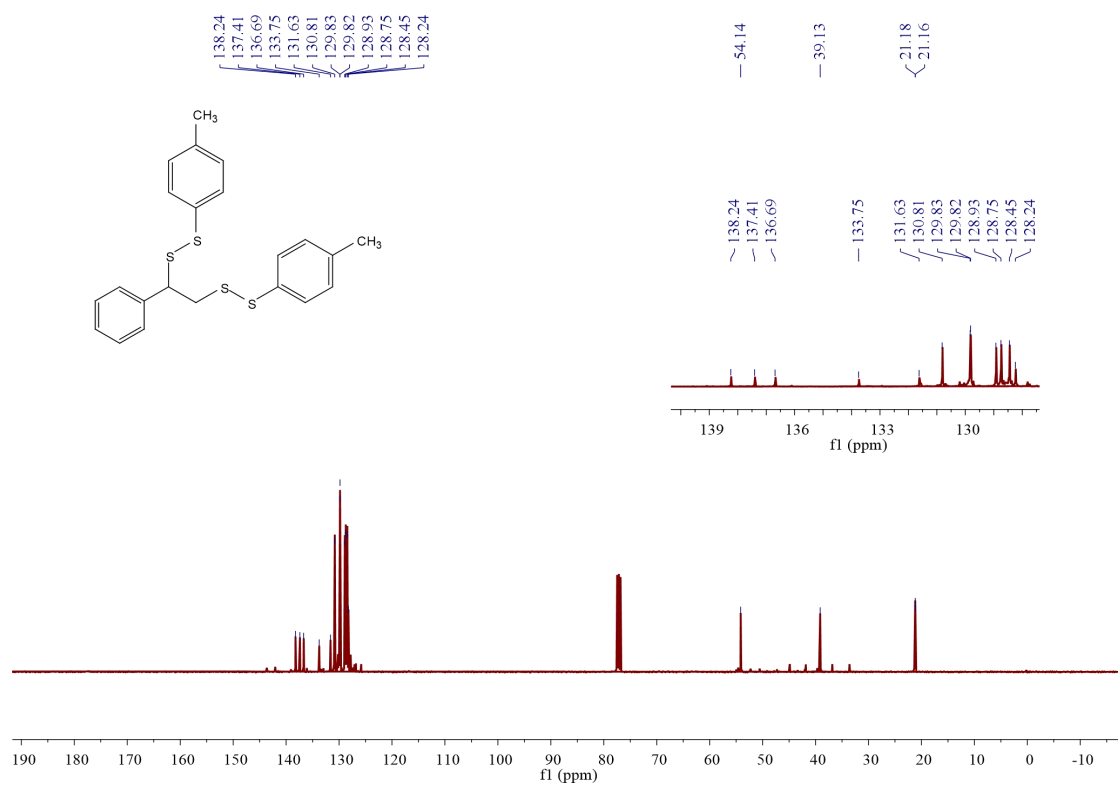


¹³C NMR spectra of 3t (101 MHz, CDCl₃)

NMR Spectra

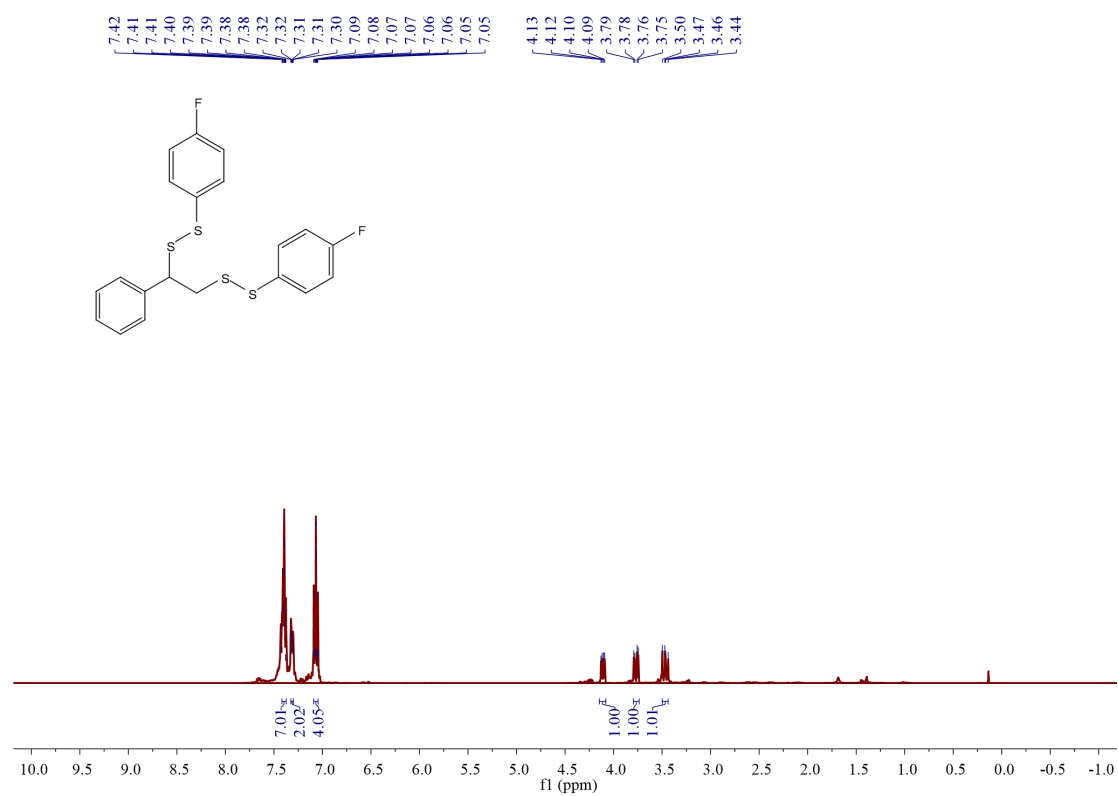


¹H NMR spectra of 3u (400 MHz, CDCl₃)

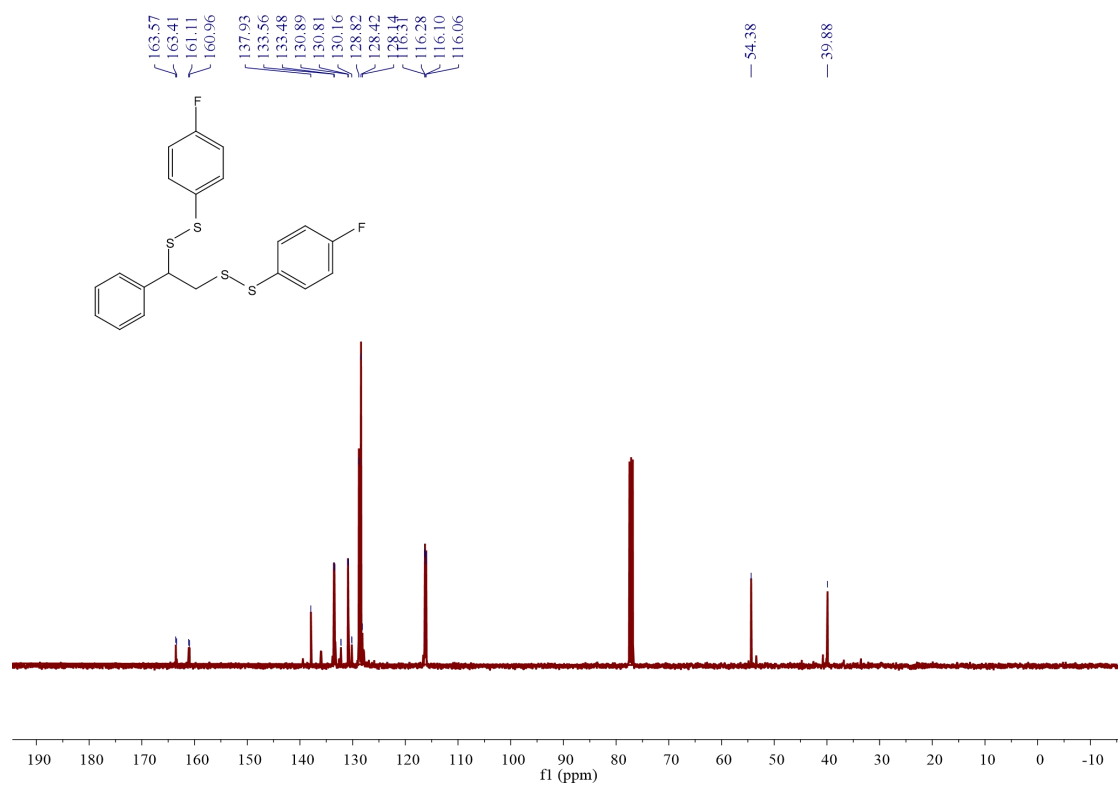


¹³C NMR spectra of 3u (101 MHz, CDCl₃)

NMR Spectra

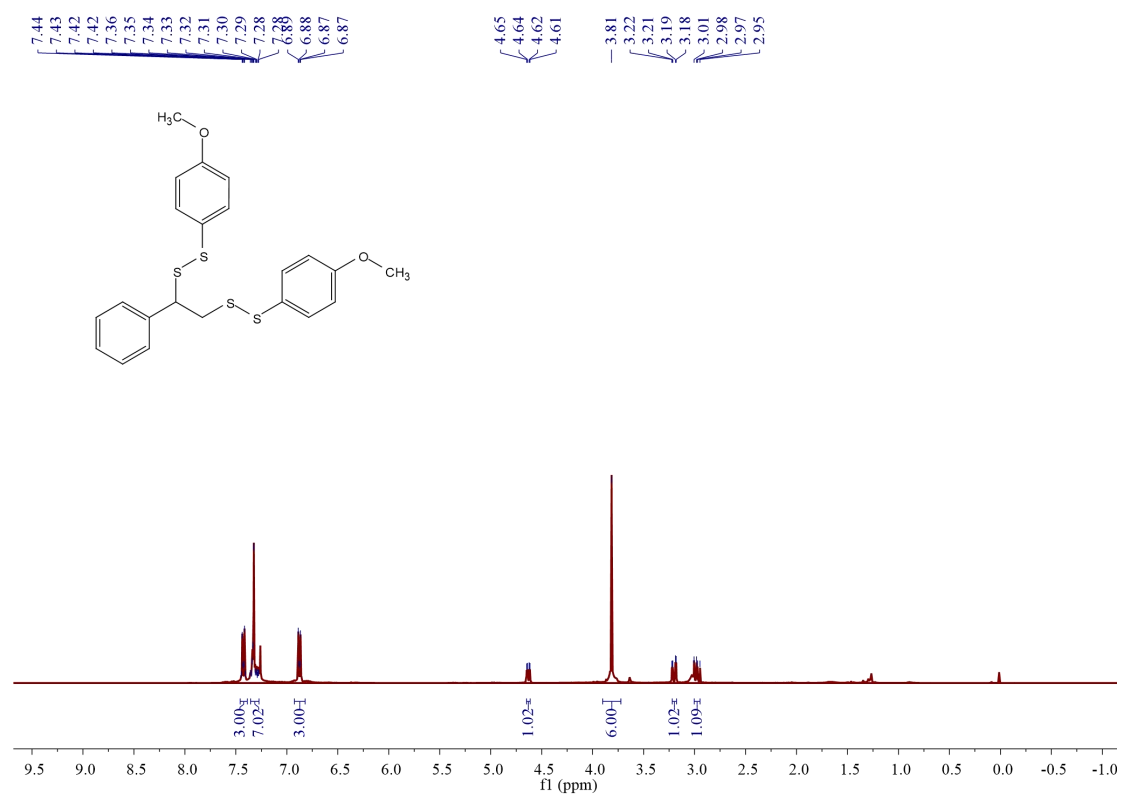


¹H NMR spectra of **3v** (400 MHz, CDCl₃)

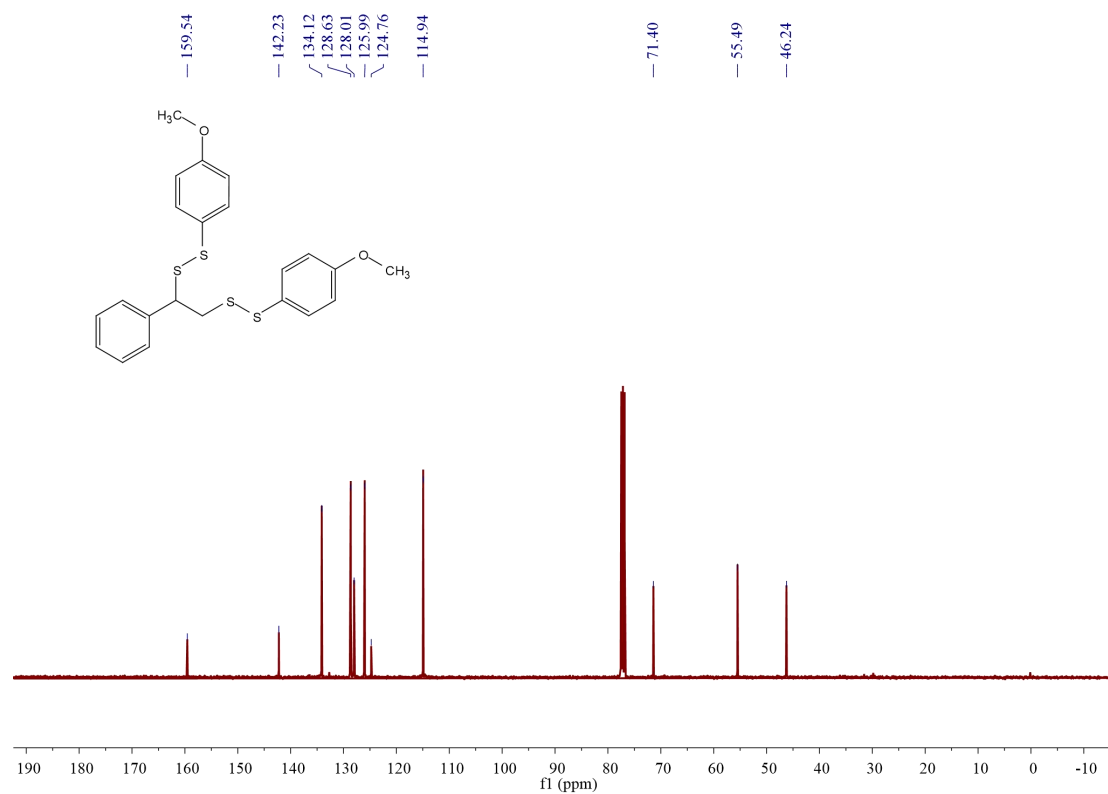


¹³C NMR spectra of **3v** (101 MHz, CDCl₃)

NMR Spectra

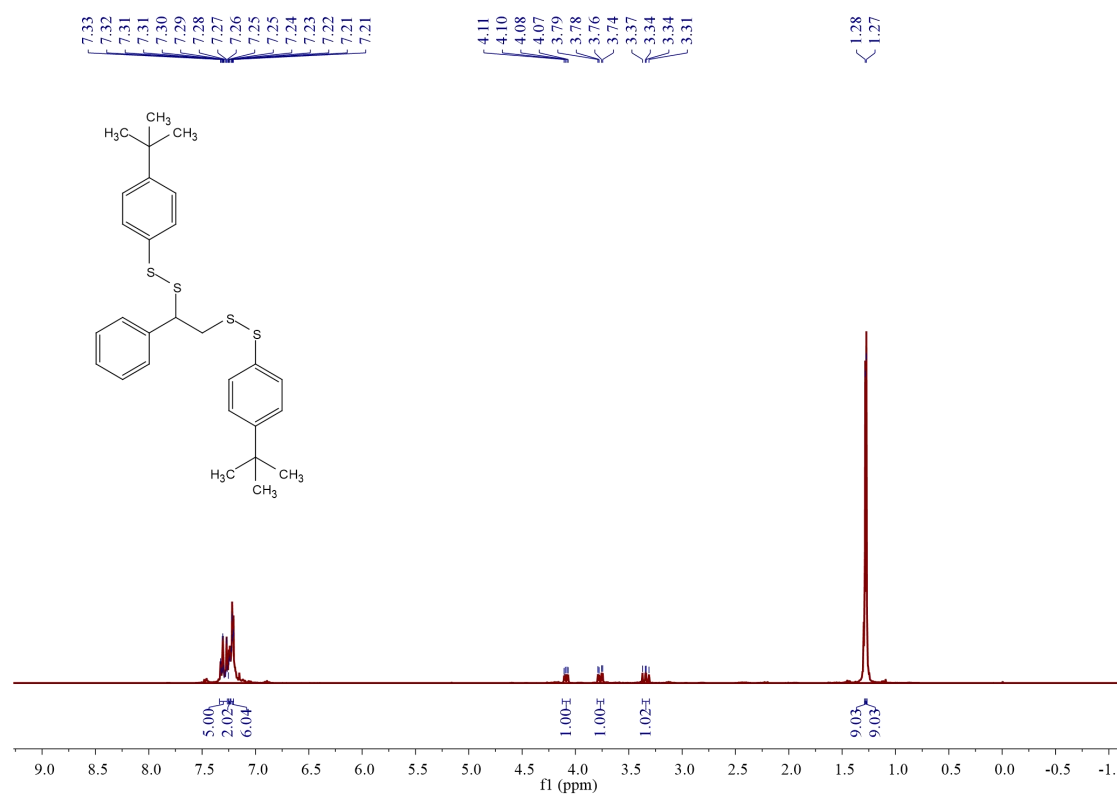


¹H NMR spectra of 3w (400 MHz, CDCl₃)

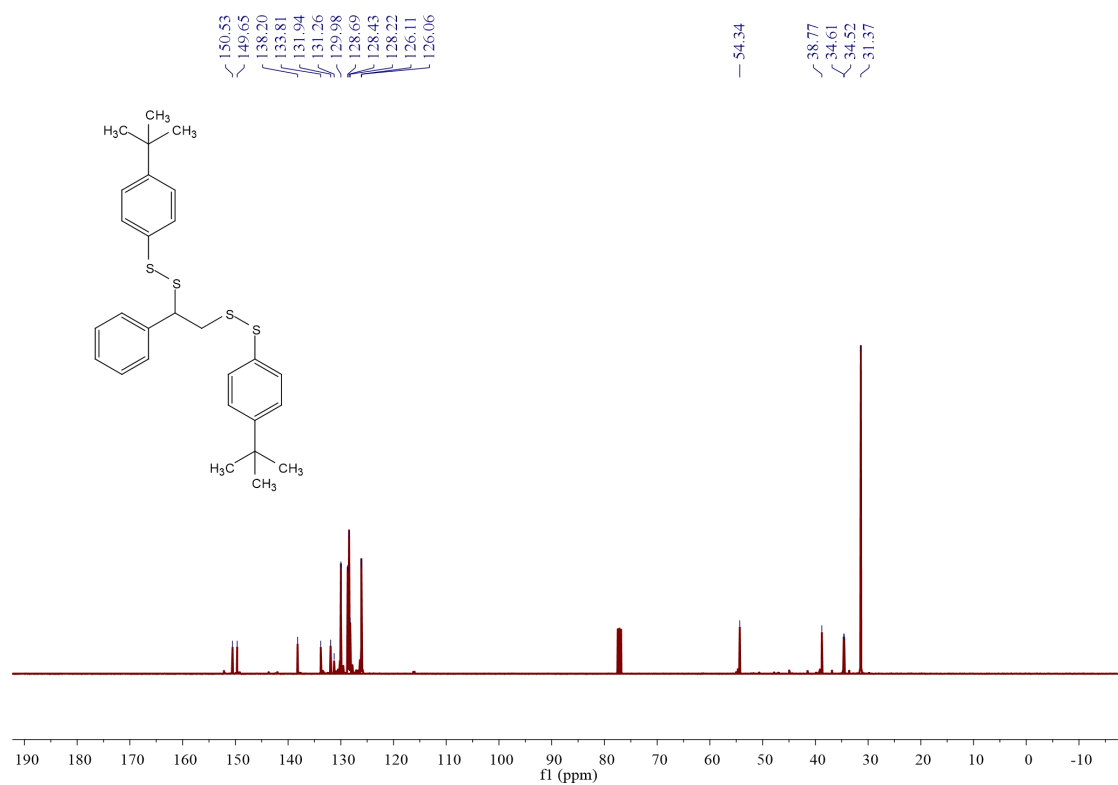


¹³C NMR spectra of 3w (101 MHz, CDCl₃)

NMR Spectra

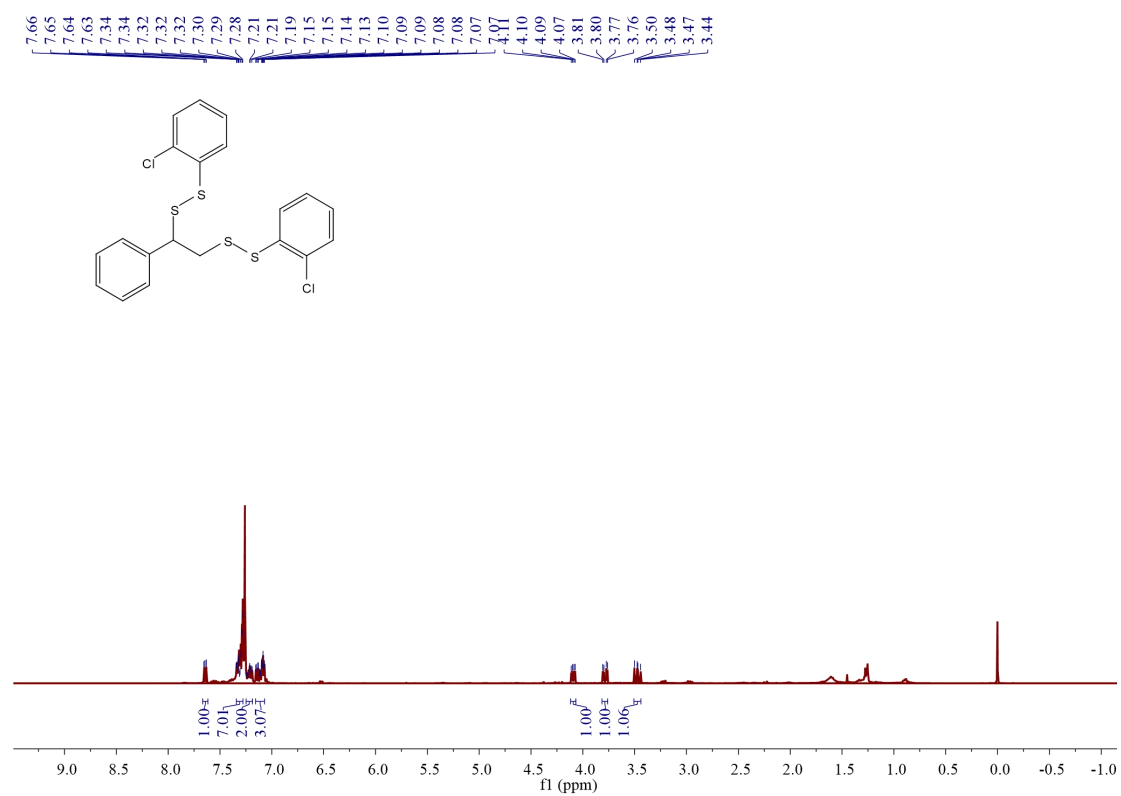


¹H NMR spectra of 3x (400 MHz, CDCl₃)

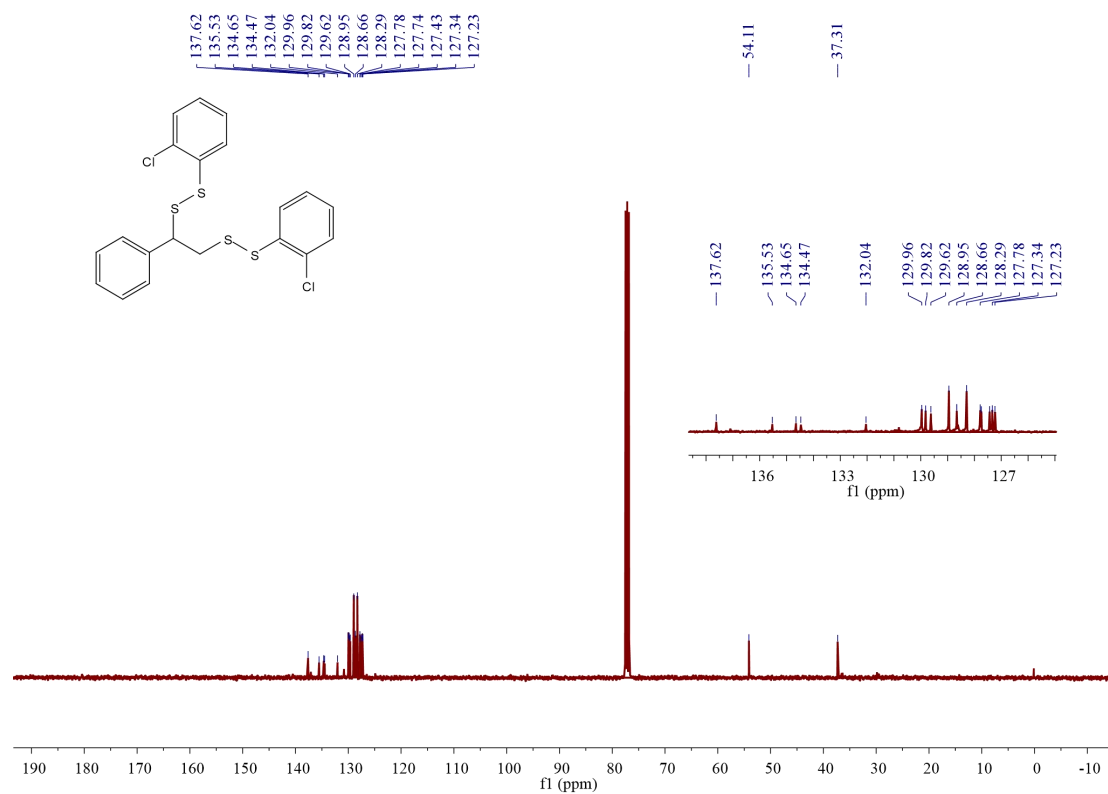


¹³C NMR spectra of 3x (101 MHz, CDCl₃)

NMR Spectra

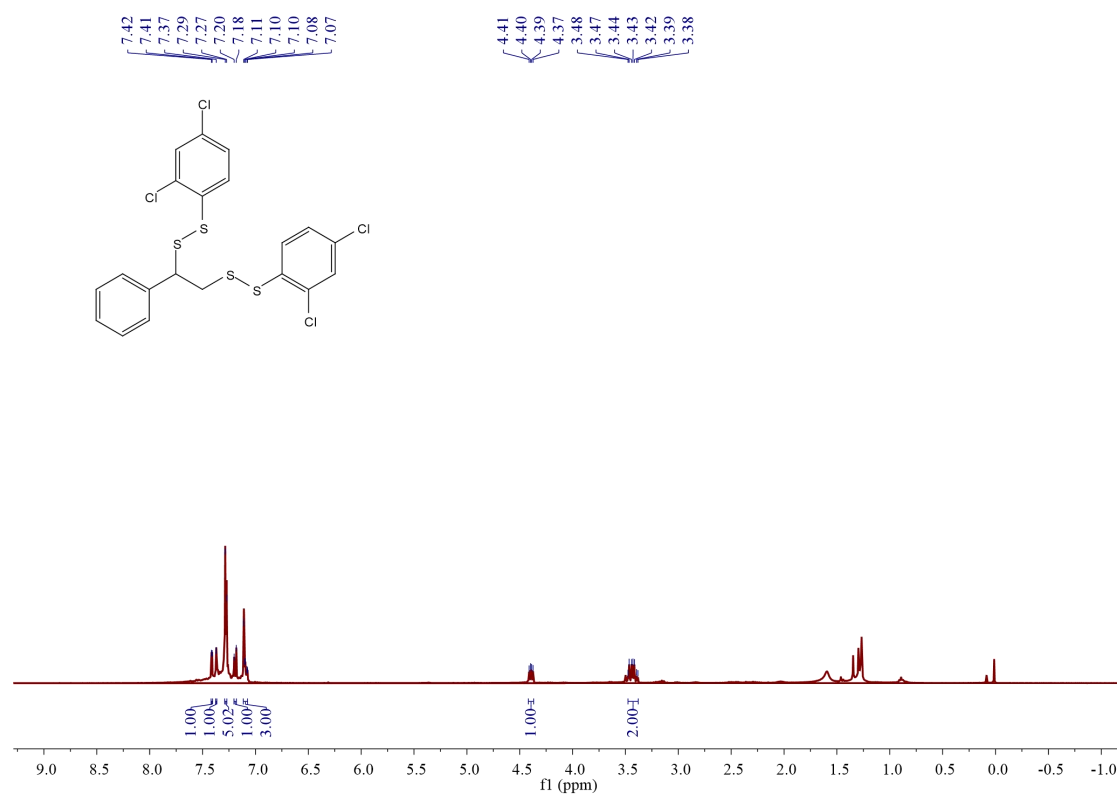


¹H NMR spectra of 3y (400 MHz, CDCl₃)

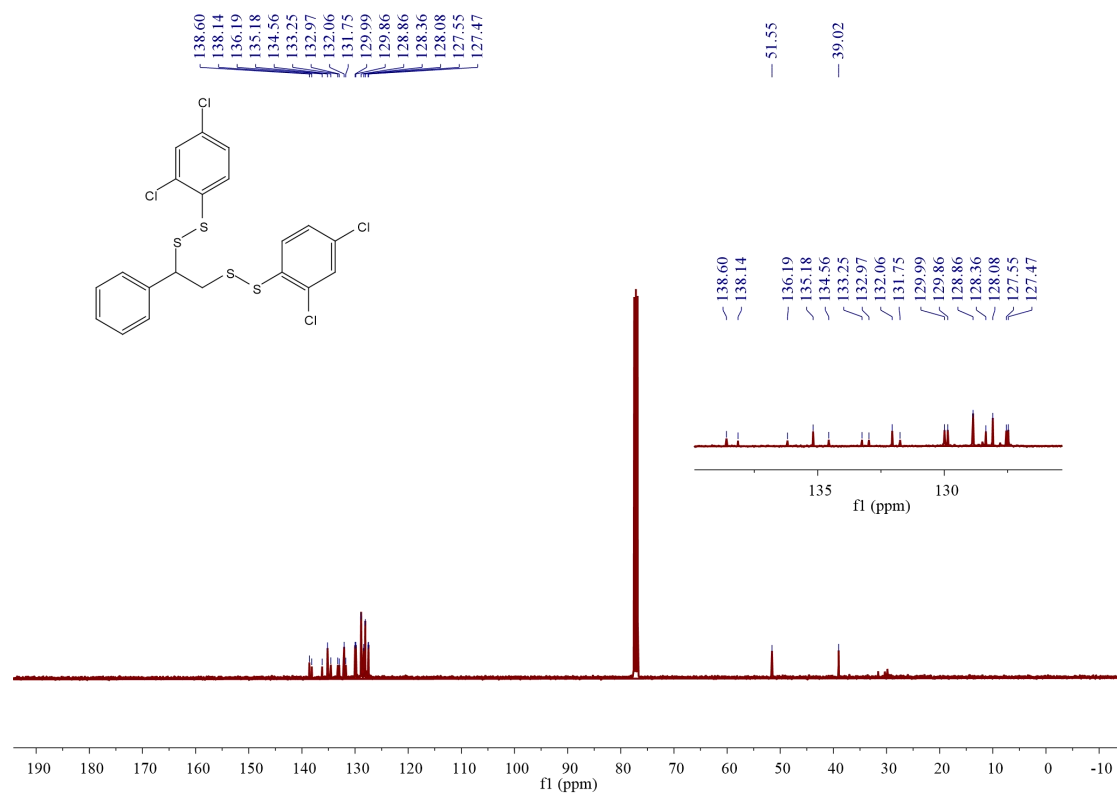


¹³C NMR spectra of 3y (101 MHz, CDCl₃)

NMR Spectra

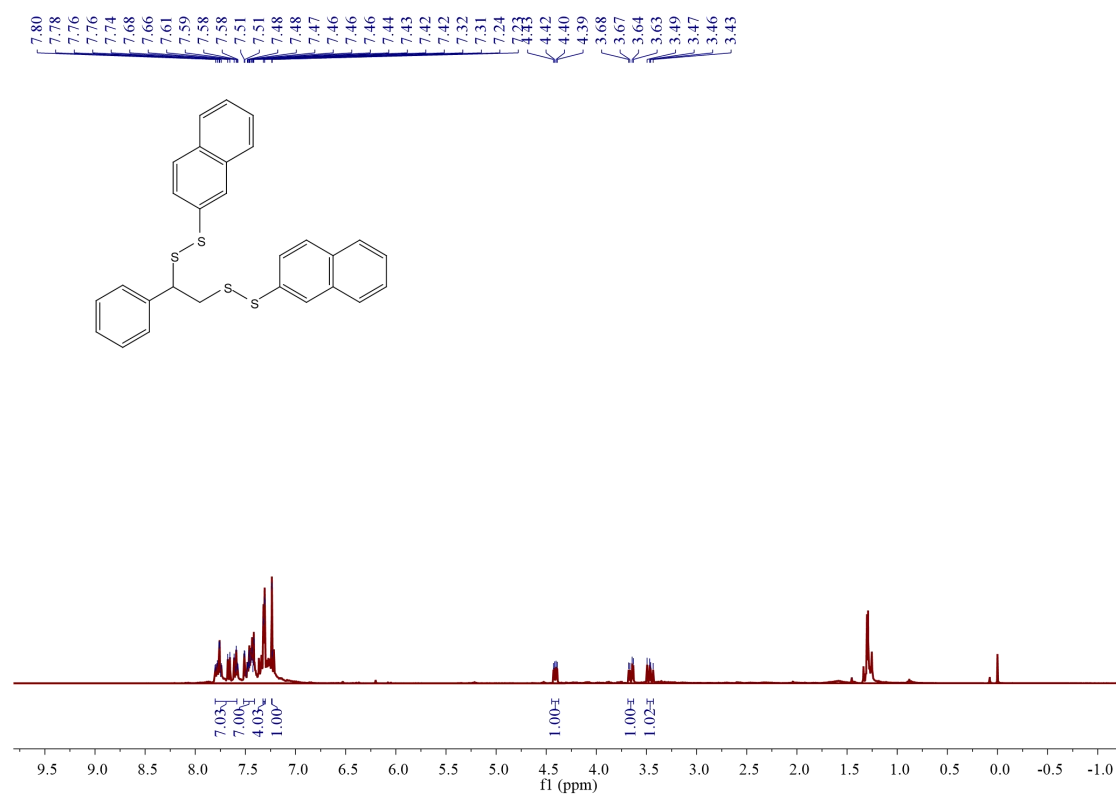


¹H NMR spectra of 3z (400 MHz, CDCl₃)

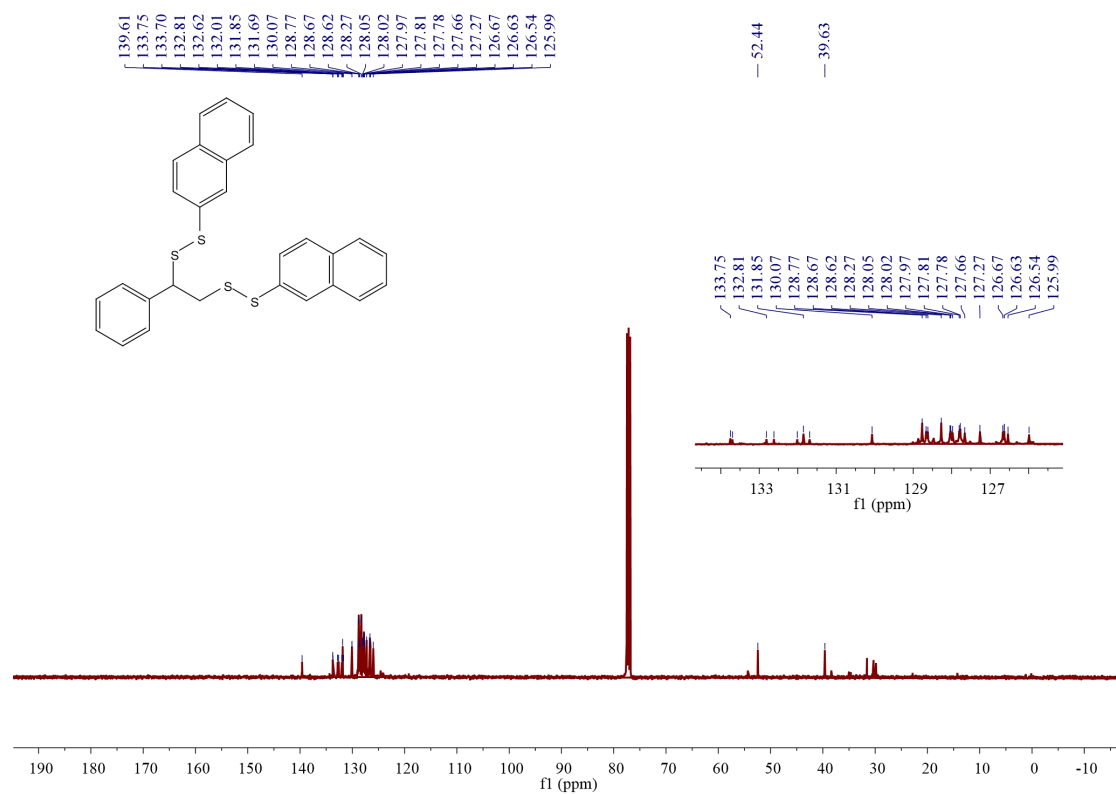


^{13}C NMR spectra of 3z (101 MHz, CDCl_3)

NMR Spectra

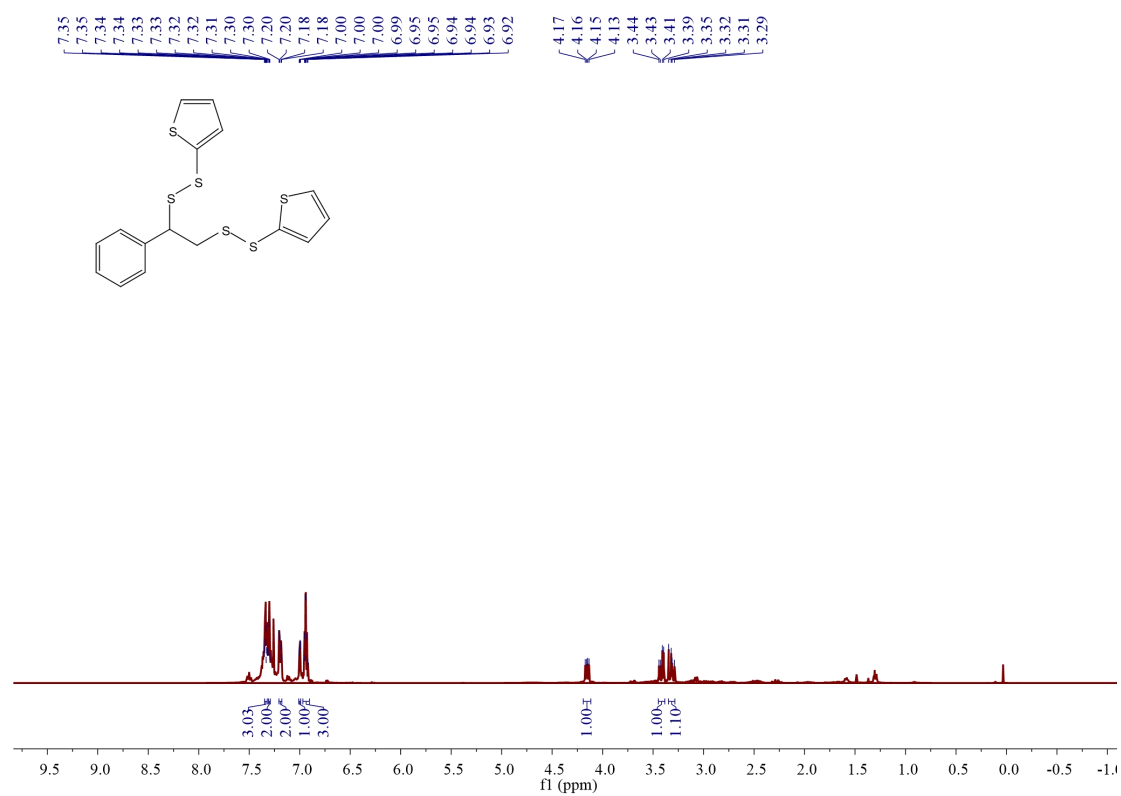


¹H NMR spectra of 3aa (400 MHz, CDCl₃)

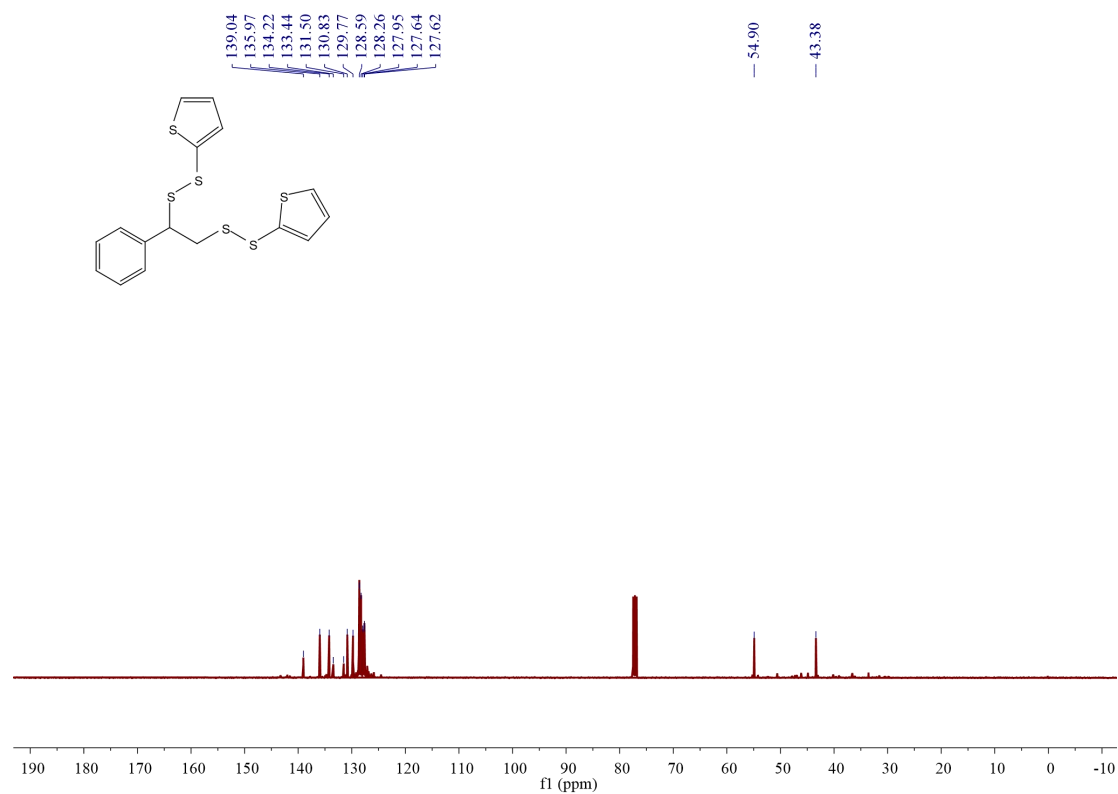


¹³C NMR spectra of 3aa (101 MHz, CDCl₃)

NMR Spectra



¹H NMR spectra of 3ab (400 MHz, CDCl₃)



¹³C NMR spectra of 3ab (101 MHz, CDCl₃)